

Final Report

Agreement Number 99FC810156

AIR-WATER GAS TRANSFER ON STEPPED SPILLWAYS

Prepared for

U.S. Department of the Interior
Bureau of Reclamation

Water Resources Research Laboratory
Denver Federal Center
Denver, CO

Prepared by

Brian W. McKenna
James F. Ruff

Engineering Research Center
Colorado State University
Fort Collins, CO

April 2001

Final Report

Agreement Number 99FC810156

AIR-WATER GAS TRANSFER ON STEPPED SPILLWAYS

Prepared for

U.S. Department of the Interior
Bureau of Reclamation

Water Resources Research Laboratory
Denver Federal Center
Denver, CO

Prepared by

Brian W. McKenna
James F. Ruff

Engineering Research Center
Colorado State University
Fort Collins, CO

April 2001

Executive Summary

AIR-WATER GAS TRANSFER ON STEPPED SPILLWAYS

When the concentration of dissolved gasses in water reach levels that are either too high or too low, the environment can be negatively impacted. Low dissolved oxygen concentrations can result in the degradation of aquatic habitat as well as the usability of the water. Likewise, an excessive concentration of total dissolved gas can also degrade the aquatic habitat by causing gas bubble disease in fish. In between these two extremes lies a safe level of dissolved gas concentration where the pressure of the dissolved gasses is equal to the pressure of gasses in the environment. This concentration is known as the saturation concentration.

Despite the fact that both of these conditions are opposites in terms of nature and causes, their solution may be one and the same. By increasing the rate or efficiency at which gasses are transferred between the air-water interface, dissolved gasses will be more likely to return to the ideal saturation concentration. Small-scale model studies have revealed that stepped spillways possess larger transfer efficiencies than smooth spillways.

As a result, a prototype-scale model study was undertaken to evaluate the transfer efficiencies of various stepped spillway configurations and compare those configurations with a similar smooth spillway. Measurements of the total dissolved gas concentrations were taken on a near prototype-scale model spillway. Measurements were made using step heights of 1 foot and 2 feet as well as a smooth slope. For each step configuration,

measurements were taken for unit discharges of 5, 10, 15, and 20 cfs/ft. Sampling locations were located at the top and bottom of the spillway as well as at $\frac{1}{4}$, $\frac{1}{2}$, and $\frac{3}{4}$ of the length of the spillway.

A method for calculating the average transfer efficiency for a specific scenario and location was proposed. This method was applied to the experimental data taken during this study in order to compare the different scenarios and locations in terms of their efficiencies. The results of the application of this method are presented. Conclusions about the results and potential applications of the findings are also discussed.

Brian W. McKenna
James F. Ruff
Department of Civil Engineering
Colorado State University
Fort Collins, CO 80523
Spring 2001

ACKNOWLEDGMENTS

Sincere thanks is extended to Colorado State University, the Agricultural Experiment Station (project COLO 0708), and the United States Bureau of Reclamation (agreement number 99FC810156) for financially sponsoring this research. Without the funding provided by these sources, this report would not have been possible.

A sincere thanks is given to everyone who contributed information, advice, and assistance during the course of this research. The authors would like to thank Dr. Robert Ward and Dr. Chester Watson for thoroughly reviewing this text. A special thanks goes out to Kathleen Frizell of the Bureau of Reclamation for her advice and assistance during all phases of this project. A sincere appreciation is expressed to the environmental group and the chem. lab at the Bureau of Reclamation for loaning the total dissolved gas meters used in the data collection phase. The authors would also like to thank Jason Ward for providing valuable direction and insight throughout the research and writing process. The authors wish to acknowledge John Brookman for his assistance with the nitrogen injection process and data collection. Lastly, a thanks is given to Jodi McKenna for her thorough editing of this text.

TABLE OF CONTENTS

EXECUTIVE SUMMARY	ii
ACKNOWLEDGEMENTS	iv
Chapter 1 INTRODUCTION	1
1.1 Background	1
1.2 Objective	4
Chapter 2 LITERATURE REVIEW	5
2.1 Total Dissolved Gas Theory	5
2.1.1 Colt (1984)	5
2.1.2 Chanson (1994)	7
2.1.3 Geldert (1996)	10
2.2 Effects of Dissolved Gas on Aquatic Habitat	11
2.2.1 Marking (1987)	11
2.2.2 Bouck, Nebeker, and Stevens (1976)	12
2.3 Effects of Hydraulic Structures on Dissolved Gas	14
2.3.1 Chanson (1994)	15
2.3.2 Toombes and Chanson (2000)	16
2.3.3 Ahman and Zapel (2000)	18
Chapter 3 DESCRIPTION OF TESTING FACILITY, EQUIPMENT, AND PROCEDURES	20
3.1 Testing Facility	20
3.2 Testing Equipment	26
3.2.1 Nitrogen Equipment	27
3.2.2 Total Dissolved Gas Meters	31
3.3 Testing Procedures	33
3.3.1 Testing Scenarios	33
3.3.2 Step Number and Stationing	34
3.3.3 Overview of Sampling Locations	36

3.3.4	Configuration of Common Sensing Meter.....	37
3.3.5	Configuration of Sweeney Aquametric Meter.....	39
3.3.6	Testing Protocol.....	45
Chapter 4	Data Analysis and Results	48
4.1	Transfer Efficiency	48
4.1.1	Equation Derivation.....	48
4.1.2	Variation with Respect to TGP% _{US}	49
4.1.3	Calculation Method.....	51
4.1.4	Results.....	53
4.1.5	Error Analysis	54
4.1.6	Relationship to Vertical Drop, Flow Rate, and Step Height... ..	56
4.2	TGP% as a Function of Vertical Drop.....	61
4.3	Data Comparison for Point Gage and Stilling Wells.....	63
4.3.1	Trend Comparison	63
4.3.2	Magnitude Comparison.....	64
Chapter 5	Summary, Conclusions, and Recommendations.....	67
5.1	Summary.....	67
5.2	Conclusions.....	68
5.3	Recommendations.....	70
	BIBLIOGRAPHY.....	72
	APPENDIX A – Raw Data.....	76
	APPENDIX B – Plots of TGP% in Head Box vs. TGP% on Slope.....	87
	APPENDIX C – Linear Regression Equations.....	105
	APPENDIX D – Plots of TGP% as a Function of Vertical Drop.....	107

LIST OF FIGURES

Figure 3-1 - Plan view of CSU/USBR DSOF.....	21
Figure 3-2 - Profile view of CSU/USBR DSOF.....	22
Figure 3-3 - Isometric view of CSU/USBR DSOF.....	23
Figure 3-4 - Photograph of overtopping facility with flow of 15 cfs/ft.....	24
Figure 3-5 - Photograph of overtopping facility without flow.....	25
Figure 3-6 - Location of gas injection point.....	28
Figure 3-7 - Nitrogen tanks.....	29
Figure 3-8 - Nitrogen regulators and fittings.....	30
Figure 3-9 - Total Dissolved Gas Meters.....	32
Figure 3-10 - Illustration of stationing used.....	35
Figure 3-11 - Detail of Stilling Well for Common Sensing Probe.....	38
Figure 3-12 - Venturi assembly with Sweeney Aquametric probe.....	39
Figure 3-13 - Venturi assembly mounted on point gage.....	40
Figure 3-14 - Detail of stilling well for SA probe.....	42
Figure 3-15 - Flow pattern through stilling well at station two.....	44
Figure 3-16 - Flow pattern through stilling well at station two.....	44
Figure 4-1 - Example data plot of TGP% HB vs. Station 1.....	50
Figure 4-2 - Positive skew in saturation level.....	53
Figure 4-3 - Transfer efficiency as a function of vertical drop.....	57
Figure 4-4 - Transfer efficiency as a function of unit discharge.....	59
Figure 4-5 - Transfer efficiency as a function of step height.....	60
Figure 4-8 - TGP% as a function of vertical drop; TGP% HB = 115%.....	62
Figure 4-9 - TGP% as a function of vertical drop; TGP% HB = 90%.....	62
Figure 4-10 - Example data plot of TGP% HB vs. Sta 2 for point gage configuration....	64
Figure 4-11 - Example comparison of point gage data to stilling well data.....	65

LIST OF TABLES

Table 2-1 - Mean hours to 20% mortality (Bouck et al. 1976).....	13
Table 2-2 - Summary of gas transfer on stepped chute experiments.....	16
Table 2-3 - Energy dissipation of stepped spillway chutes (Ahman and Zapel 2000)	19
Table 3-1 - Summary of testing scenarios	34
Table 3-2 - Summary of sampling station locations	36
Table 4-1 - Tabulation of transfer efficiencies (E) for each scenario and location	54
Table 4- 2 ² - R ² values for TGP% at station HB vs. station 1, 2, 3, and TB plots	55
Table 4- 3 ³ - Transfer efficiency as a function of vertical drop equations.....	58
Table 4- 4 ⁴ - Transfer efficiency as a function of unit discharge equations.....	59

Table 4-2

Chapter One

INTRODUCTION

1.1 Background

Gasses dissolved in water can have negative effects on the environment when they reach concentrations that are too high or too low. When the gas of concern is dissolved oxygen (DO), concentrations below a certain threshold can be dangerous to aquatic organisms by depriving organisms of the oxygen necessary for them to function. On the other end of the spectrum, the amount of total dissolved gasses (TDG) can also be harmful to aquatic organisms when they reach concentrations that are too high. Excessive TDG levels have been known to cause the potentially lethal condition of gas bubble disease. The safest level of dissolved gasses occurs when the pressures of the gasses dissolved in the water are in equilibrium with atmospheric pressures. This concentration is referred to as the saturation level.

Low DO levels have historically been a problem in many water bodies. Low DO concentrations can occur as the result of a number of natural and man-made causes. For example, natural causes include the oxygen demand of organic material and naturally occurring pools that keep the water stagnant and prevent oxygenation. Additionally, low DO can occur as the result of man-made causes in reservoirs created by hydraulic structures such as weirs and dams. The stagnant pools created by hydraulic structures prevent oxygenation of the water and promote the growth of oxygen consuming organic materials. Further, stratification of reservoirs as the result of solar heating of the surface

can prevent the exchange of oxygen to the bottom of the reservoir even more. Other man-made sources of low DO include nitrate and phosphate pollution of lakes and estuaries from by agricultural runoff and wastewater discharge. The nitrates and phosphates promote the growth of organic material, thus increasing the amount of oxygen demand. It is true that the oxygen can be replenished to the water through contact between the water and the atmosphere; however, when the rate of depletion exceeds the rate of replenishment, low DO levels can cause a significant environmental problem.

Excessive TDG, or TDG supersaturation, is a growing concern in many areas. Excessive TDG can be the result of natural causes such as waterfalls, the mixing of waters of different temperatures, and sudden temperature changes in water. More often, however, TDG supersaturation is the result of a hydraulic structure such as a spillway. The supersaturation is caused by the entrainment of atmospheric gasses as water passes over a spillway. As the spilled water plunges deep into the stilling basin, the entrained air is exposed to extremely high hydrostatic pressures that force the entrained air into solution. As the rate of spill increases, the levels of TDG increase as well. Likewise, the depth of the stilling basin is directly proportional to the amount of supersaturation produced. Consequently, high head dams spilling large amounts of water into deep stilling basins can lead to dangerous levels of TDG supersaturation.

Such is the case in the Columbia River Basin where the combination of high flows and large dams with deep stilling basins has led to excessive TDG levels throughout much of the basin. TDG levels regularly exceed the federal standard of 110% of the saturation level during peak spring and summer flows. Supersaturation as high as 140% of saturation has been recorded in the immediate tailwater of many dams while

supersaturation as high as 120% has been recorded in the forebays of dams downstream of large spills (Ruffing et al. 1996). The policy used in the past by dam operators was to store water during the peak runoff periods and then release it slowly. The philosophy was to keep peak spillway releases as low as possible and thereby keep TDG levels to a minimum. However, in 1995 the National Marine Fisheries Service demanded an increase in the amount of water spilled to aid salmon, listed as an endangered species, in their migration. The increased spill was intended to not only produce more current in the river but also provide a safer downstream passage over the spillways rather than through the turbines. As a result of the increased spills to save salmon, dam operators are now required to release enough water to increase fish survival while at the same time they are creating water quality conditions known to be lethal to the fish they were intending to save (Ruffing 1996).

Although low DO and TDG supersaturation lie at opposite ends of the spectrum in terms of their natures and their causes, their solution may be one in the same. Increasing the rate or efficiency at which gasses are transferred between an air-water interface will bring all dissolved gas levels, whether DO or TDG, closer to the ideal saturation level. A stepped spillway is one alternative that has proven to be effective in increasing the transfer efficiency of the air-water interface in small-scale model studies (Toombes et al. 2000). Additionally, small-scale stepped spillways have proven their ability to dissipate the energy of flow, which can reduce the stilling basin depth necessary to contain a hydraulic jump (Ahman and Zapel 2000). A shallower stilling basin can lessen the potential for TDG supersaturation by minimizing the hydrostatic pressure acting upon the aerated flow. Despite the success of small-scale models, little research

has been done with prototype scale stepped spillways, particularly as it pertains to gas transfer.

1.2 Objective

The objective of this thesis is to determine the transfer efficiencies of different stepped spillway configurations and apply this to the potential use of stepped spillways to improve water quality. Special emphasis will be placed on the use of stepped spillways to reduce TDG supersaturation. Total dissolved gas measurements were taken on a near prototype scale model spillway at varying step heights and flow rates to achieve this objective. Total dissolved gas measurements were also taken on a smooth spillway of identical dimensions in order to compare the transfer efficiencies of the stepped spillways with a baseline. The relationship of transfer efficiency to variables such as flow rate, step height, and vertical drop were evaluated. The results of the model study and conclusions about the possible applications of the results are presented.

Chapter Two

LITERATURE REVIEW

2.1 Total Dissolved Gas Theory

2.1.1 Colt (1984)

Colt (1984) is an excellent comprehensive source discussing the solubility of gasses in water with a specific emphasis on the causes, measurement, computation, and reporting of gas supersaturation.

In the discussion on dissolved gas supersaturation, Colt lists several causes, both natural and man made that can produce supersaturation. Those causes include sudden temperature changes, mixing waters of different temperatures and air bubble entrainment. The most applicable cause to the author's study is that of air bubble entrainment. Colt suggests two mechanisms in which bubble entrainment can create supersaturation: "when bubbles are carried down into the water or gas and water are present together at elevated pressures" (Colt 1984). The former mechanism often occurs as a result of water flowing over spillways, falls or rapids. The latter mechanism often occurs in closed conduit systems as a result of "leaks on the suction side of the pumps, clogging of intake structures so that flowing water does not completely fill the pipe, or an intake pump that is not completely submerged" (Colt 1984).

Colt also discusses the computation and reporting of gas supersaturation. Colt explains that gas supersaturation can be described using the total gas pressure (tgp). The total gas pressure is defined as follows:

$$\text{tgp} = \left[\sum_i^n P_i^l \right] + P_{\text{vap}} \quad (2-1)$$

where: P_i^l = partial pressure (or gas tension) of the i^{th} gas in
the liquid solution

P_{vap} = vapor pressure of water

The total gas pressure then, is the sum of the pressures of each atmospheric gas (nitrogen, argon, carbon dioxide and oxygen) dissolved in the liquid plus the vapor pressure of water.

The total gas pressure alone, however, does not fully describe the situation. The total gas pressure must be compared to the local barometric pressure (BP) in order for it to be meaningful and comparable. Colt presents two different ways to relate the total gas pressure to the barometric pressure. The first way is to take the difference between the tgp and the barometric pressure. This yields a term known as the ΔP .

$$\Delta P = \text{tgp} - \text{BP} \quad (2-2)$$

where: tgp = total gas pressure

BP = local barometric pressure

Colt also suggests reporting the total gas pressure as a percent of the local barometric pressure which he calls the total gas pressure (%) or TGP(%).

$$\text{TGP}(\%) = \left[\frac{\text{tgp}}{\text{BP}} \right] \times 100\% \quad (2-3)$$

where: tgp = total gas pressure

BP = local barometric pressure

Combining equation (2-2) with equation (2-3), the total gas pressure (%) can be written in its most common form as follows:

$$\text{TGP}(\%) = \left[\frac{\text{BP} + \Delta\text{P}}{\text{BP}} \right] \times 100\% \quad (2-4)$$

Colt concludes by discussing the preferred method for measuring gas supersaturation. Colt states that “direct measurement of ΔP is the preferred method of analysis” (Colt 1984). ΔP can be directly measured using an instrument known as a “Weiss saturometer”. “Weiss saturometers” use the membrane-diffusion method (MDM) to measure ΔP directly by measuring the pressure difference between the dissolved gasses and the atmosphere. This type of instrument consists of a gas permeable, silicone rubber tubing (known as the gas collector) connected to a differential pressure measuring device. Gasses in the water permeate into the silicone tubing and the saturometer measures the pressure difference between the inside of the tubing and atmosphere. This value is then reported as the ΔP . By combining a Weiss saturometer with a barometer, the total gas pressure percent can be measured directly.

2.1.2 Chanson (1994)

The next fundamental concept of dissolved gasses is the mathematical description of their transfer from air to water and vice versa. According to Chanson, the mass transfer of any chemical across an interface is described by Fick’s law. Fick’s law states that the mass transfer rate of a chemical across an interface is directly proportional to the negative product of the coefficient of molecular diffusion and the gas concentration gradient.

$$\frac{d}{dt}M_{\text{gas}} \propto -D_{\text{gas}} \left(\frac{d}{dx}C_{\text{gas}} \right) \quad (2-5)$$

where: M_{gas} = mass of gass

D_{gas} = coefficient of molecular diffusion

C_{gas} = gas concentration

The analysis of the gas concentration gradient is very complex when air entrainment exists. Assuming the chemical in question is a dissolved gas (i.e. oxygen or nitrogen) and the interface is between air and water, equation (2-5) can be written as:

$$\frac{d}{dt}M_{\text{gas}} = K_m A \left(\frac{P_{\text{gas}}}{H_{\text{gas}}} - C_{\text{gas}} \right) \quad (2-6)$$

where: K_m = mass transfer coefficient

A = gas-liquid interface area

P_{gas} = partial pressure of the chemical in air

H_{gas} = Henry's law constant

K_M is a function of the liquid film coefficient (K_L) and the gas film coefficient (K_G). However, in the case of atmospheric gases, K_L is much greater than K_G , such that K_M can be considered equal to K_L . Additionally, Henry's law states that "the weight of any gas that will dissolve in a given volume of a liquid, at constant temperature, is directly proportional to the pressure that the gas exerts above the liquid." This can be written in equation form as follows:

$$C_s = \frac{P_{\text{gas}}}{H_{\text{gas}}} \quad (2-7)$$

where: C_s = concentration of dissolved gas at equilibrium

By simplifying and dividing by the total air-water mixture volume, equation (2-6) becomes the basic air-water gas transfer equation:

$$\frac{d}{dt}C_{\text{gas}} = K_L a (C_s - C_{\text{gas}}) \quad (2-8)$$

where: a = specific surface area, defined as the air-water interface
area per unit volume of air and water

Integrating equation (2-8) along a given distance of an open channel or over a hydraulic structure, such as a spillway, allows the overall gas transfer to be described in terms of the deficit ratio (r) defined as:

$$r = \frac{C_s - C_{\text{US}}}{C_s - C_{\text{DS}}} = e^{-K_L a t} \quad (2-9)$$

where: C_{US} = upstream dissolved gas concentration

C_{DS} = downstream dissolved gas concentration

Chanson also suggests that the gas transfer along a channel or over a structure can be described as a function of the deficit ratio, in terms of the transfer efficiency (E).

$$E = 1 - \frac{1}{r} \quad (2-10)$$

$$E = \frac{C_{\text{DS}} - C_{\text{US}}}{C_s - C_{\text{US}}} \quad (2-11)$$

The transfer efficiency is more descriptive than the deficit ratio. A transfer efficiency between zero and one ($0 < E < 1$) indicates a normal aeration or degassing situation; the downstream gas concentration (C_{DS}) is closer to the saturation concentration (C_s) than the upstream gas concentration (C_{US}). Additionally, for this situation, the greater the transfer efficiency, the better the structure or channel is at transferring gas. If, for some reason,

the upstream gas concentration is greater than the saturation concentration and the downstream gas concentration is less than saturation or vice versa, the transfer efficiency will be greater than one ($1 < E$). The other possibility is that the downstream gas concentration is further from the saturation concentration than the upstream gas concentration. In this case the transfer efficiency would be less than zero ($0 > E$).

2.1.3 Geldert (1996)

Geldert suggests that the dimensionless deficit ratio (r) and the transfer efficiency (E) equations can be rewritten in terms of the total gas pressure percent (TGP%) defined in equation (2-4). This eliminates the need to determine the saturation concentration since it is assumed to be 100%. Additionally, most total dissolved gas meters (such as the ones used in this project) report data in terms of TGP%. By rewriting the equations in terms of TGP%, the need to convert the total dissolved gas meter reading to a concentration is eliminated. The new deficit ratio and transfer efficiency equations are respectively written as:

$$r = \frac{100 - \text{TGP}\%_{\text{US}}}{100 - \text{TGP}\%_{\text{DS}}} \quad (2-12)$$

$$E = \frac{\text{TGP}\%_{\text{DS}} - \text{TGP}\%_{\text{US}}}{100 - \text{TGP}\%_{\text{US}}} \quad (2-13)$$

Hereafter, any reference to the deficit ratio or the transfer efficiency will be understood to mean the total gas pressure percent form of the equations.

2.2 Effects of Dissolved Gas on Aquatic Habitat

2.2.1 Marking (1987)

The history of gas embolisms and their effect on fish have been recognized since at least 1670, according to Marking. The term “gas bubble disease” first came about around the turn of the century when Gorham (1901) described the phenomenon of gas bubble disease as consisting of the following:

Vesicles of gas invading all the superficial parts of the fish, especially fins, eyeballs, and in loose connective tissue of the orbits, so that the eyes were forced from their sockets; less commonly bubbles formed beneath the lining of the mouth, in the gill arches, or beneath the skin, so that scales were raised from the surface. The swimming behavior of the fish was disturbed, especially in maintenance of horizontal equilibrium. (Marking 1987)

Marking credits Gorham as being the first to recognize that gas bubble disease is the result of a reduction in partial pressures of dissolved gasses and not the result of a pathogen. Gorham first noticed gas bubble disease occurring in fish as they were taken from great depths to the surface of a water body very rapidly. The change in depth subjected the fish to a change in partial pressure that resulted in the formation of the bubbles in the tissue described above.

Gas bubble disease was also observed around 1900 in fish held in an aquarium. The fact that the fish were suffering from gas bubble disease despite the fact that the depth of water was not rapidly changing proved to be a mystery. Three years later, however, Marsh (1903) solved the mystery by recognizing that the intake pump was forcing air bubbles into solution by pressurizing the water supply line. Marsh recognized that gas bubble disease could occur from supersaturation of water as well as rapid changes in depth.

Marking admits that the exact level of toxicity of supersaturation varies depending on the species and their habitat. Threshold concentrations for species such as the speckled dace have been estimated as high as 123%. On the other hand, threshold concentrations for salmonid eggs, fry and fingerlings have been estimated as low as 103%. Habitat conditions also play a large part in the toxicity of supersaturation. The general criterion of 110% has been criticized as being too low for rivers deeper than 1m and too high for fish hatcheries. Fish in hatchery systems are generally much more susceptible to gas bubble disease because they are confined to shallow depths. Wild fish can compensate for supersaturation by sounding to depths sufficient for compensating the partial pressures.

While there is some uncertainty as to the exact threshold of toxicity of supersaturation, the fact that gas supersaturation causes gas bubble disease is indisputable. Marking also makes it clear that gas bubble disease can potentially lead to mortality in many species.

2.2.2 Bouck, Nebeker, and Stevens (1976)

In an attempt to define more precisely the threshold concentration of supersaturation, Bouck et al. (1976) performed extensive experiments on several species of pacific salmonids as well as largemouth bass in shallow water holding tanks. The fish were continuously exposed to total gas pressures (%) ranging from 100% to 140% and then monitored to determine the rate of mortality. The experiment produced the following values for the mean time in hours at which 20% mortality occurred:

Table 2-1 – Mean hours to 20% mortality (Bouck et al. 1976)

Salmonids	Supersaturation Level		
	115%	120%	125%
Adults	309	48	18.3
Smolts	154	41	17.2
Juveniles	125	53.5	23.6

Additionally, all salmonid fish tested at 125% saturation died in six days or less while total mortality never occurred during the 30-day test period at 115% saturation. On the other hand, large mouth bass, a predator of juvenile salmon, proved to be much more resilient to supersaturation. Large mouth bass were able to survive for longer periods at higher supersaturation levels than salmonids without their feeding instincts being inhibited. This makes salmonids even more susceptible to death during periods of supersaturation because of predation from other stronger species.

While the results of this study are valuable in assessing the tolerance of salmonids to supersaturation, the authors are quick to point out the limitations of their study. In their discussion, the authors state the following:

Perhaps some readers may want to extrapolate beyond these data to natural circumstances in a river, reservoir, or lake. We urge extreme caution in such endeavors because the research design did not permit the testing of remedial behavioral responses such as avoidance, sounding, or other aspects resulting in less than continuous exposure to supersaturation stress. (Bouck et al. 1976)

Therefore, this study sufficiently proves that supersaturation is lethal to salmonids. However, it fails to address the ability of salmonids to avoid or compensate for supersaturated water.

2.3 Effects of Hydraulic Structures on Dissolved Gas

In searching for studies similar to the author's study, it became apparent that very few data sets or predictive equations exist that can be applied to the author's study. Most data sets measuring dissolved gasses upstream and downstream of hydraulic structures fit into one of two categories. The first category includes data sets where the hydraulic structure of interest was a large dam with a spillway and stilling basin. These data sets are very valuable for formulating predictive equations, however, the large amount of gas transfer that occurs in the stilling basins of these structures covers up the mechanisms at work on the spillway itself. The second category of data sets includes rather small structures such as weirs, free-overfalls and short cascades where the overall hydraulic head is on the order of five feet or less. The dimensions of these structures are so much smaller than the model used in this study that the results can not be accurately extrapolated.

Despite most references not being directly applicable to this study, several references are helpful in describing the general mechanisms at work in air-water gas transfer at hydraulic structures. As mentioned in Chapter One, large dams have two potential ways to create dissolved concentrations that can have an adverse effect on the environment. One way is through the plunging of spillway releases into a deep stilling basin resulting in supersaturation. The other way is through the depletion of dissolved oxygen because of the stagnant pool created upstream of the dam. The references summarized in this section describe how stepped spillways may be a way to reduce both of these negative impacts.

2.3.1 Chanson (1994)

In his text, *Stepped Cascades, Channels, Weirs and Spillways* (Peramon 1994), Chanson devotes an entire chapter to the subject of “Air-Water Gas Transfer on Stepped Chutes”. Chanson suggests that, “on stepped chutes, both the aeration of the flow and the strong turbulent mixing enhance the air-water transfer of chemicals” (Chanson 1994). Enhanced air-water transfer simply means that the concentration of the dissolved chemical in question will return to its saturation concentration faster. This is applicable whether the chemicals are supersaturated or under saturated. The chemicals can be anything from atmospheric gasses to polluted matters. The mathematical reason for this can be understood by recalling the governing equation (eq 2-8) for gas transfer.

$$\frac{d}{dt}C_{\text{gas}} = K_L a(C_s - C_{\text{gas}}) \quad (2-14)$$

On a stepped chute, the turbulent mixing of the flow increases the mass transfer coefficient (K_L), thus increasing the rate of exchange of gas. The aeration of the flow also increases the rate of exchange of gas by increasing the area of gas-liquid interface (a) due to the cumulative bubble surface areas. According to Chanson, an air content of 10% creates a specific interface area of 600 m² per cubic meter of air and water assuming a bubble diameter of 1mm.

Chanson goes on to provide a review of seven previous experiments performed to determine gas transfer on stepped chutes. All of the experiments tested structures that were relatively small. Most of the structures tested were less than five feet tall with step heights less than six inches. Additionally, six of the experiments measured dissolved oxygen while one experiment measured volatile organic components. The table below

provides a summary of the dimensions tested in all of the various experiments including the author's.

Table 2-2 – Summary of gas transfer on stepped chute experiments.

	Slope (deg)	Unit flow rate (ft ² /s)	h _{step} (ft)	d _{crit} /h _{step}	H _{dam} (ft)
Minimum	6	3.01x10 ⁻⁴	0.082	0.002	2.95
Maximum	45	10.38	1.00	9.12	6.99
Author's	26.6	5 - 20	0, 1, and 2	0.46 and 2.32	50

Most of the experiments attempted to derive an equation to describe the deficit ratio in terms of variables, such as the dam height, step height, critical flow depth, and temperature. While these equations may be useful for other structures of similar scale, Chanson warns against using their results to predict gas transfer on larger structures. He claims that the smaller models “underestimate grossly the entrainment of bubbles and hence the aeration efficiency” (Chanson 1994). Nevertheless, two experimenters’ conclusion can probably be considered valid for all sizes of structures. Tebbutt and Essery (1977) suggested that the best transfer efficiency is achieved with small water discharges under nappe flow situations.

2.3.2 Toombes and Chanson (2000)

Toombes and Chanson (2000) took a unique approach in comparing the aeration efficiency of smooth and stepped chutes. They performed their experiment using a flume 84 feet in length set at a slope of 4 degrees. After the smooth invert chute was tested to

determine its efficiency, 10 steps were constructed inside the flume. The steps were 0.47 feet high and 7.87 feet long.

Their experiment was unique in that they did not directly measure any gas concentrations. Instead, they measured air-water velocities and air bubble counts. They then used these measurements to estimate the gas concentration according to the following equation:

$$\Delta C_{\text{gas}} = (C_s - C_{\text{gas}})_{\text{US}} \left(1 - \exp\left(-\frac{K_L a}{V} \Delta x\right) \right) \quad (2-15)$$

where: V = flow velocity over the interval Δx

The above equation is merely the discrete integral of the basic gas transfer equation presented previously. To determine the air-water interface area (a), Toombes and Chanson used the following equation derived using mass conservation for air:

$$a = \frac{4F_{\text{ab}}}{v} \quad (2-16)$$

where: F_{ab} = number of bubbles impacting the air probe per
second

v = local air-water velocity

Using this approach Toombes and Chanson concluded that the aeration efficiency of the stepped chute was between 15% and 40% depending on the flow rate. The aeration of the smooth chute, however, was only about 3%. This means that “the stepped chute design is basically 10 times more efficient than the smooth chute for the same flow rate and bed slope” (Toombes and Chanson 2000).

While this paper reinforced the concept of improved aeration on stepped versus smooth chutes, the accuracy of the values reported for aeration efficiency may be

questionable since the values were never verified against actual gas concentration measurements. The only evidence of any verification is their statement, “The overall aeration efficiency is comparable with measured prototype performances” (Toombes and Chanson 2000). Additionally, their results are not comparable with the author’s results because of the large discrepancy in channel slope and step height.

2.3.3 Ahman and Zapel (2000)

Ahman and Zapel suggest another way that stepped spillways can reduce dissolved gas levels. In addition to the greater transfer efficiency of stepped chutes, the energy dissipation of stepped chutes is also greater than for smooth chutes. By increasing the amount of energy dissipation that occurs along the spillway, the depth of the stilling basin necessary to force a hydraulic jump is reduced. A shallower stilling basin will have less hydrostatic pressure acting on the entrained air and therefore create less total dissolved gas supersaturation.

In order to quantify the amount of energy dissipation that could be achieved with a stepped spillway, Ahman and Zapel tested a 1:8 scale physical model with varying slopes and step heights. By measuring the velocities, water depth, and air concentration, the amount of energy dissipation for each configuration could be determined. The results of their analysis are found in table 2-3

Table 2-3 – Energy dissipation of stepped spillway chutes (Ahman and Zapel 2000)

Slope (H:V)	Step Height (ft)	Energy Dissipation
2:1	4	82%
3:1	4	81%
2:1	2	79%
3:1	2	78%
1:1	2	74%

Ahman and Zapel concluded that “the stepped spillway provides a reasonable alternative for structural gas abatement improvements” (Ahman and Zapel 2000). However, they are quick to point out that air entrainment can not be accurately modeled at the scale they used. The result is that prototype velocities and thus stilling basin depths are over predicted in the model. Additionally, they recognized that gas transfer could not be modeled properly either. Consequently, “verifying the gas abatement performance... can only be accomplished through prototype testing” (Ahman and Zapel 2000). Therefore, while the 1:8 scale model is valuable in making an estimate of energy dissipation, a more accurate quantification of both the energy dissipation and the gas transfer can only be done at prototype scale.

Chapter Three

DESCRIPTION OF TESTING FACILITY, EQUIPMENT, AND PROCEDURES

3.1 Testing Facility

The tests for this study were performed on the Colorado State University (CSU)/ United States Bureau of Reclamation (USBR) Dam Safety Overtopping Facility (DSOF). The facility is located just west of Fort Collins, Colorado, at the Engineering Research Center on the Foothills Campus of Colorado State University. The facility consists of a supply pipeline, concrete head box, chute, and tail box. The model is near-prototype in that the vertical drop of the chute is similar to that of many small dams currently in operation. The width of the chute, however, has been constricted to allow for higher unit discharges. The near-prototype scale of the facility holds many advantages over smaller models. Because surface tension forces of smaller models are so great compared to entrainment forces, aeration effects are greatly reduced. Since aeration is fundamental to gas transfer, smaller models cannot accurately predict the amount of aeration or degassing taking place. Consequently, model studies of gas transfer must be done at near-prototype scales. The size of the DSOF can be seen in the scale drawings of the plan, profile, and isometric views of the facility found in Figures 3-1, 3-2, and 3-3 respectively. Additionally, photographs of the facility with and without flow are found in Figures 3-4 and 3-5 respectively.

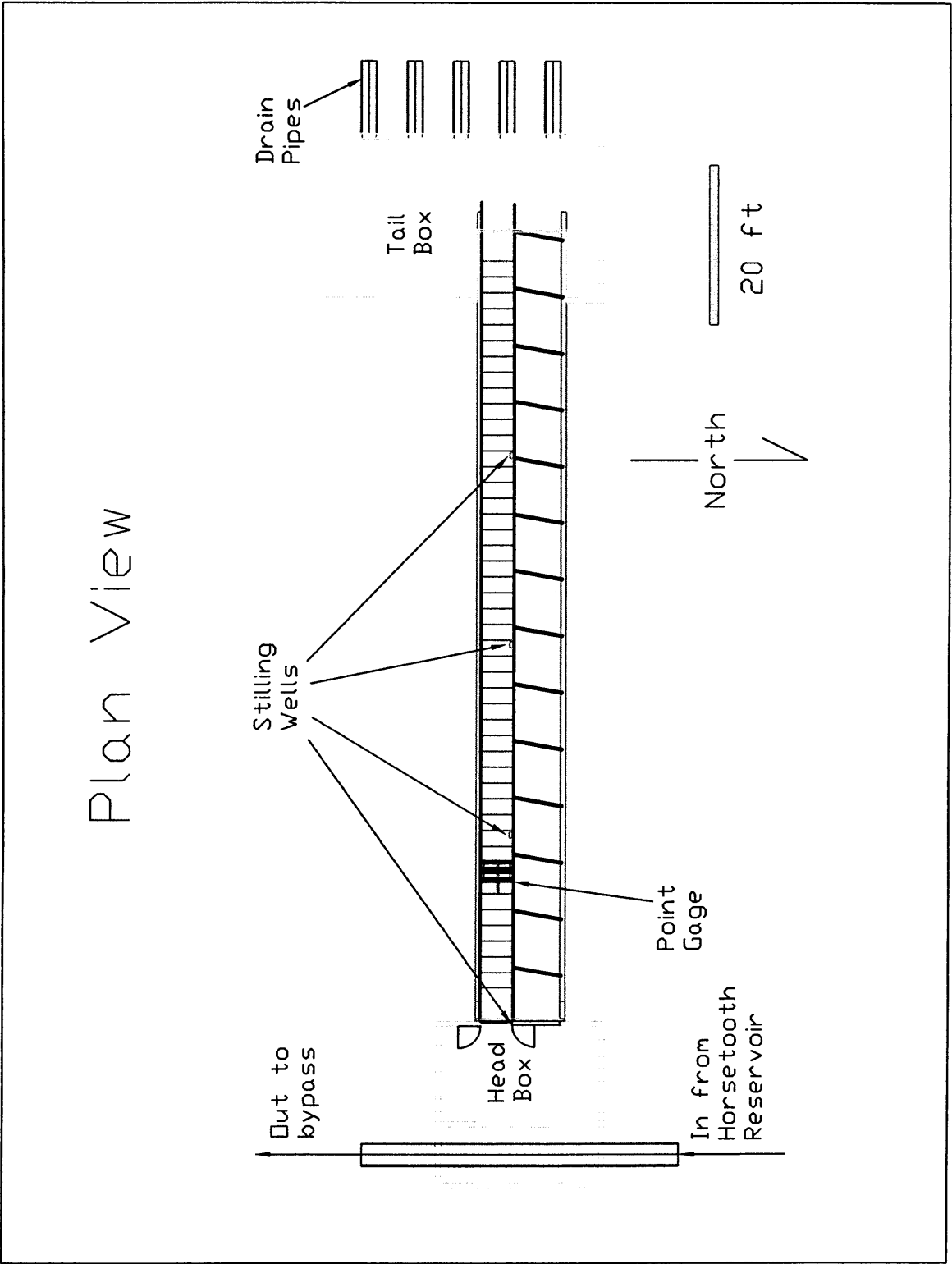


Figure 3-1-Plan view of CSU/USBR DSOF

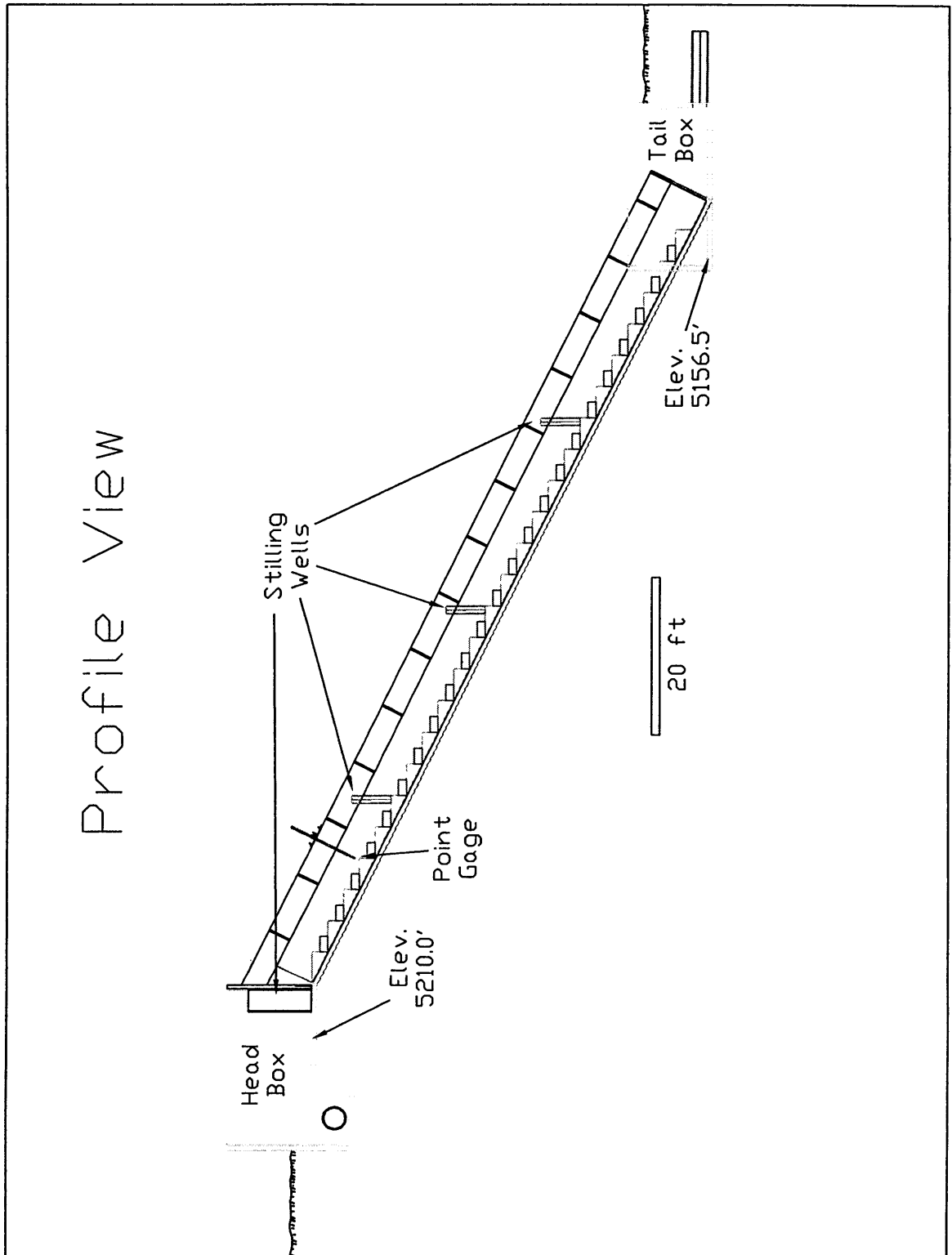


Figure 3-2– Profile view of CSU/USBR DSOF

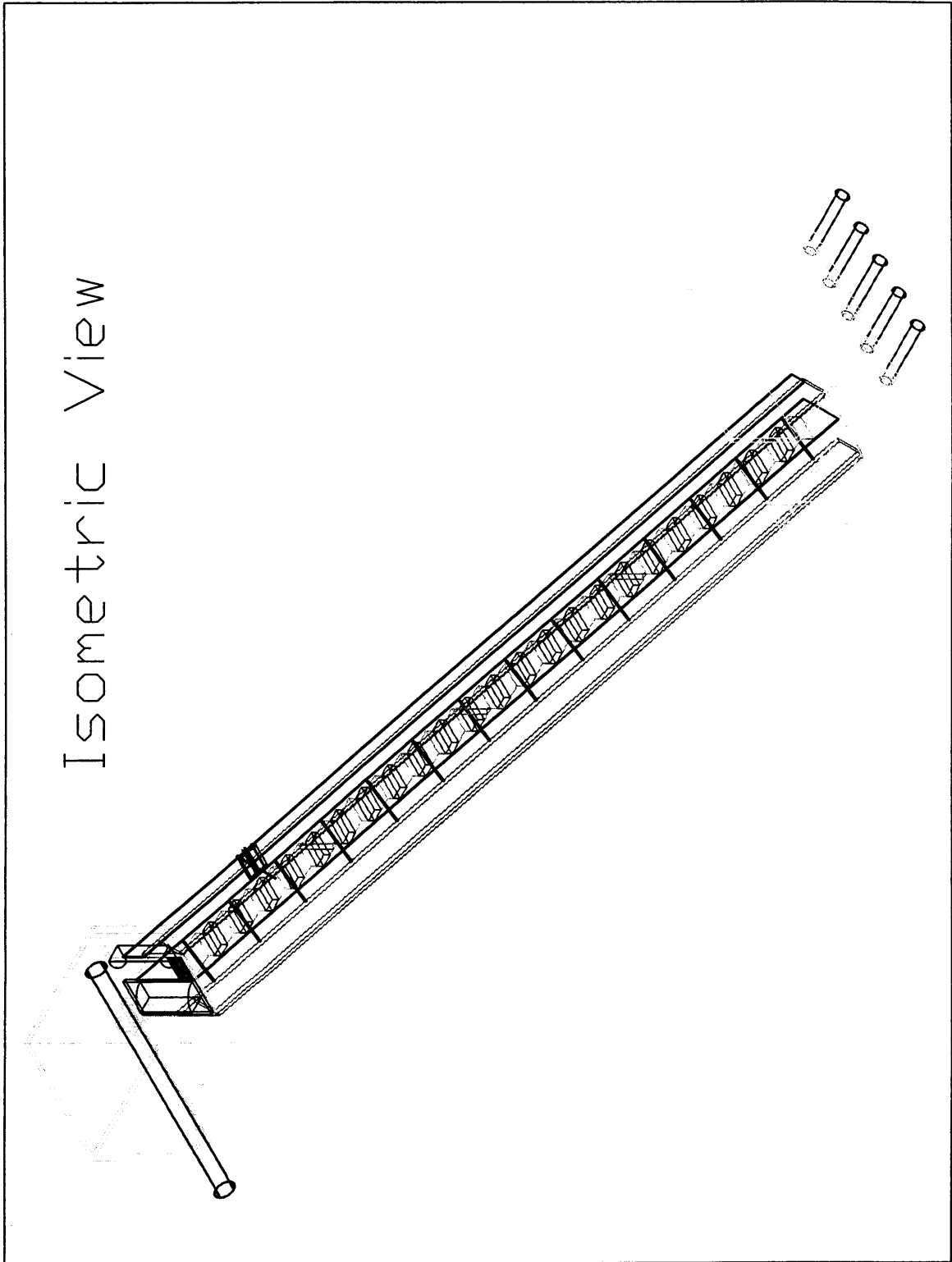


Figure 3-3–Isometric view of CSU/USBR DSOF



Figure 3-4– Photograph of overtopping facility with flow of 15 cfs/ft



Figure 3-5 –Photograph of overtopping facility without flow

At a 2H: 1V slope, the 100-foot long flume provides approximately 50 feet of vertical drop. The concrete flume is 10 feet wide; however, for this study, a temporary 7-foot tall wood wall was constructed in the flume to constrict the width to 4 feet. Rounded transition walls guide the water from the headbox into the flume to minimize transition losses and eddies. A sharp crested, wood weir 22 inches tall was installed at the downstream end of the transition walls in order to prevent the flow from breaking contact with the spillway as it passed over the crest. The gas transfer measurements were taken in the flume on three different surfaces: smooth concrete, 1-foot high wood steps, and 2-foot high wood steps. Water is supplied to the head box of the flume via a 36-inch pipeline from Horsetooth Reservoir. A series of valves along the pipeline are used to control discharge. The 2,640-foot long pipeline is capable of delivering a flow of up to 130 cfs at a maximum static head of approximately 250 feet. During this study, however, the maximum flow rate used was 80 cfs due to the limitations of the measuring instruments as well as a lower than usual reservoir head.

3.2 Testing Equipment

There were two distinct types of equipment used in this study. The first type consisted of the equipment that was used to inject nitrogen gas into the pipeline. This included liquid nitrogen tanks, regulators, valves, fittings, and air-hoses. The second type of equipment used was comprised of the instruments necessary to measure the dissolved gas levels of the water. The following two subsections describe in detail these two types of equipment.

3.2.1 Nitrogen Equipment

Typical dissolved gas levels in the supply reservoir ranged from approximately 92% to 98% of saturation. In order to be able to vary the levels of dissolved gas in the water reaching the spillway, it was necessary to have a mechanism that could increase the amount of dissolved gas to achieve supersaturation. Knowing that supersaturation can occur when “gas and water are present together at elevated pressures” (Colt 1984), led the author to explore ways that gas could be injected into the pressurized supply pipeline. Two basic questions had to be answered pertaining to the injection method: What gas should be used to inject into the pipeline? and Where should the point of injection be located?

After researching the possibilities for gasses that could be used, it was decided that nitrogen gas would be the best alternative. The following factors led to this decision:

- *Commercial availability* - The tanks could be delivered to the site the next working day after they were ordered.
- *Relatively low cost* - Each tank cost approximately \$60.
- *Large volume of gas in each tank* - Since the tanks contained gas in liquid form, they held a much larger volume of gas than other available gasses. Each tank of liquid nitrogen contained approximately 4,365 cubic feet of nitrogen gas. This volume of gas could last through approximately one day of testing.
- *Natural occurrence of nitrogen supersaturation* - Typically, when supersaturation occurs due to spillways, nitrogen is the predominant gas involved because the atmosphere is comprised of 78% nitrogen.

In determining the location of the injection point there were three factors that had to be taken into consideration. First, the injection point had to be located where there was access to the pipeline. Since most of the pipeline is buried, access could only be obtained where it was above ground or in one of the below ground valve houses. Additionally, the location had to be accessible to a truck so that the nitrogen tanks could be delivered. The second factor was that the injection point had to be located upstream of a point of high pressure so that the gas could supersaturate the water. The final consideration was that the injection point had to be located such that the gas and water would have a sufficient length of contact time before the water reached the spillway.

Considering these three factors, the best location for the injection point was determined to be the valve house located near the southwest corner of the Engineering Research Center. This location is show in Figure 3-6.

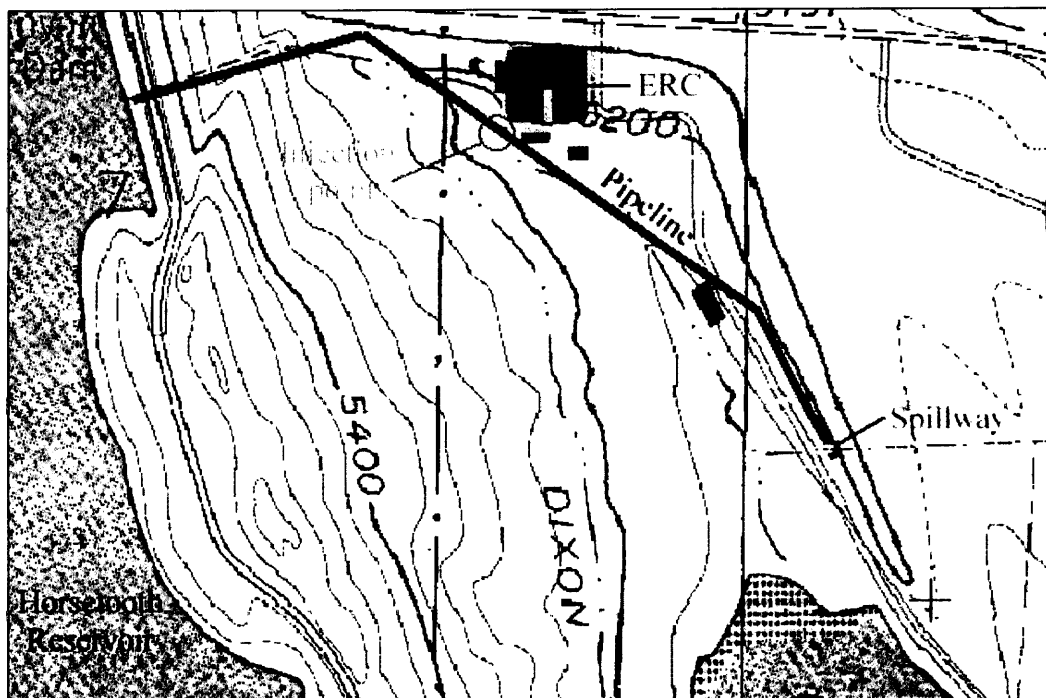


Figure 3-6—Location of gas injection point

Large tanks of liquid nitrogen were used to inject gas through an air hose and into a drain valve in the pipeline. Connected to each liquid nitrogen tank was a high-pressure regulator that was used to control the flow of gas from the tank. Due to the high flow rate and temperature of the nitrogen, each tank could only be used from 15 to 90 minutes, depending on the exact flow rate, before the tank and regulator would freeze. At times, the ice covering the tank and regulator was over an inch thick. When the ice became too thick, the opening of the regulator froze shut, thereby preventing the flow of nitrogen. In order to avoid this, the tanks had to be monitored closely and then switched when the regulator began to freeze. By rotating tanks, each tank had time to thaw before it needed to be used again. A photograph of a liquid nitrogen tank showing early signs of freezing is shown in Figure 3-7.



Figure 3-7– Nitrogen tanks

It was necessary to make the tank rotations as seamless as possible so that dissolved gas levels in the headbox of the spillway did not fluctuate significantly. To accomplish this, each regulator was equipped with a quick release fitting to connect it to the air hose. Additionally, the air hose was fitted with a ball valve at the end connecting it to the regulator. Since two tanks were simultaneously connected to the pipeline, the tanks could be switched by simply closing the ball valve on one tank and opening it on the second tank. If conditions required more than two tanks to be rotated, the quick release fittings allowed several tanks to be rotated quickly and efficiently by switching the air hose from one tank to another. Figure 3-8 shows the nitrogen tanks as well as their accompanying hardware.

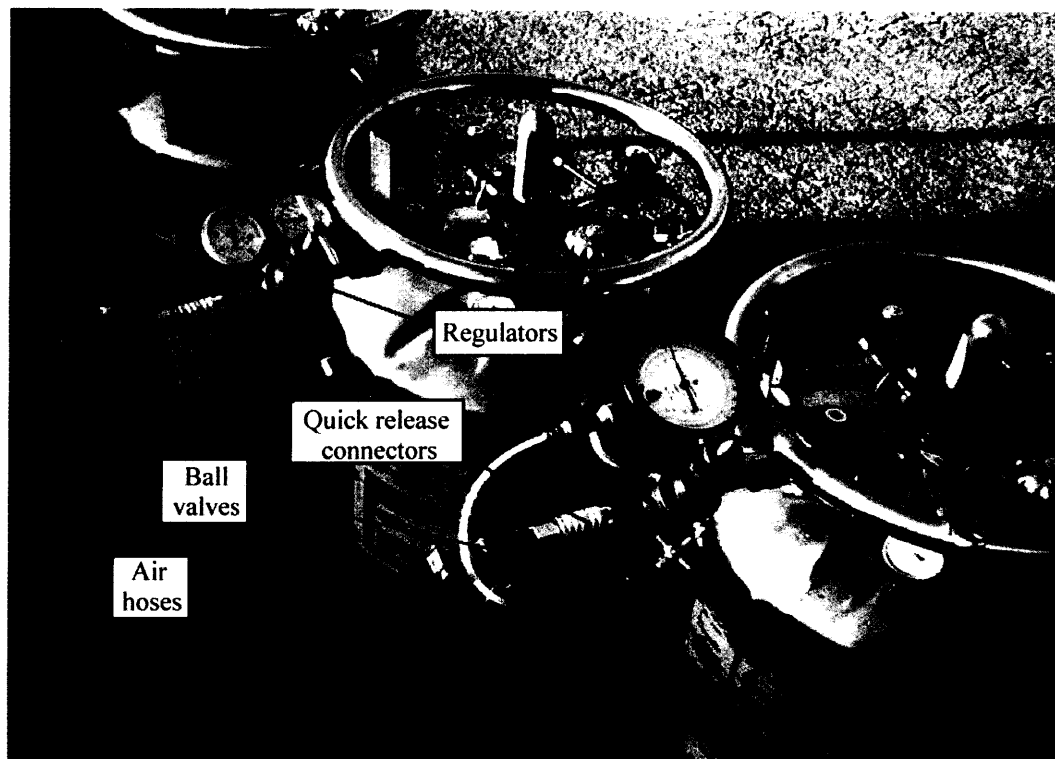


Figure 3-8 – Nitrogen regulators and fittings

3.2.2 Total Dissolved Gas Meters

Total dissolved gas meters were used to measure TGP%, water temperature, ΔP , and barometric pressure. Two different meters were used in order to obtain simultaneous readings at the top of the spillway as well as along the spillway slope and in the tail box. One meter was made by Common Sensing Inc. (CS) while the other meter was manufactured by Sweeny Aquametrics (SA). Although each meter was manufactured by a different company, both were very similar. Both meters were “Weiss saturometer” style instruments that directly measured ΔP . (For a further discussion of “Weiss saturomteters,” refer to the discussion of Colt (1984) in Chapter Two section 1.1 of this text.)

The instruments consisted of three major components: Analyzer, Conductor Cable, and Sensor Module. The Analyzer of each meter consisted of a liquid-crystal display (LCD) that reported the measured values, a barometer that measured the atmospheric pressure, and the electronic circuitry necessary to process the readings from the sensors. The Conductor Cable connected the Analyzer to the Sensor Module. It contained electrical conductors as well as a nylon pressure tube that allowed the differential pressure gage in the probe to sense atmospheric pressure. The Sensor Module was the portion that was actually placed in the water. It contained a temperature sensor as well as a silicone tube gas-collector connected to a pressure sensor. The silicone tube gas-collector was permeable to atmospheric gasses such as nitrogen, oxygen, carbon dioxide and water vapor. However, it was impermeable to water in its liquid state. Therefore, gasses dissolved in the water were able to pass through the silicone tubing into the gas-collector so that the pressure sensor could measure the pressure of the gasses

dissolved in the water. A picture of both meters with their components labeled is found in Figure 3-9.

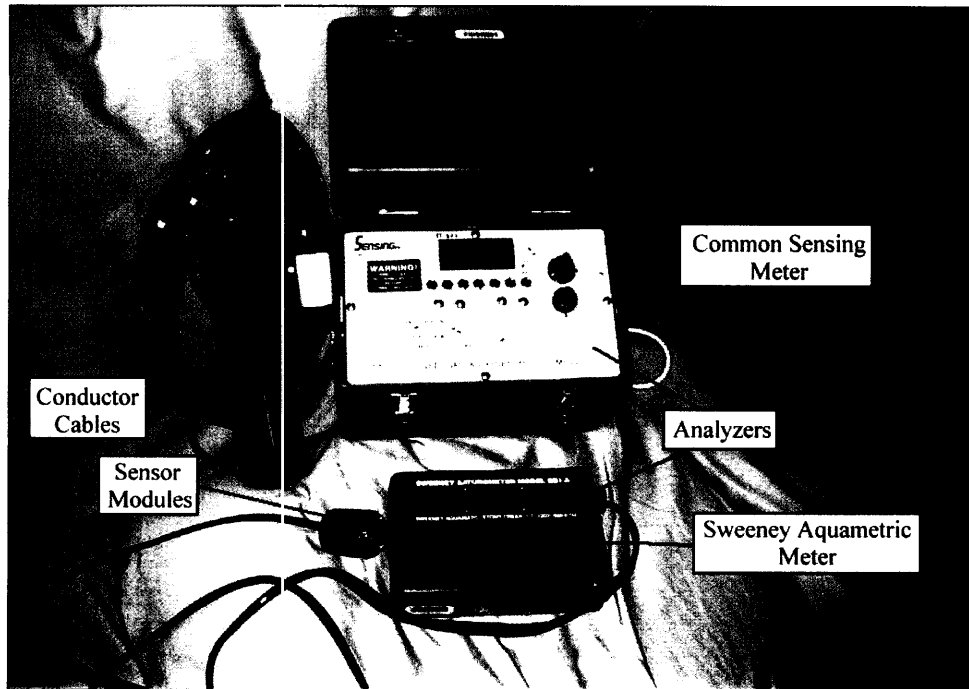


Figure 3-9– Total Dissolved Gas Meters

Although the meters were similar in concept, several differences made each one suitable for distinct uses and locations during the experiment. The most obvious difference was the size and portability of the two meters. The SA meter (shown at the bottom of Figure 3-9) was much smaller and lighter than the CS meter. Additionally, the SA meter was powered by a 9-volt battery while the CS meter had to be plugged in to an electrical outlet. For these reasons, among others, it was more practical to use the CS meter to measure the dissolved gas levels in the head box so that it did not have to be moved frequently. The SA meter was better suited to take readings at several places along the slope and in the tail box.

3.3 Testing Procedures

The goal of the tests that were run at the DSOF was to determine how the dissolved gas levels in the water would change as the water flowed from the head box, down the spillway, and into the tail box. To accomplish this goal, specific details such as the location of the meters, flow rates to be analyzed, step heights to be analyzed, testing protocol, etc. had to be established. The remainder of this chapter is devoted to explaining the scenarios and procedures that were used.

3.3.1 Testing Scenarios

Twelve different scenarios were tested and compared. The twelve scenarios consisted of three step configurations with four different flow rates for each configuration. Tests were run with no steps in the flume as well as with steps that were both 1 foot and 2 feet tall. These specific step heights were chosen because of the fact that they are commonly used in roller compacted concrete (RCC) dams. RCC steps are typically based on the lift heights of the concrete being placed. Lift heights are often 1 foot or 2 feet high. The smooth spillway configuration was tested to give a baseline for the performance of the steps

Four flow rates were tested ranging from 5 cfs/ft to 20 cfs/ft in increments of 5 cfs/ft. These flow rates were selected in order to provide a realistic overtopping condition, as well as to provide data during both skimming and nappe flow regimes on the steps. For the 2-foot steps, skimming flow occurred at 15 cfs/ft and 20 cfs/ft while nappe flow occurred at 5 cfs/ft and 10 cfs/ft. For the 1-foot steps, nappe flow occurred at

5 cfs/ft and skimming flow occurred for all other flow rates. The following table summarizes the different scenarios along with the accompanying flow regime.

Table 3-1 – Summary of testing scenarios

Scenario	1	2	3	4	5	6	7	8	9	10	11	12
Step height (ft)	2	2	2	2	1	1	1	1	0	0	0	0
Flow rate (cfs/ft)	5	10	15	20	5	10	15	20	5	10	15	20
Flow regime	N	N	S	S	N	S	S	S	NA	NA	NA	NA

Note: A step height of “0” indicates a smooth spillway; N = Nappe flow; S = Skimming flow; NA = Not Applicable because there are no steps

3.3.2 Step Numbering and Stationing

Steps were numbered by assigning a step number of one to the top step and then ascending for each successive step below. While this numbering system was sufficient to compare locations for a specific step height, comparing locations when the step heights were different became very confusing. What was known as step six for the 2-foot high steps became step 11 for the 1-foot high steps. Furthermore, when there were no steps in the flume, this labeling system became impossible.

Consequently, both the vertical distance as well as the linear distance from the crest was used to describe stationing between the different step configurations. Therefore, a measurement taken at the tip of step six for the 2-foot steps would share the same station label as a measurement taken on step 11 for the 1-foot steps. In both cases, the vertical drop is 10 feet and the linear distance is 22.4 feet. The same location on the smooth slope would have a slightly different station label however. Due to the fact that the crest moved back 4 feet and the floor was lowered 2 feet (because of

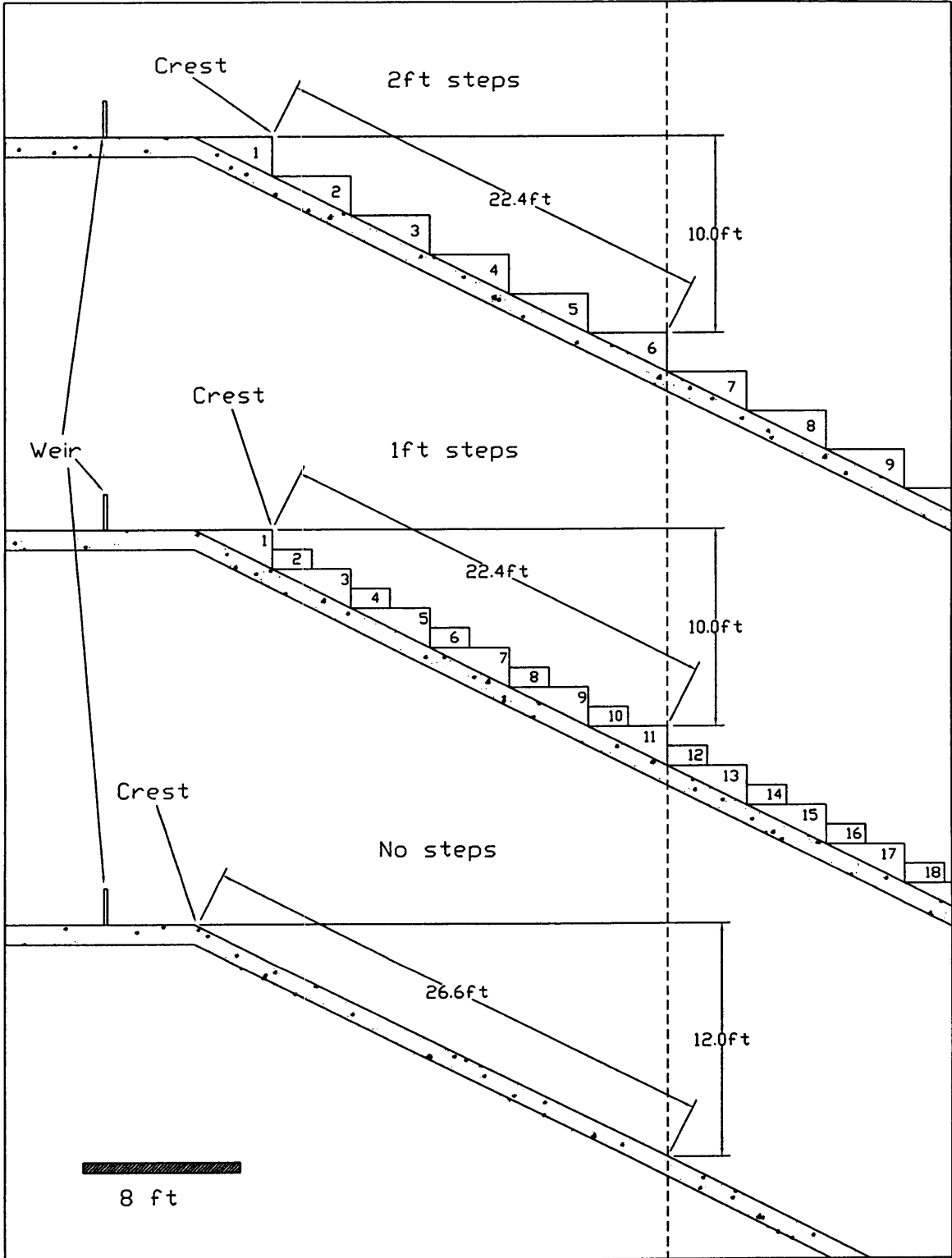


Figure 3-10 – Illustration of stationing used

the missing steps), the vertical drop is 12 feet while the linear distance is 26.6 feet. The stationing system used for all three configurations is illustrated in Figure 3-10.

3.3.3 Overview of Sampling Locations

Five sampling locations were selected to measure the dissolved gas levels in the water. A permanent sampling station was located in the head box (station HB), three sampling stations were located along the spillway face (stations 1, 2, and 3), and one sampling location was located in the tail box (station TB). The sampling stations on the spillway face were located at approximately one-fourth, one-half, and three-fourths the length of the spillway. The following table summarizes the exact locations of the sampling stations for each step configuration.

Table 3-2 – Summary of sampling station locations

Station	Step config	Step #	Vert Drop (ft)	Lin Dist (ft)
HB	2 foot		0	-10.06
	1 foot	-	0	-10.06
	smooth	-	0	-6.06
1	2 foot	6	10	22.36
	1 foot	11	10	22.36
	smooth	-	12	26.83
2	2 foot	12	22	49.19
	1 foot	23	22	49.19
	smooth	-	24	53.67
3	2 foot	18	34	76.02
	1 foot	35	34	76.02
	smooth	-	36	80.5
TB	2 foot	-	50	110
	1 foot	-	50	110
	smooth	-	50	110

Note that the vertical drop and linear distance for each station is the same for the 1 and 2 foot steps. For the smooth slope, however, the vertical drop and linear distance are slightly different because of the change in the crest location and the elevation of the floor. Nevertheless, because the locations are in close proximity, data taken at a given station is considered comparable for all step configurations although the locations are not identical between the steps and the smooth slope. While this small discrepancy in location is noted here, future references to sampling stations will make the assumption that the locations are close enough to be considered identical for the steps and the smooth slope.

3.3.4 Configuration of Common Sensing Meter

The probe for the CS meter was located in the head box of the spillway throughout the testing. The probe was placed in a stilling well so that the probe would be sufficiently secured and so that it could be removed easily for inspection and cleaning. The stilling well was three inches in diameter and made of PVC pipe. It had four slots measuring 1 inch wide by 5.5 inches long, equally spaced around the circumference of the pipe. These slots were made to replicate the openings in the probe itself and to allow water to flow through freely. The stilling well was secured to the right transition wall (looking downstream), 1.35 feet upstream of the weir. It was placed here so that it would be in the flow of the water passing over the crest without significantly disturbing the flow patterns around it. The exact dimensions and location of the stilling well for the CS probe can be found in Figure 3-11.

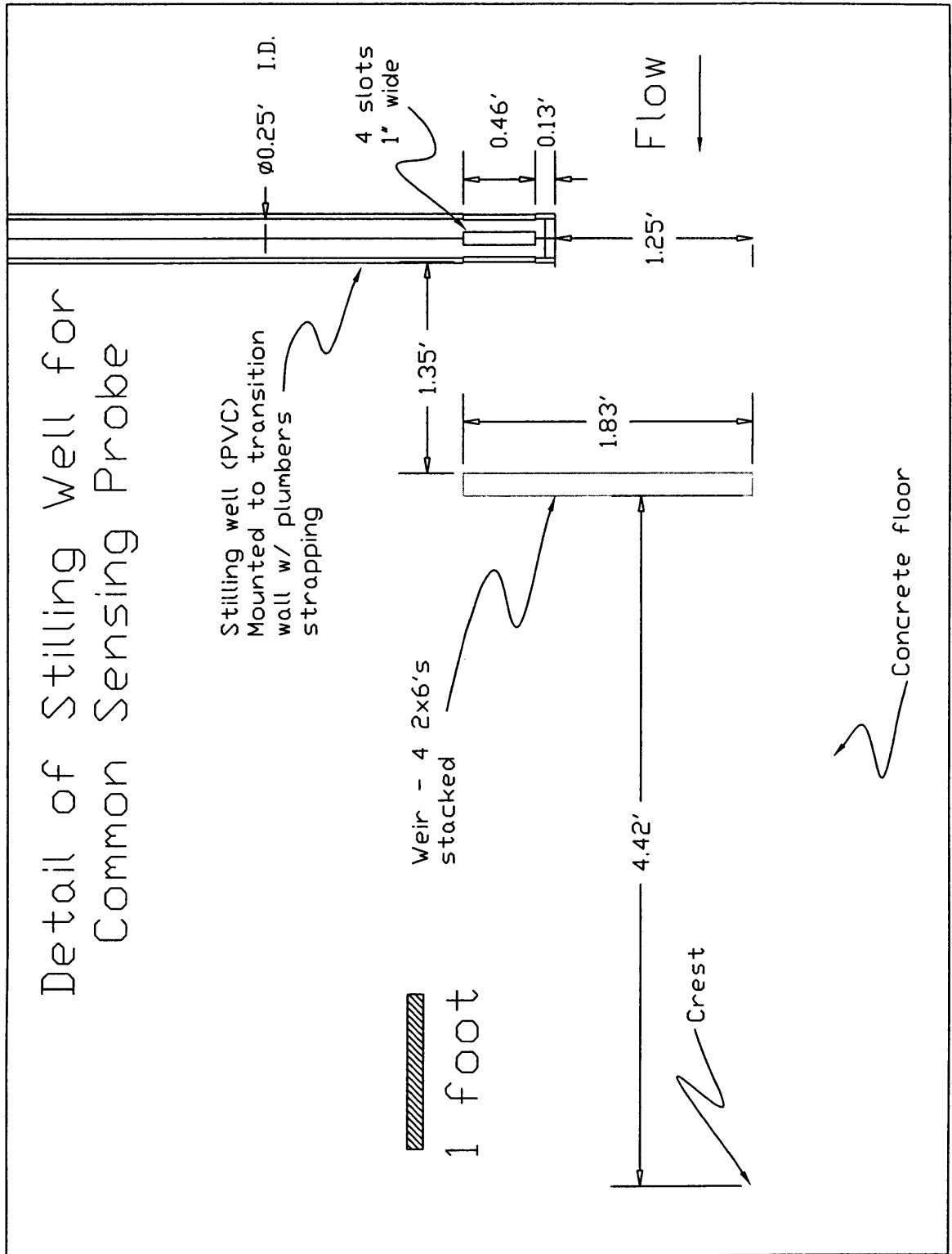


Figure 3-11– Detail of Stilling Well for Common Sensing Probe

3.3.5 Configuration of Sweeney Aquametric Meter

The configuration of the SA meter was a large source of frustration during this project. After two months of data collection, circumstances dictated that the original configuration of the meter be altered. As could be expected with any water quality sampling, changing the configuration led to differences in the data. This section contains a description of the original configuration of the SA meter, the reasons for changing the configuration, and a description of the altered configuration. A discussion of the discrepancies in the data produced by the two configurations is found in Chapter Four.

Originally, the SA probe was placed inside a venturi assembly made by Sweeney Aquametric. The venturi assembly consisted of a steel casing designed with openings at each end so that water could flow through freely. Figure 3-12 is a photograph of the venturi assembly. Notice the opening in the side where the probe slides in as well as the openings in the top and bottom where water can flow through.

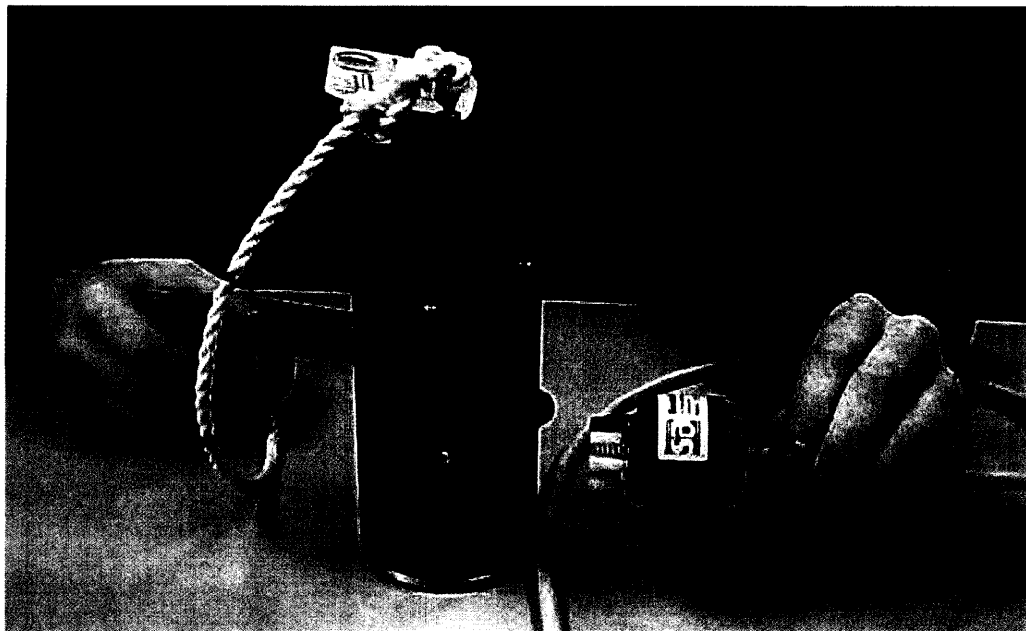


Figure 3-12– Venturi assembly with Sweeney Aquametric probe

The venturi assembly was attached to a movable point gage to secure the probe and the venturi assembly in the flow. The venturi assembly was attached to the point gage via a steel mounting bracket that was bolted directly to the arm of the point gage. The point gage was positioned so that the probe itself was located three inches directly above the tip of the step. The venturi assembly was positioned so that it was perpendicular to the flow with the opening for the probe facing downstream so that probe would be protected from any particles in the water. Figure 3-13 shows the venturi assembly holding the probe and mounted onto the point gage. The photograph was taken looking downstream. Also visible in the photograph is the air concentration probe and the Pitot-static used in the concurrent study on energy dissipation (Ward 2000).

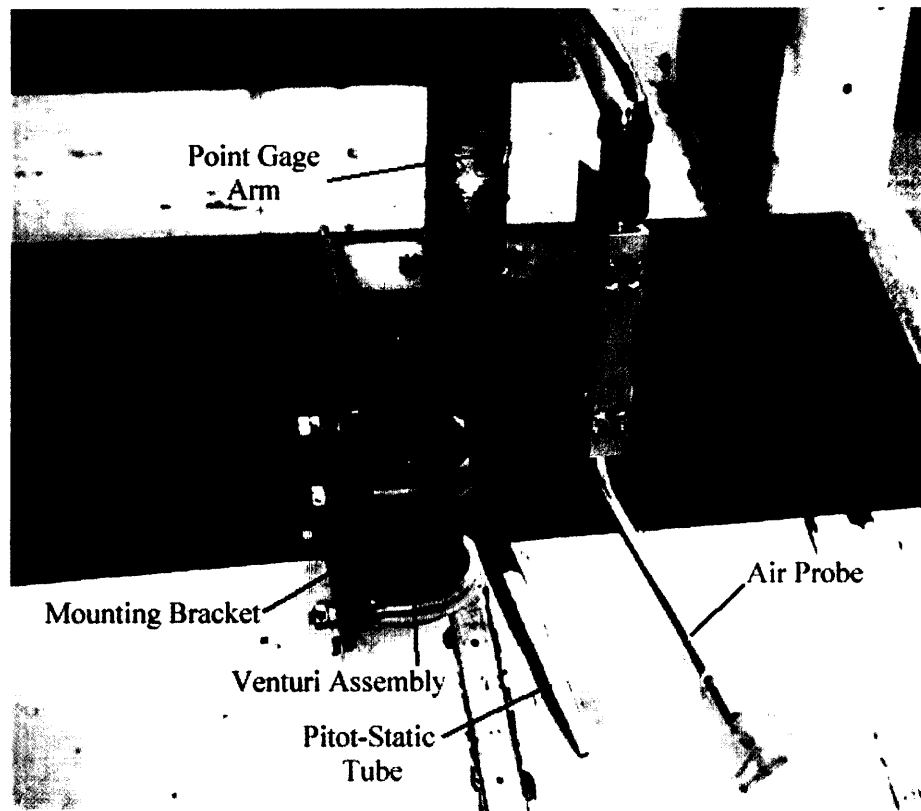


Figure 3-13 – Venturi assembly mounted on point gage

An extensive data set totaling 180 data points was collected using the point gage configuration just described. However, the data set was by no means complete when problems arose with the probe. Due to the extremely high velocity and turbulence of the water at the bottom of the spillway, the silicone tubing in the gas collector of the probe tore on two different occasions within a matter of a few weeks. Each time this occurred, the probe had to be sent back to the manufacturer for repair and calibration. Considering the time (about one week) and expense (about \$350) involved with repairing the meter, it became apparent that the configuration had to be altered so that the probe would be better protected from the high velocities and turbulence. The manufacturer of the meter recommended that the probe be placed in a stilling well without the use of the venturi assembly. The manufacturer explained that while the venturi assembly would protect the probe from particles in the water, it was designed to be used in still water conditions to increase the velocity of flow over the gas collector. Therefore, the venturi assembly itself may have been causing the damage to the probe. (Sweeney, J. 2000)

Several options for a stilling well for the SA probe were explored. While the ideal situation may have been to place the stilling well in the center of the flume, there was no feasible way to secure the stilling well in the middle of the flume. Therefore, it was decided that the stilling well would be located on the side of the flume so that it could be attached to the wall of the flume. The stilling wells were made of 6-inch PVC pipes. The pipes were sawed in half lengthwise with the concave side facing the flume wall. This enabled the flow patterns through the stilling wells to be observed using the Plexiglas window located at station two. Several stilling wells with various modifications of hole locations and sizes were tested to determine which variation most

Detail of Stilling Well for Sweeney Aquametric Probe

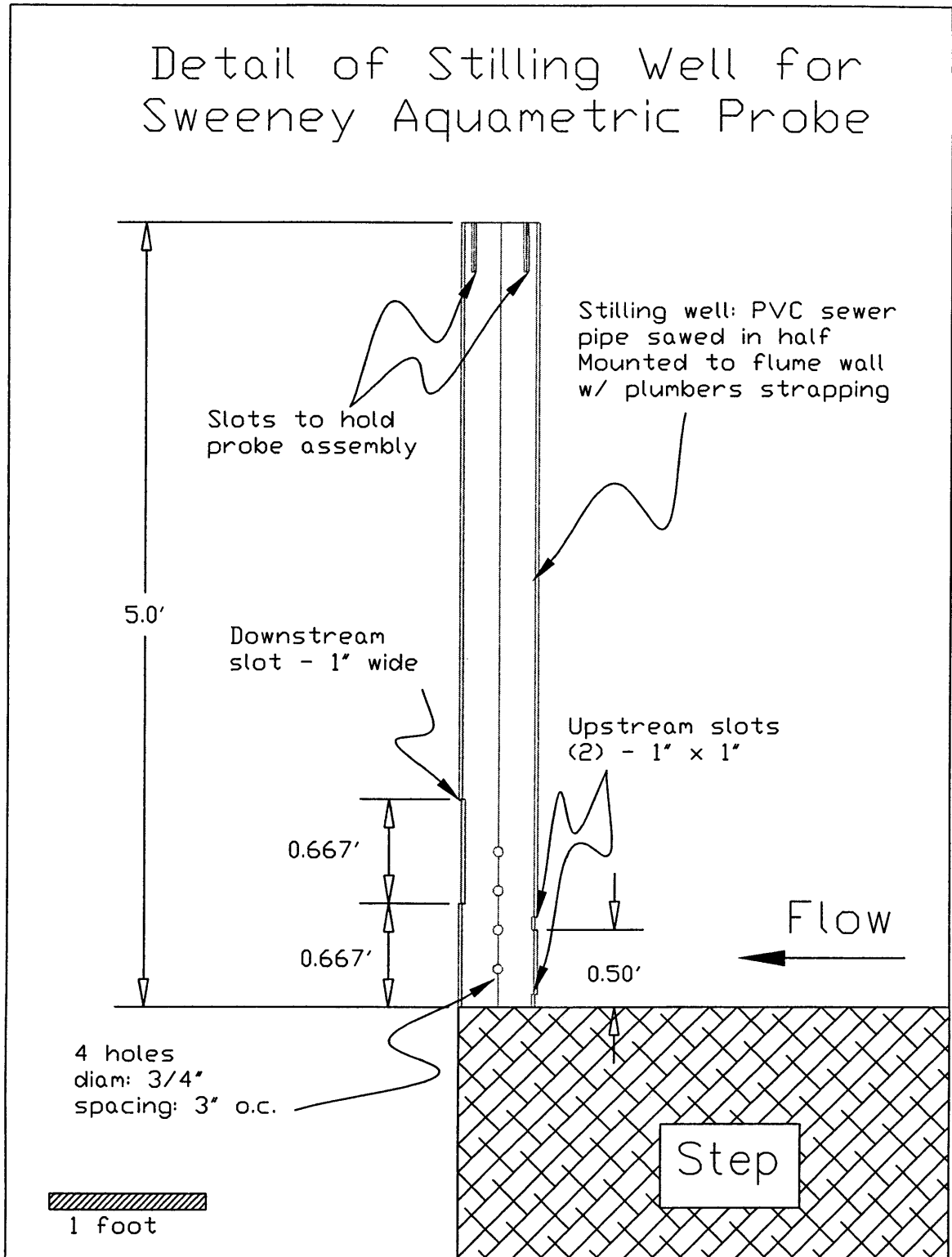


Figure 3-14- Detail of stilling well for SA probe

replicated the data taken on the point gage and at the same time produced a desirable flow pattern. While the data from the point gage could not be replicated exactly, several variations produced data that was very similar while also producing flow patterns that provided sufficient exchange of water without causing excessive turbulence within the stilling well. The details for the final stilling well design used for stations one, two, and three are found in Figure 3-14. The final design placed the downstream end of the stilling well at the tip of the step being analyzed. Two square holes measuring one inch by one inch were cut in the upstream side of the stilling well to allow flow to enter. One hole was located all the way at the bottom of the stilling well while the other was located six inches above the base of the stilling well. Water was allowed to flow out of the stilling well through a one-inch by eight-inch slot on the downstream side. The bottom of this slot was located eight inches above the base of the stilling well so that the stilling well would remain full during testing. Additionally, four circular holes measuring three fourths of an inch in diameter were located on the side parallel to the flow. These holes were spaced three inches apart on center.

The SA probe was attached to a rod made of a half-inch diameter PVC pipe with metal hooks at the top. The probe was lowered into the stilling well on the rod until the hooks on the rod rested in the slots cut in the top of the stilling well. The slots were cut $3\frac{3}{4}$ inches deep so that the probe would be located at the same depth as it was when it was mounted on the point gage. The hooks and slots also helped to stabilize the rod and the probe so that they were not banged around as much by the flow. Figure 3-15 is a photograph showing the rod and probe inside the stilling well at station two. Figure 3-16 is a photograph showing the flow patterns through the stilling well.



Figure 3-15– Flow pattern through stilling well at station two



Figure 3-16– Flow pattern through stilling well at station two

3.3.6 Testing Protocol

The key to any successful testing protocol is consistency. For this reason, every effort was made to be consistent with regard to methods of operation and data collection. At the start of each day of testing before any water was turned on, both meters were compared to each other to determine whether they were accurately reporting barometric pressure, temperature, ΔP , and TGP%. After it was determined that the meters were functioning properly, the flow of water to the head box was started by opening a valve in the pipeline. After the flow was started, another valve located approximately 40 feet from the head box was closed slightly to ensure that there was enough pressure in the line to create supersaturated water. This valve was adjusted to produce eight to ten pounds per square inch of pressure in the pipeline just upstream of the valve. Once the flow of water was started, the nitrogen tank was opened to begin injecting the nitrogen gas into the pipeline.

After the flow of water and nitrogen were started, there was a long delay before the first reading could be taken. This delay was the result of three main factors. The first factor was the large distance from the nitrogen injection point to the head box. The large distance created a long travel time for the nitrogen to reach the head box. For example, at a flow rate of 20 cubic feet per second the velocity of the water in the three-foot diameter pipeline would be 2.83 feet per second. At this velocity, it would take the water approximately 9 minutes to travel the 1,500 feet from the injection point to the head box. The second factor was that upon reaching the head box, the supersaturated water would have to mix with the water already in the head box. Since the head box is 20 feet square and the water could be four feet deep or more, there was a significant amount of water

that had to be mixed before the readings produced by the meters would stabilize. The final factor causing the delay was the slow response times of the meters. Once the dissolved gas concentration of the water changed, it took time for the gasses to pass in and out of the silicone tube gas-collector. According to the protocol used by the US Army Corps of Engineers, this process can take up to 30 minutes depending on how much the dissolved gas levels change (Ruffing et al. 1996). These three factors added up to create a delay anywhere from 20 minutes to one hour depending on dissolved gas concentration and flow rate.

This delay could be seen by watching the response of the meter in the headbox. The meter would start out close to the TGP% of the reservoir, which was usually between 92% and 98%. Once the nitrogen flow was started, it would take several minutes before the meter changed at all. Then it would begin to climb quickly until it got closer to the actual reading at which time it would slow and approach the actual reading asymptotically. In order to have a set criterion to determine when the reading could be considered accurate, the protocol of the US Army Corps of Engineers was again employed. Their protocol states that “total pressure readings that stabilized for two minutes were considered equilibrated” (Ruffing et al. 1996). Because readings had to be taken in the head box and on the slope at the same time, the TGP% readings of both meters had to stabilize for two minutes simultaneously to be considered equilibrated. After a measurement was stabilized at one station, the measurements were recorded and the SA meter was moved to the next station. This second reading could usually be obtained within about 10 minutes because the head box was already mixed so the only factor causing a delay was the response time of the meter. This procedure was repeated

until a measurement was taken at each station. Next the flow of water and/or nitrogen was altered slightly and the process was repeated until three to five data points were recorded at each station for each scenario.

Chapter Four

DATA ANALYSIS AND RESULTS

4.1 Transfer Efficiency

The purpose of the data taken in this study was to determine the change in dissolve gas concentrations between two points on the spillway. Knowing that the transfer efficiency is a function of the concentration of dissolved gas at two different points, this data could be used to determine the transfer efficiency for different conditions on the spillway. The data was analyzed to determine how the transfer efficiency was affected by changes in the four major independent variables of this experiment. The four major variables for this experiment were the step height, flow rate, location along the slope (or vertical drop), and the concentration of dissolved gas in the head box. Using graphical and numerical methods to analyze the data led to several important conclusions about the transfer efficiency as well as the behavior of dissolved gasses along the spillway.

4.1.1 Equation Derivation

Recalling the definition of the transfer efficiency from Chapter Two, the transfer efficiency is a function of the concentration of dissolved gas upstream, downstream, and at saturation. The transfer efficiency is derived by taking the discrete integral of the basic transfer equation derived from Fick's Law. The definition of the transfer efficiency shown below is found in Chapter Two as equation 2-13.

$$E = \frac{TGP\%_{DS} - TGP\%_{US}}{TGP\%_S - TGP\%_{US}} \quad (4-1)$$

If it is assumed that the downstream reading is dependent upon the upstream reading, then $TGP\%_{DS}$ becomes the dependent variable and $TGP\%_{US}$ becomes the independent variable. Thus, equation 4-1 can be rearranged as follows:

$$E(TGP\%_S - TGP\%_{US}) = TGP\%_{DS} - TGP\%_{US} \quad (4-2)$$

$$TGP\%_{DS} = E * TGP\%_S - E * TGP\%_{US} + TGP\%_{US} \quad (4-3)$$

$$TGP\%_{DS} = (1 - E)TGP\%_{US} + E * TGP\%_S \quad (4-4)$$

Equation 4-4 suggests that the downstream reading (station 1, 2, 3, or TB) is a function of the upstream reading (station HB), the transfer efficiency, and the saturation concentration which is assumed to be approximately 100%.

4.1.2 Variation with Respect to $TGP\%_{US}$

In order to determine how the transfer efficiency varied with the upstream reading (station HB), the data was plotted as an x-y scatter plot. One data point was plotted for each simultaneous reading between the head box and the slope. Each data point was plotted with the head box reading as the abscissa and the reading from the slope or tail box as the ordinate. The data was segregated into data groups by flow rate, location, and step size so that the upstream concentration variable could be isolated. Once the data was plotted, it was qualitatively examined to determine how the transfer efficiency changed as

the reading in the head box changed. An example of this data plot for all flow rates at station 1 with the 1-foot steps is shown below in Figure 4-1.

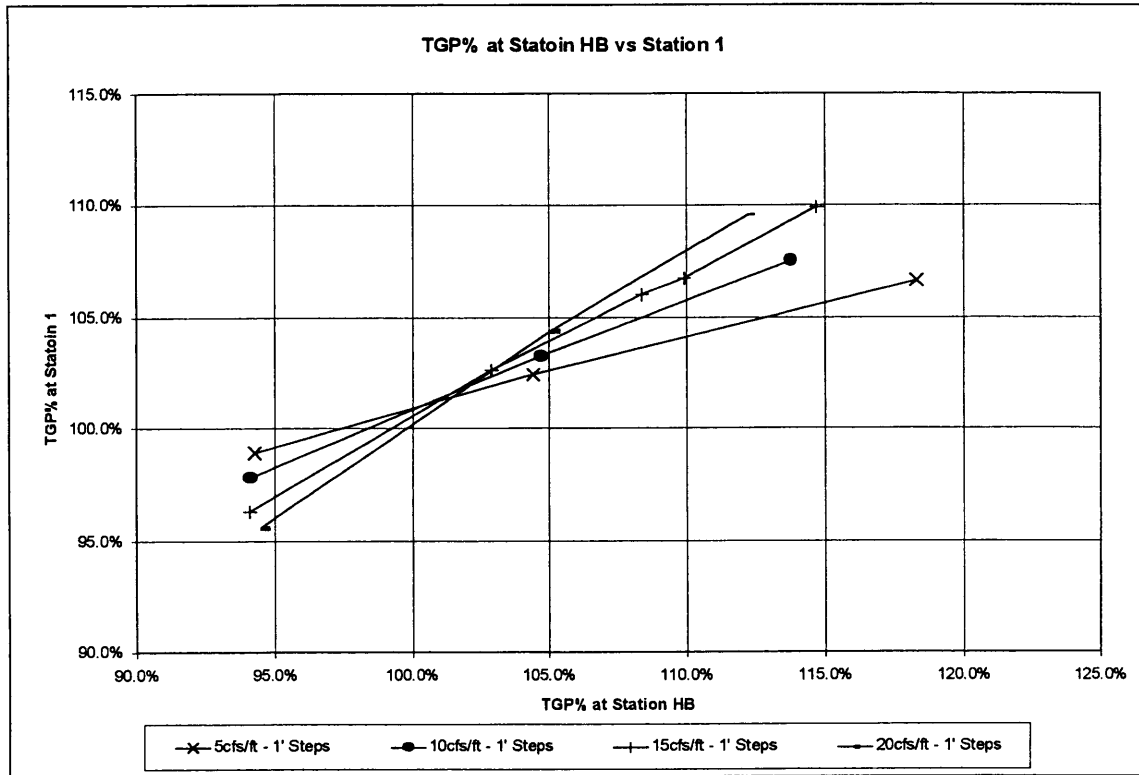


Figure 4-1 – Example data plot of TGP% HB vs. Station 1

As can be seen in Figure 4-1, the data plots quickly revealed that for a given location, step height, and flow rate, the data was approximately linear. This linear relationship of the data was seen at every location, step height, and flow rate. Additionally, the scatter associated with the data points was extremely small. (See Appendix B for the complete set of data plots showing this linear relationship along with the small scatter of the data points.) The implication of this observation is that since the data is linear, the transfer efficiency must be constant for all values of the upstream concentration at any given location, step height and flow rate. Furthermore, equation 4-4

indicates that both the slope and the y-intercept of the equation are defined by the efficiency. Recall equation 4-4 shown below:

$$\text{TGP}\%_{\text{DS}} = (1 - E)\text{TGP}\%_{\text{US}} + E * \text{TGP}\%_{\text{S}} \quad (4-4)$$

The slope of this equation is defined as one minus the transfer efficiency (1 – E) while the y-intercept is defined as the product of the transfer efficiency and the saturation concentration (E*TGP%_S).

4.1.3 Calculation Method

The exact value of the transfer coefficient was determined by acquiring the slope and y-intercept of the data using Microsoft Excel's linear regression feature. This method provided two ways that the transfer efficiency could be calculated; using either the slope or the y-intercept. A table listing the slope and y-intercept for each scenario is found in Appendix C. The transfer efficiency was calculated from the slope by taking one minus the slope. The transfer efficiency was calculated from the y-intercept by assuming that the saturation concentration (TGP%_S) was equal to 100% so that the y-intercept was equal to the transfer efficiency. The latter method will be referred to as E' to avoid confusion.

$$E = 1 - \text{slope} \quad (4-5)$$

or

$$E' = y - \text{intercept} \quad (4-6)$$

Theoretically, each method should have produced identical results. However, E' was consistently 0.1% to 1.7% higher than E. Although this discrepancy is rather small,

it deserves an explanation. The most likely reason that E' was slightly higher is the assumption that the saturation concentration ($TGP\%_s$) was 100%. Since the y-intercept was equal to the transfer efficiency times $TGP\%_s$, a slightly higher saturation level would result in a slightly higher E' . This phenomenon of having saturation level greater than 100% was observed during the experiment. It is known that water flowing down an aerated spillway will always tend to approach the saturation level. In this experiment however, the $TGP\%$ readings at the bottom of the spillway in the tail box always tended to be slightly higher than 100%. Readings typically ranged from 101.0% to 102.0% in the tail box with a mean value of 101.5%. It could be argued that the spillway was simply not long enough to bring the water back to saturation. However, $TGP\%$ greater than 101.0% were typically recorded in the tail box even when the $TGP\%$ in the head box was much less than 100.0%. This means that the $TGP\%$ of the water crossed over 100% at some point before reaching the tail box. Exploration of the reason for this observed phenomenon was outside of the scope of this project; however, possible explanations include the high velocity of flow, extreme turbulence in the flow, inaccuracies in the meter, and air entrainment. Figure 4-2 shows how the saturation level observed in the tail box was skewed positively by plotting the number of occurrences for each measured value from 100.0% to 102.5%.

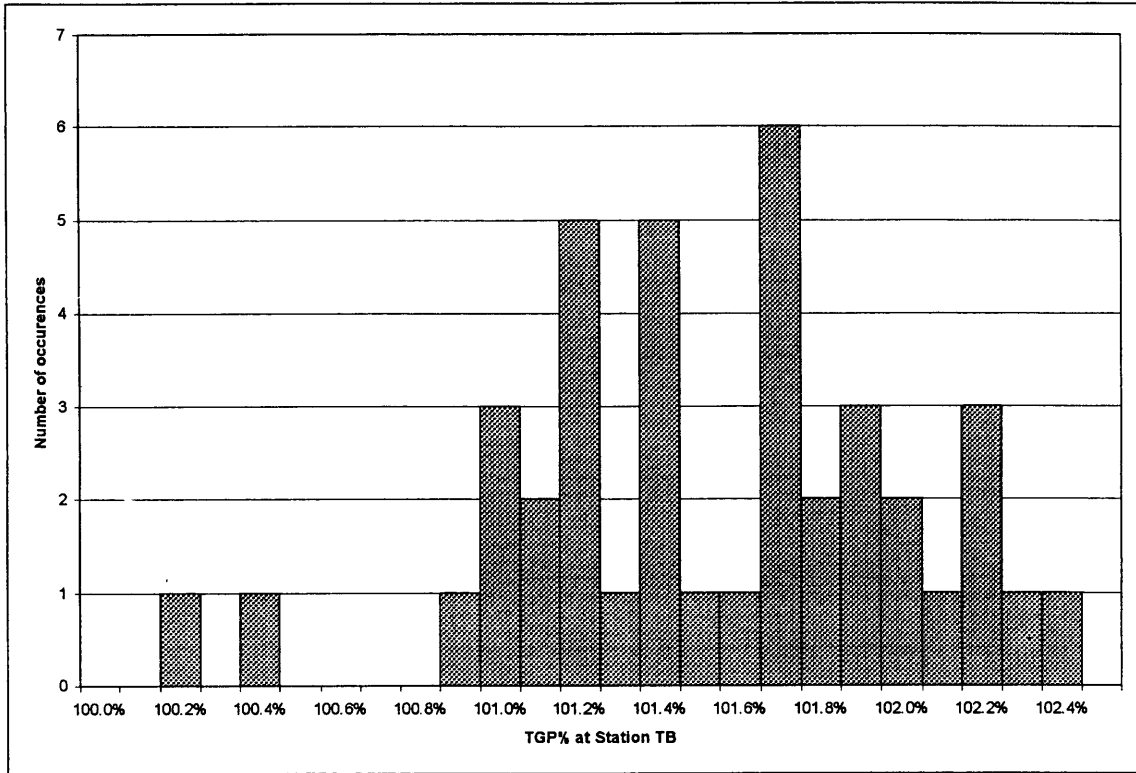


Figure 4-2 - Positive skew in saturation level

The observation of this phenomenon, coupled with the observation that E' was always slightly larger than E , indicates that E , as calculated from the slope, is the correct value for the transfer efficiency. Therefore, future references to the transfer efficiency will be to E and not E' .

4.1.4 Results

A transfer efficiency was calculated for each location and scenario using the slopes of the data plots (found in Appendix C) and equation 4-5. Table 4-1 contains the values for the transfer efficiencies for each scenario and location.

Table 4-1 - Tabulation of transfer efficiencies (E) for each scenario and location

Scenario	1	2	3	4	5	6	7	8	9	10	11	12
h_{step} (ft)	2	2	2	2	1	1	1	1	0	0	0	0
Flow (cfs/ft)	5	10	15	20	5	10	15	20	5	10	15	20
E at Sta. 1	0.723	0.559	0.452	0.363	0.680	0.507	0.344	0.211	0.505	-	0.044	-
E at Sta. 2	0.927	0.857	0.800	0.741	0.922	0.821	0.749	0.660	0.867	0.697	0.395	-
E at Sta. 3	0.988	0.962	0.947	0.928	0.978	0.937	0.926	0.909	0.943	0.783	0.581	-
E at Sta. TB	0.988	0.980	0.986	0.972	0.991	0.965	0.964	0.960	0.963	0.912	0.880	-

As stated in Chapter Two, transfer efficiency typically ranges from zero to one under normal conditions. A larger transfer efficiency indicates a larger amount of aeration or degassing of the flow which is typically more desirable. While the relationship of transfer efficiency to variables such as step height, flow rate, and vertical drop are considered in further detail later in this chapter, important qualitative observations can be made by looking at the data in Table 4-1. First, and not surprisingly, the transfer efficiency increases as the vertical drop increases. (Sta. 1 is near the tope of the spillway and Sta. TB is in the tail box of the spillway.) Second, as the flow rate increases, the spillway loses transfer efficiency. This can be attributed to the fact that the specific surface area (a) is larger at smaller flow rates because of the higher air to water volume ratio. Lastly, the results reveal that the 2-foot steps were the most efficient while the smooth slope was the least efficient. This too can be attributed to the increased specific surface area (a) that the larger steps provide.

4.1.5 Error analysis

Because no other comparable data sets were found, the calculated transfer efficiencies could not be compared to established values for error analysis. Therefore,

the accuracy of the data was difficult to assess. The precision of the data, however, was easily determined by quantitatively examining the scatter of the data using the R^2 values. An R^2 valued was calculated for each data group in the plots of TGP% in the head box versus the TGP% along the slope or in the tail box. (See Appendix B for plots) Analysis of the R^2 values indicated that there was in fact very little scatter in the data and thus the data was very precise. Table 4-2 shows the R^2 values for each data grouping, along with the number of data points included in that grouping.

Table 4-3 - R^2 values for TGP% at station HB vs. station 1, 2, 3, and TB plots

Scenario	1	2	3	4	5	6	7	8	9	10	11	12
h_{step} (ft)	2	2	2	2	1	1	1	1	0	0	0	0
Flow (cfs/ft)	5	10	15	20	5	10	15	20	5	10	15	20
Sta1 R^2	0.992	0.998	1.000	0.997	0.999	1.000	0.998	0.999	-	-	1.000	-
Sta1 # pts	4	4	4	3	3	3	5	3	2	1	3	1
Sta2 R^2	0.998	0.999	0.998	1.000	0.993	0.996	0.994	0.999	-	1.000	1.000	-
Sta2 # pts	3	3	4	3	3	5	5	3	2	3	4	1
Sta3 R^2	0.986	1.000	0.997	1.000	0.953	0.992	0.819	0.999	-	0.992	1.000	-
Sta3 # pts	3	3	4	3	3	3	5	3	2	3	4	1
StaTB R^2	0.645	0.708	0.700	0.322	0.987	0.757	0.618	0.906	-	0.978	-	-
StaTB # pts	4	4	4	4	3	3	7	3	2	4	2	0

As can be seen from the Table 4-3, the R^2 values of the data groups, and thus the precision of the data, was very good. The mean R^2 value for all of the different data groups was 0.938. The measurements taken in the tail box show the least amount of precision. This is most likely due to the water in the tail box not being completely homogenous. While the R^2 values for the tail box are low in comparison to the other stations, the data is still precise enough to meet the objectives of the experiment. Figure

4-2 further demonstrated the precision of the data in the tail box. It showed that while the data may have been slightly scattered in the tail box, the overall range of the measurements was relatively small with respect to the precision of the meters. This figure showed that measurements in the tail box ranged from 101.0% to 102.4% for all scenarios. Thus, while the R^2 values are slightly low, the precision of the data is still acceptable.

4.1.6 Relationship to Vertical Drop, Flow Rate, and Step Height

As discussed briefly in “Results,” there was a definite correlation between the transfer efficiency, and the three variables vertical drop, flow rate, and step height. This section provides graphical representations of these relationships as well as equations that can be used to predict transfer efficiency under specific conditions. It is important to note that the predictive equations presented here are only applicable to structures possessing identical geometry to the model used in this study. The equations can not be extrapolated to predict efficiencies for other structures of different slope, scale, step height, etc.

As expected, the transfer efficiency increased as the vertical drop increased. Thus, the longer the spillway, the more efficient it will be at transferring gasses. Figure 4-3 is a plot of the transfer efficiency versus the vertical drop. Each step height and flow rate display similar behavior; the transfer efficiency increases as vertical drop increases and asymptotically approaches a transfer efficiency of 1.0 at the bottom of the spillway. This asymptotic trend confirms the fact that once saturation has been achieved, increased spillway length or vertical drop will have no effect on the transfer.

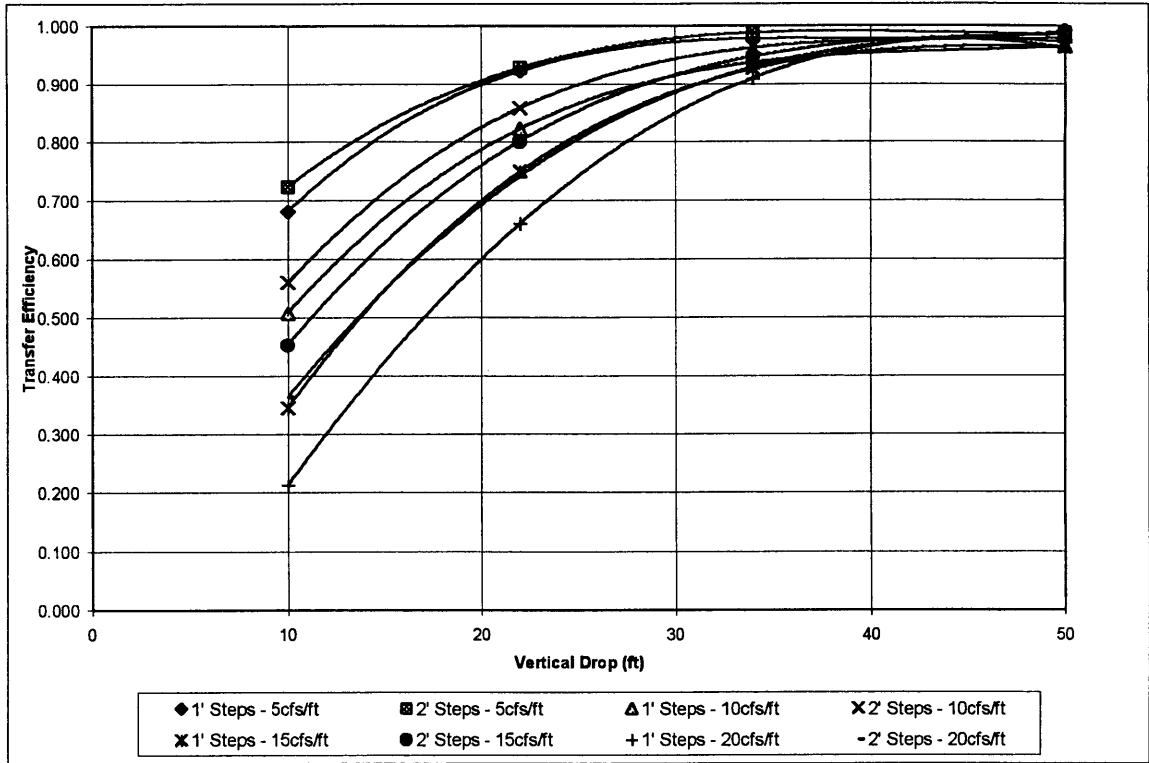


Figure 4-3- Transfer efficiency as a function of vertical drop

The curves in Figure 4-3 were best approximated using a third order polynomial. An equation was derived for each curve using Microsoft Excel's polynomial regression feature. Although the cubic functions are not very convenient to work with, they provide accurate predictions of the transfer efficiency when the step height, flow rate, and vertical drop are known. Table 4-4 displays the equations derived for each curve. Because there were only four points for each curve, the R^2 value for each equation was one.

Table 4-4– Transfer efficiency as a function of vertical drop equations

Flow(cfs/ft)	h_{step} (ft)	Equation
5	2	$E = 8 \times 10^{-6}(\text{VD})^3 - 0.001 (\text{VD})^2 + .0432(\text{VD}) + 0.3847$
5	1	$E = 1 \times 10^{-5}(\text{VD})^3 - 0.0015(\text{VD})^2 + .0572(\text{VD}) + 0.2431$
10	2	$E = 1 \times 10^{-5}(\text{VD})^3 - 0.0013(\text{VD})^2 + .0595(\text{VD}) + 0.087$
10	1	$E = 1 \times 10^{-5}(\text{VD})^3 - 0.0014(\text{VD})^2 + .0617(\text{VD}) + 0.0167$
15	2	$E = 9 \times 10^{-6}(\text{VD})^3 - 0.0013(\text{VD})^2 + .0628(\text{VD}) - 0.0568$
15	1	$E = 9 \times 10^{-6}(\text{VD})^3 - 0.0014(\text{VD})^2 + .0704(\text{VD}) - 0.2324$
20	2	$E = 5 \times 10^{-6}(\text{VD})^3 - 0.001 (\text{VD})^2 + .0593(\text{VD}) - 0.1358$
20	1	$E = 2 \times 10^{-6}(\text{VD})^3 - 0.0008(\text{VD})^2 + .0616(\text{VD}) - 0.3264$

Note: VD = vertical drop in feet

There was also a strong correlation between the transfer efficiency and the flow rate. As the flow rate increased, the transfer efficiency decreased as anticipated. The interesting aspect of this relationship was that for every station and step height, the transfer efficiency decreased in approximately a linear manner. In fact, each line was approximated quite accurately using a linear regression. Figure 4-4 displays this linear trend with the transfer efficiency plotted as a function of the unit discharge.

It is interesting to note that the lines are paired according to their location. The line for the 2-foot steps at station one is near the line for the 1-foot steps at station one. This same pattern exists for every other station as well. This suggests that the location (or vertical drop) had a much larger influence over the efficiency than the step height did. The fact that the lines grow closer together at the top of the plot represents the asymptotic trend seen in Figure 4-3. As the water moves further down the spillway and approaches saturation, the location will have less and less of an impact on transfer efficiency.

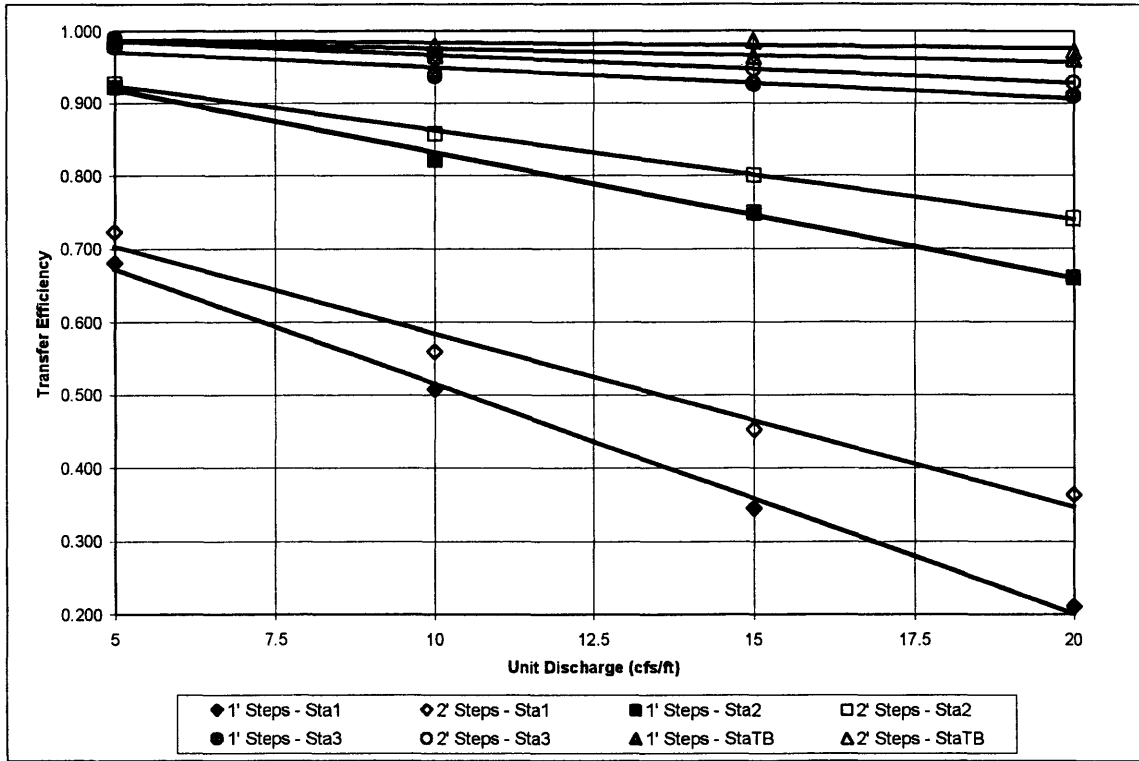


Figure 4-4- Transfer efficiency as a function of unit discharge

Predictive equations were derived from Figure 4-4 using Excel's linear regression function. The equations along with their respective R^2 values are found in Table 4-5.

Table 4-5– Transfer efficiency as a function of unit discharge equations

Station	h_{step} (ft)	Equation	R^2
TB	2	$E = -0.000798 (q) + 0.991$	0.556
TB	1	$E = -0.001876 (q) + 0.994$	0.735
3	2	$E = -0.003914 (q) + 1.005$	0.988
3	1	$E = -0.00436 (q) + 0.992$	0.916
2	2	$E = -0.01233 (q) + 0.986$	0.998
2	1	$E = -0.017184 (q) + 1.003$	0.997
1	2	$E = -0.02375 (q) + 0.821$	0.980
1	1	$E = -0.03141 (q) + 0.828$	0.997

The last relationship to be examined is that of transfer efficiency to step height. While the data revealed a definite correlation between step height and transfer efficiency, the influence of step height was not as large as was expected. Of the three variables examined in this section, step height was found to be the least significant in changing efficiency. Figure 4-5 is a plot of the transfer efficiency as a function of the smooth slope, 1-foot steps and 2-foot steps.

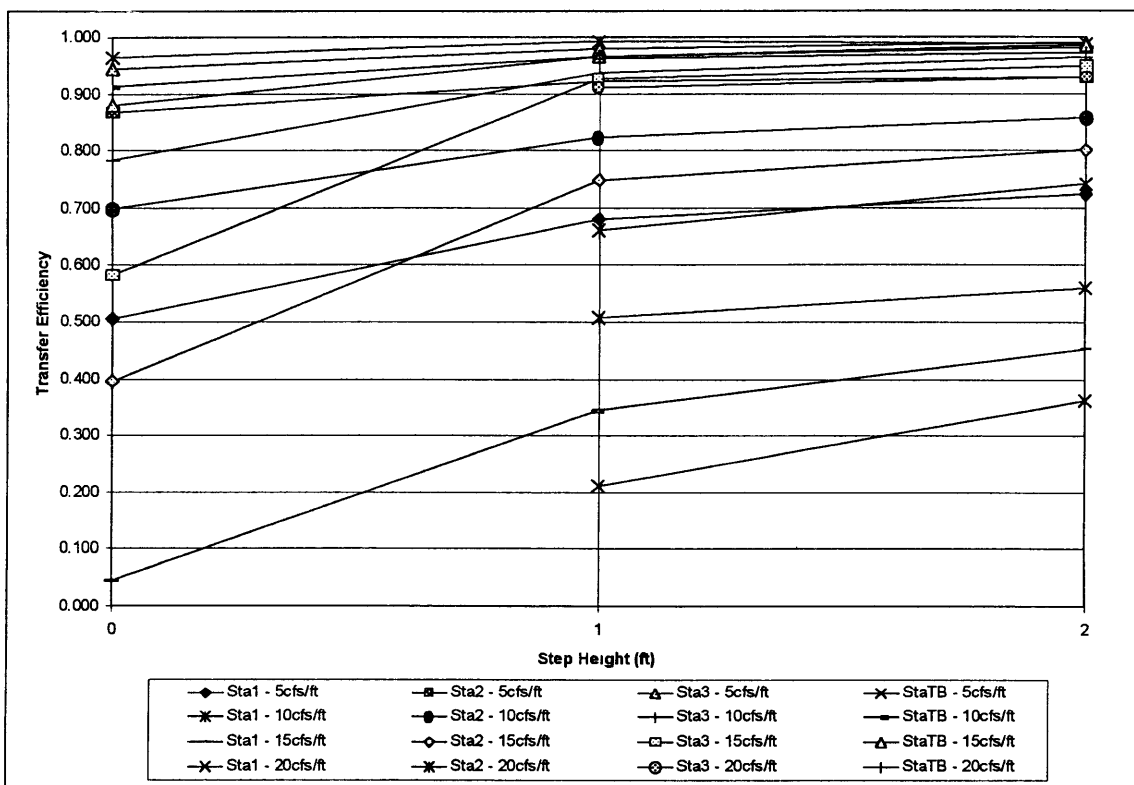


Figure 4-5 - Transfer efficiency as a function of step height

Due to the limited number of step heights tested and the fact that the data did not fit a continuous function, no predictive equations were developed to describe the relationship between transfer efficiency and step height. However, several qualitative conclusions can be drawn from Figure 4-5. Most importantly, there is a larger difference between the

smooth slope and the 1-foot steps than there is between the 1-foot and 2-foot steps. This is easily observed by noticing the steeper slope of the lines on the left side of the figure. In addition, it can be observed by the flatness of the lines between the 1-foot and 2-foot steps, that the change in step height did not significantly effect the transfer efficiency.

4.2 TGP% as a Function of Vertical Drop

The gas transfer on the spillway was also analyzed by plotting the TGP% as a function of the vertical drop from the head box. Due to the fact that the head box reading rarely remained stable long enough to acquire a reading at every location, the plots of TGP% as a function of vertical drop had to be derived by interpolating individual points. The interpolations were performed using the equations given in Appendix C. These equations were derived from linear regressions of the data plots of TGP% along the slope as a function of the TGP% reading in the headbox (found in Appendix B). Using these equations, the TGP% at every station and for every scenario could be calculated using a constant TGP% reading in the head box. Drawing a straight line between each location for a given scenario indicates the TGP% that could be expected at any point along the spillway for a given TGP% in the head box. Figures 4-6 and 4-7 show examples of these plots for head box readings of 115% and 90%. Additionally, Appendix D contains plots of the TGP% as a function of vertical drop for head box readings of 115%, 110%, 105%, 95% and 90%.

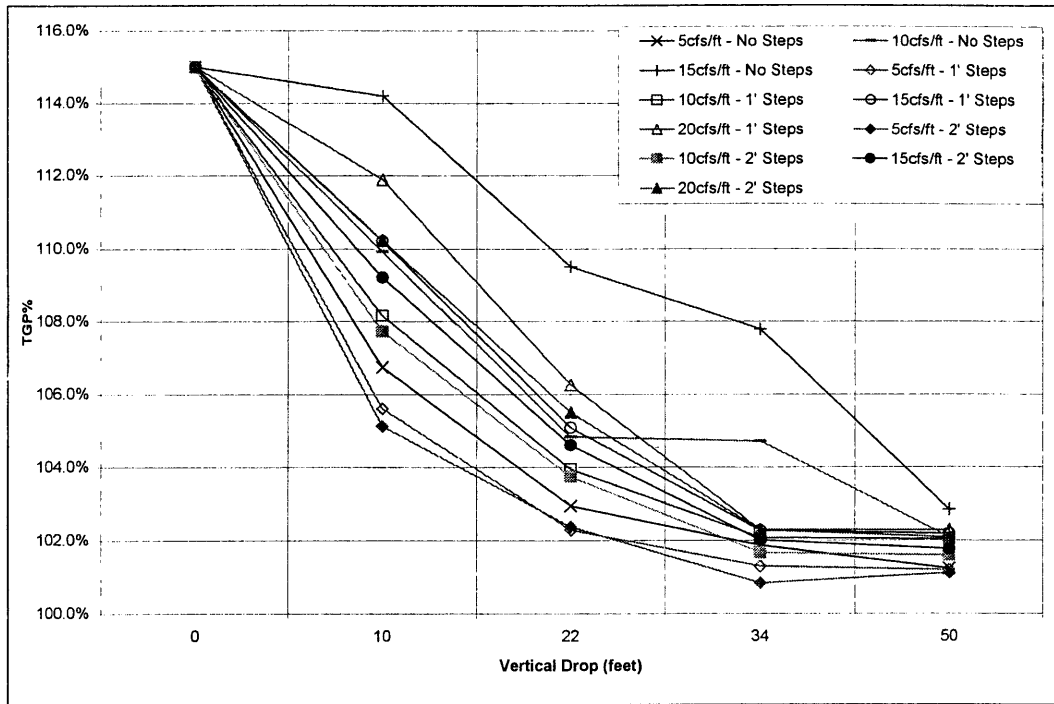


Figure 4-8- TGP% as a function of vertical drop; TGP% HB = 115%

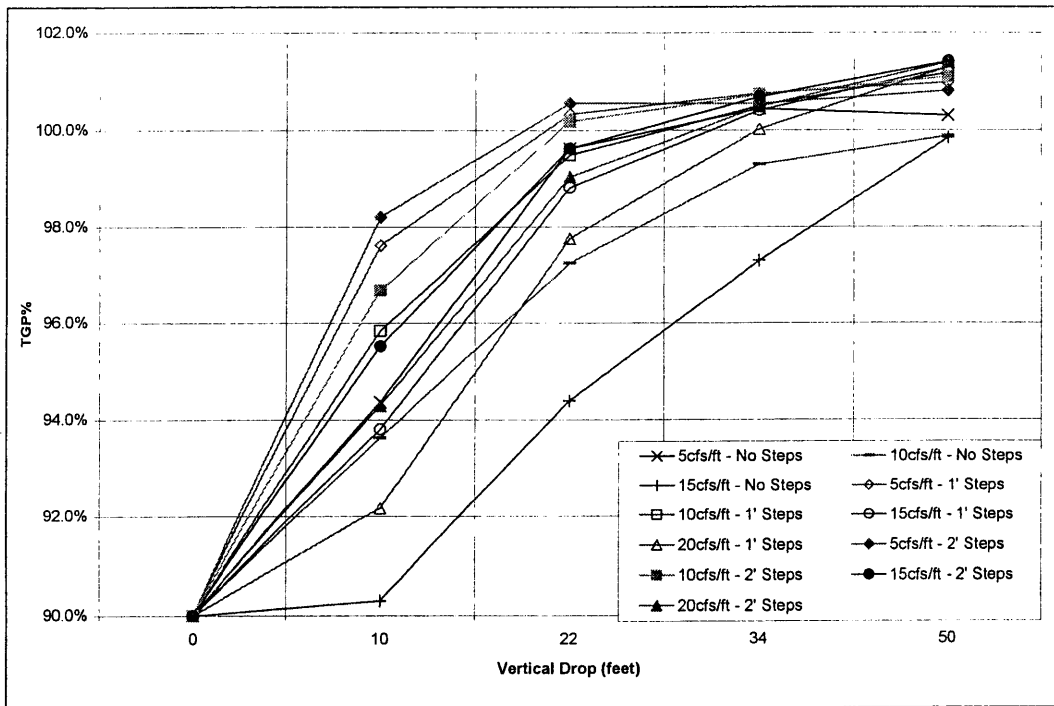


Figure 4-9- TGP% as a function of vertical drop; TGP% HB = 90%

4.3 Data Comparison for Point Gage and Stilling Wells

As mentioned in Chapter Three, the configuration of the SA meter had to be altered before a complete data set was acquired with the original configuration. Because of the differences in configurations, the two data sets could not be used together. Hence, all of the data analysis in this chapter was done using only the data for the second configuration, that is when the SA probe was in the stilling well configuration. Since the data set with the SA probe mounted on the point gage was incomplete, extensive data analysis was not possible. However, the two data sets were compared to determine the general differences in both trend and magnitude between the two data sets.

4.3.1 Trend Comparison

Based upon the limited amount of data available for the point gage configuration, the trend in the data appears to be the same as it was for the stilling well configuration. In both cases plotting the TGP% on the slope as a function of the TGP% in the head box reveals a linear relationship. This relationship was discussed in further detail in section 1.2 of this chapter. Figure 4-10 is an example of the linear relationship for the point gage data at station two.

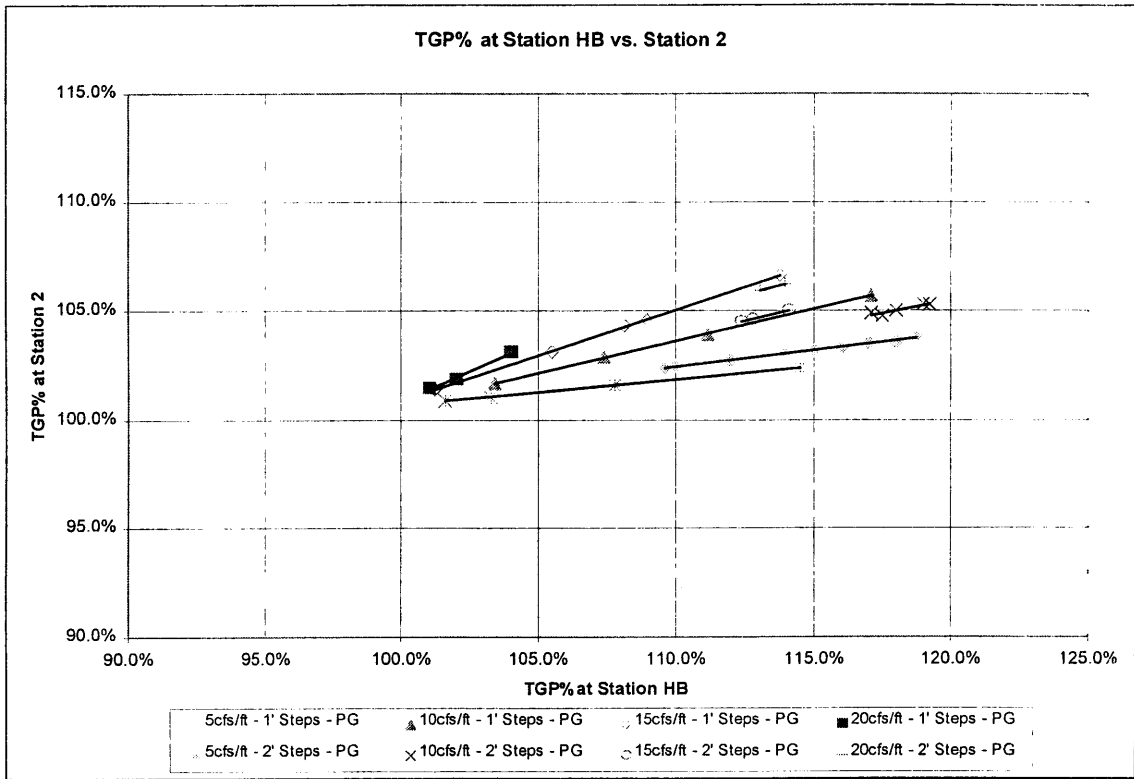


Figure 4-10- Example data plot of TGP% HB vs. Station 2 for point gage configuration

While the range of data taken with the point gage was not as large as it was with the stilling wells, there is in some cases, a higher concentration of data points. For example, nine data points were taken on the 2-foot steps at 5cfs/ft. All of these data points lie between 109% and 118% on the x-axis. Even with this concentration of data points however, Figure 4-10 shows very little scatter in the data. This reinforces the evidence that the data taken in both configurations was very precise.

4.3.2 Magnitude Comparison

Although the general trend observed between the two configurations was the same, the magnitude of individual data points between the two configurations was not. When the water was supersaturated, measurements made with the stilling wells tended to

be slightly lower than measurements made with the point gage for a given head box reading. When the water was less than saturated, the opposite was true; measurements taken with the point gage were slightly higher. This is observed graphically by noticing that the slope of the regression line for the stilling well measurements is slightly flatter than the slope for the point gage regression line in Figure 4-11.

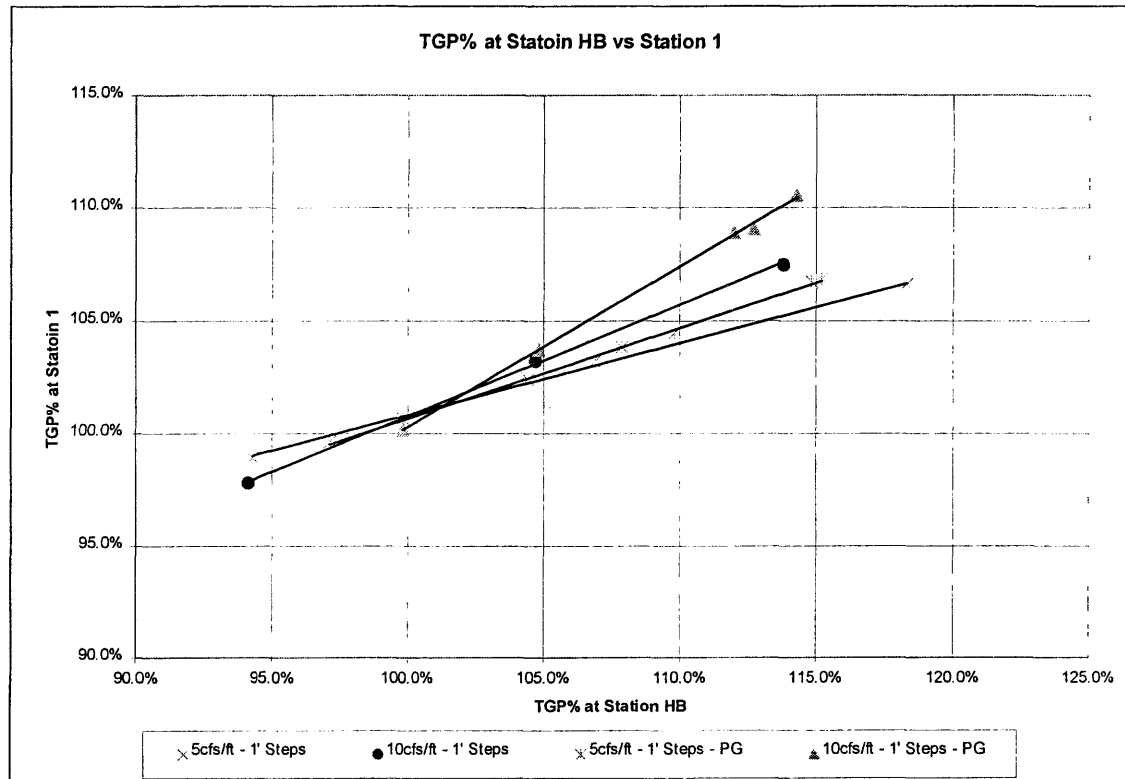


Figure 4-11- Example comparison of point gage data to stilling well data

Because the slope of the line is equal to one minus the transfer efficiency, the smaller slope of the stilling well data indicates that the stilling wells were measuring a slightly higher transfer efficiency than the point gage. The exact reason for this discrepancy is unknown, although, it is suspected that the configuration of the holes in the stilling wells was increasing the contact of the water with air, thereby increasing

efficiency. The difference between the two configurations was enough that the data sets could not be used together. However, in most cases, the two configurations were only about 1% to 2% different from each other. Considering how different the configurations were, the data sets were close enough that the small difference in data does not negate the validity of the results found using the stilling well data.

Chapter Five

SUMMARY, CONCLUSIONS, AND RECOMMENDATIONS

5.1 Summary

The need for a design that could increase low DO levels while at the same time reducing TDG was presented. Whenever dissolved gasses deviate greatly from the saturation concentration, environmental problems can ensue. Low DO levels, occurring naturally and artificially, can be detrimental to the aesthetics, drinking water quality, and aquatic habitat of water bodies. Additionally, TDG supersaturation, resulting from large spillway releases into deep stilling basins, can be lethal for many types of fish by causing gas bubble disease. Many endangered salmon species are especially at risk to contract gas bubble disease during their annual migration. The key to improving the water quality with regard to dissolved gasses is to improve the transfer efficiency so that the dissolved gas levels can return to saturation as quickly as possible. Theoretical equations as well as small-scale model studies have suggested that stepped spillways may be a viable solution to improving the dissolved gas quality of water.

Consequently, a prototype-scale model study was undertaken to evaluate the transfer efficiency of stepped spillways. Measurements of TDG were taken at the CSU/USBR DSOF with three different step configurations and at four different flow rates. Supersaturation was produced by injecting nitrogen gas into the pressurized pipeline supplying the spillway. Simultaneous measurements were taken for various

TGP% readings at the top of the spillway as well as at three locations along the spillway and in the tail box of the spillway.

These measurements provided a means by which transfer efficiencies were calculated. It was found that the transfer efficiency for any given scenario at any given location was always constant for all values of dissolved gas concentration in the head box of the spillway. Therefore, a single transfer efficiency was calculated for each scenario and at each location along the spillway. The calculated transfer efficiencies were evaluated in terms of their relationship to the following three variables: vertical drop, flow rate, and step height. Regression equations were presented to describe the relationship between transfer efficiency and vertical drop as well as transfer efficiency and flow rate. A graphical method for evaluating the transfer efficiency was also presented by using regression equations to plot the TGP% on the spillway as a function of the vertical drop.

5.2 Conclusions

The results revealed that the stepped spillways were more efficient at transferring dissolved gasses than the smooth spillway was. Additionally, the larger 2-foot steps produced higher transfer efficiencies than the smaller 1-foot steps. As expected the larger steps created more turbulence and aeration of the flow, thereby increasing the transfer efficiency. However, before stepped spillways can be justified as a viable option for improving water quality, the significance of the differences in transfer efficiency of different step heights must be examined. This is best done by comparing the influence of

step height on transfer efficiency with the influences of the other main variables, vertical drop and flow rate.

It was observed that on the 2H:1V slope used in this study, the vertical drop had a much larger influence on the transfer efficiency than the step height did. For example, after a vertical drop of 50-feet, the transfer efficiency at 5cfs/ft for the 2-foot steps was 0.988, while the smooth spillway transfer efficiency dropped to only 0.963. While this difference does show that the 2-foot steps were more efficient, at the bottom of the spillway this difference was almost negligible. The conclusion that can be drawn from this is that if the vertical drop of the spillway is large enough (greater than 50 feet for a 2H:1V slope), there will be little to no difference observed in the transfer efficiency of a stepped spillway versus a smooth spillway. For shorter spillways, however, the difference was much more noticeable. At a vertical drop of only 10 feet, the transfer efficiencies at 5cfs/ft for the 2-foot steps and the smooth spillway were 0.723 and 0.505 respectively. When the flow rate was 15cfs/ft the difference between steps and no steps was even larger. The 2-foot steps produced a transfer efficiency of 0.452, while the smooth spillway was an order of magnitude less at 0.044. Thus, while the steps may not produce noticeable benefits for a long spillway, shorter spillways will have noticeable improvements in the transfer efficiency with steps as opposed to without.

The influence of flow rate on transfer efficiency was also very great compared to the influence of step height. The transfer efficiency varied greatly for any given location and step height when the flow rate was changed. For example, at a vertical drop of 10 feet, increasing the flow rate from 5cfs/ft to 20cfs/ft caused the transfer efficiency to drop from 0.723 to 0.363 on the 2-foot steps. Likewise, the transfer efficiency of the 1-foot

steps changed from 0.680 to 0.211 with the same increase in flow rate. In addition, a larger change in transfer efficiency was typically observed by reducing the flow rate 5cfs/ft rather than increasing the step size from 1-foot to 2-foot. This principle can be applied to both the operation of existing structures as well as the design of new structures. Existing structures should be operated in such a way that the unit flow rate is minimized. This can be accomplished by reducing the volume of water allowed to spill at any given time. It can also be accomplished by increasing the width of the spillway by opening as many gates as possible if the spillway is a controlled spillway. In the design of new structures, increasing the width of the spillway may improve the transfer efficiency as much as steps would. Cost-benefit ratios should be calculated to determine whether a wider, smooth spillway or a narrower, stepped spillway is a better alternative.

5.3 Recommendations

This thesis is by no means an exhaustive look at air-water gas transfer on stepped spillways. In fact, it has only scratched the surface. Further work needs to be done at the prototype-scale. Future work should attempt to expand the scope of the variables included in this study. For example, higher flow rates, higher and lower TGP% readings in the head box, and larger as well as smaller step heights should all be explored. Additionally, variables that were not considered in this thesis, such as spillway slope and step angle, should also be considered in future studies.

Furthermore, this thesis did not consider the energy dissipating effects of stepped spillways. The greater energy dissipation of stepped spillways can reduce the depth of the stilling basin needed to contain a hydraulic jump. A reduction in stilling basin depth

can further reduce TDG supersaturation by minimizing the hydrostatic pressures acting on the entrained air. Some work has been done to examine the feasibility of using stepped spillways to reduce supersaturation in this way (Ahmann and Zapel 2000). In the future, studies should attempt to combine the existing knowledge of gas transfer on the slope presented in this thesis with the known effect that stepped spillways can have on reducing stilling basin depth. By using an integrated approach that considers degassing effects on the slope as well as supersaturation effects in the stilling basin, a more accurate comparison of step and smooth spillways can be obtained.

BIBLIOGRAPHY

BIBLIOGRAPHY

1. Ahmann, M.L., and Zapel, E.T. (2000). "Stepped spillways, a dissolved gas abatement alternative." *Hydraulics of Stepped Spillways*, Minor and Hager, eds., Balkema, Rotterdam. 45-52.
2. Bouck, G.R., Nebeker, A.V., and Stevens, D.G. (1976). *Mortality, Saltwater Adaptation and Reproduction of Fish During Gas Supersaturation*. U.S. Environmental Protection Agency Report No. EPA-600/3-76-050.
3. Chanson, H. (1994). *Hydraulic design of Stepped Cascades, Channels, Weirs, and Spillways*, Pergamon, Tarry Town, New York. 113-151.
4. Colt, J. (1984). *Computation of dissolved gas concentrations in water as functions of temperature, salinity, and pressure*. American Fisheries Society Special Publication 14.
5. Geldert, D.A. (1996). "Parametric Relations to Predict Dissolved Gas Supersaturation Below Spillways," MS Thesis, University of Minnesota, Minneapolis, MN.
6. Geldert, D.A., and Gulliver J.S. (1996). "Prediction of Dissolved Gas Supersaturation Downstream of Hydraulic Structures." *Water Quality '96: Proceedings of the 11th Seminar*, 26 February – 01 March 1996, Seattle, Washington. 513-521.
7. Geldert, D.A., Gulliver, J.S., and Wilhelms, S.C. (1998). "Modeling Dissolved Gas Supersaturation Below Spillway Plunge Pools." *Journal of Hydraulic Engineering*, ASCE, 124(5). 298-304.
8. Gulliver, J.S. (1991). "Introduction to Air-Water Mass Transfer." *Air-Water Mass Transfer*, S.C. Wilhelms and J.S. Gulliver, eds., ASCE, New York, 1-8.
9. Johnson, P.L. (1975). *Prediction of Dissolved Gas at Hydraulic Structures*. US Bureau of Reclamation Technical Report No. GR-8-75.
10. Marking, L.L. (1987). *Gas Supersaturation in Fisheries: Causes, Concerns, and Cures*. Fish and Wildlife Leaflet 9, United States Department of the Interior, Fish and Wildlife Service.

11. Murphy, A.P., Lichtwardt, M.A., and Bisgaard S. (1998). "Novel Methods for Generating and Treating Air Supersaturated Water." *Proceedings of ASME Fluids Engineering Division Summer Meeting '98*, June 21-25, 1998, Washington, DC.
12. Novak, P., and , Gabriel P. (1997). "Oxygen Uptake at Barrages of Elbe Cascade." *Proceedings, 27th International Association of Hydraulic Research Congress*, San Francisco, Vol. D, F.M. Holly Jr. and A. Alsaffar eds., 489-529.
13. Rice, C.E. and Kadavy, K.C. (1996). "Model Study of a Roller Compacted Concrete Stepped Spillway." *Journal of Hydraulic Engineering*, ASCE, 122(6). 292-297.
14. Rindels, A.J. (1990). "Gas Transfer at Spillways, Hydraulic Jumps, and Overfalls," PhD Thesis, University of Minnesota, Minneapolis, MN.
15. Rucker, H. and Harshbarger, D. (1997). "Monitoring Dissolved Oxygen and Total Dissolved Gs in Tailraces." *Proceedings, 27th International Association of Hydraulic Research Congress*, San Francisco, Vol. D, F.M. Holly Jr. and A. Alsaffar eds. 477-482.
16. Ruffing, F.E. (1996). "Total Dissolved Gas Studies on the Lower Columbia: An Overview." *Water Quality '96: Proceedings of the 11th Seminar*, 26 February – 01 March 1996, Seattle, Washington. 274-280.
17. Ruffing, F.E., Flint, N.A., and Kalli, G.A. (1996). "Total Dissolved Gas Studies on the Lower Columbia: Transect Studies." *Water Quality '96: Proceedings of the 11th Seminar*, 26 February – 01 March 1996, Seattle, Washington. 282-296.
18. Sweeney Aquametrics, Inc. *Manual for Sweeney Aquamatic Saturometer Model DS-1A*. Stoney Creek, CT.
19. Sweeney, J. (2000). Sweeney Aquametrics, Inc., personal communications.
20. Toombes, L. and Chanson, H. (2000). "Air-water Flow and Gas Transfer at Aeration Cascades: A Comparative Study of Smooth and Stepped Chutes." *Hydraulics of Stepped Spillways*, Minor and Hager, eds., Balkema, Rotterdam. 77-84.
21. Ward, J.P., (2001). "Hydraulic Design of Stepped Spillways." PhD Thesis, Colorado State University, Fort Collins, CO.
22. Watson, C.C., Walters, R.W., and Hogan, S.A. (1998). "Aeration Performance of Low Drop Weirs." *Journal of Hydraulic Engineering*, ASCE, 124(1). 65-71.

23. Weber, L.J. and Mannheim, C. (1997). "A Unique Approach for Physical Model Studies of Nitrogen Gas Supersaturation." *Proceedings, 27th International Association of Hydraulic Research Congress*, San Francisco, Vol. D, F.M. Holly Jr. and A. Alsaffar eds. 518-523.
24. Wilhelms, S.C. and Schneider, M.L. (1997). "Total Dissolved Gas in the Near-Field Tailwater of Ice Harbor Dam." *Proceedings, 27th International Association of Hydraulic Research Congress*, San Francisco, Vol. D, F.M. Holly Jr. and A. Alsaffar eds. 513-517.

APPENDIX A
DATA

General										HB Reading (CS Meter)					Reading 2 (SA Meter)				
h _{STEP}	Probe	Tank	Press	Flow	Date & Time	Temp	BP	ΔP	TGP%	Loc	Sta	Temp	BP	ΔP	TGP%	Comments			
2	PG	2	-	20	06/21 01:26 PM	8.5	627	094	115.0%	S12	2	10.0	627	020	103.2%	Stable for ~ 1minute			
2	PG	2	-	20	06/21 01:31 PM	8.5	627	101	116.0%	S12	2	10.0	627	021	103.3%	Stable for ~ 1minute			
2	PG	2	-	20	06/21 01:35 PM	8.5	627	106	117.0%	S12	2	10.0	627	022	103.5%	Stable for ~ 1minute			
2	PG	2	-	20	06/21 01:38 PM	8.5	627	113	118.0%	S12	2	10.0	627	023	103.6%	Stable for ~ 1minute			
2	PG	2	-	20	06/21 01:42 PM	8.6	627	117	118.7%	S12	2	10.0	627	024	103.8%	Stable for ~ 1minute			
2	PG	3	75	77	06/22 11:12 AM	8.1	625	089	114.3%	S6	1	9.8	625	068	110.8%	Stable for ~ 1minute			
2	PG	3	75	77	06/22 11:18 AM	8.1	625	093	114.9%	S6	1	9.8	625	072	111.5%				
2	PG	4	75	77	06/22 11:54 AM	8.2	625	069	110.9%	S6	1	9.8	625	045	107.2%				
2	PG	3	75	77	06/22 12:33 PM	8.2	625	018	102.9%	S6	1	9.8	625	012	101.9%				
2	PG	3	78	77	06/22 12:54 PM	8.2	625	038	106.1%	S6	1	9.8	625	028	104.5%				
2	PG	3	80	77	06/22 01:19 PM	8.2	624	059	109.6%	S6	1	9.8	625	046	107.3%				
2	PG	4	85	60	06/22 02:03 PM	8.5	625	030	104.9%	S6	1	9.9	625	021	103.4%				
2	PG	4	90	60	06/22 02:28 PM	8.6	625	073	111.7%	S6	1	9.9	625	046	107.4%				
2	PG	3	92	60	06/22 03:06 PM	8.6	624	046	107.4%	S6	1	10.0	624	031	105.0%				
2	PG	4	95	60	06/22 03:45 PM	8.6	623	089	114.3%	S6	1	10.0	623	058	109.3%				
2	PG	4	77	40	06/23 08:58 AM	8.3	625	013	102.1%	S6	1	9.9	625	008	101.2%				
2	PG	4	82	40	06/23 09:38 AM	8.3	624	043	107.0%	S6	1	9.9	625	023	103.6%				
2	PG	3	86	40	06/23 09:50 AM	8.3	624	038	106.1%	S6	1	10.0	625	021	103.3%				
2	PG	3	94	40	06/23 10:38 AM	8.3	623	081	113.1%	S6	1	10.0	624	044	107.0%				
2	PG	5	97	40	06/23 10:58 AM	8.4	623	112	118.1%	S6	1	10.0	624	062	109.9%				
2	PG	4	87	20	06/23 11:36 AM	8.6	623	056	109.1%	S6	1	10.2	624	026	104.2%				
2	PG	5	97	20	06/23 12:24 PM	8.6	623	119	119.1%	S6	1	10.1	623	059	109.5%				
2	PG	5	92	20	06/23 01:29 PM	8.3	623	082	113.2%	S6	1	9.9	623	041	106.5%				
2	PG	5	86	20	06/23 02:34 PM	8.7	623	026	104.2%	S6	1	10.1	623	014	102.3%				
2	PG	5	77	80	06/26 11:07 AM	8.2	633	025	103.9%	S18	3	9.9	632	012	101.8%				
1	PG	-	-	80	07/25 09:56 AM	11.2	636	-019	97.1%	S35	3	11.3	628	002	100.3%				
1	PG	1	85	80	07/25 10:16 AM	11.1	636	001	100.1%	S35	3	11.3	628	007	101.1%				
1	PG	1	85	80	07/25 11:43 AM	11.2	636	033	105.3%	S35	3	11.5	628	017	102.8%				
1	PG	1	86	80	07/25 12:08 PM	11.2	636	056	108.9%	S35	3	11.5	628	023	103.8%				
1	PG	2	87	80	07/25 12:48 PM	11.3	636	087	113.7%	S35	3	11.5	628	032	105.1%	Less than 2min of stab			

General										HB Reading (CS Meter)					Reading 2 (SA Meter)				
hSTEP	Probe	Tank	Press	Flow	Date & Time	Temp	BP	ΔP	TGP%	Loc	Sta	Temp	BP	ΔP	TGP%	Comments			
1	PG	2	88	80	07/25 01:30 PM	11.2	636	062	109.7%	S35	3	11.4	627	024	103.8%				
1	PG	2	88	80	07/25 01:56 PM	11.1	636	115	118.2%	S35	3	11.3	627	041	106.5%	Less than 2min of stab			
1	PG	1	80	60	07/25 03:01 PM	11.1	636	003	100.6%	S35	3	11.3	626	008	101.4%				
1	PG	1	80	60	07/25 03:31 PM	11.1	636	026	104.1%	S35	3	11.3	626	013	102.1%				
1	PG	1	81	60	07/26 08:43 AM	11.1	636	050	107.9%	S35	3	11.3	627	018	102.8%				
1	PG	1	82	60	07/26 09:11 AM	11.1	636	059	109.4%	S35	3	11.4	628	019	103.0%				
1	PG	4	-	60	07/26 11:46 AM	11.3	636	068	110.8%	S35	3	11.6	627	025	104.0%				
1	PG	-	-	20	07/28 08:55 AM	11.3	638	070	111.0%	S35	3	11.7	630	008	101.3%				
1	PG	-	-	20	07/28 09:35 AM	11.3	638	069	110.9%	S35	3	11.7	630	008	101.3%				
1	PG	-	-	20	07/28 10:25 AM	11.3	638	063	110.0%	S35	3	11.7	630	008	101.3%				
1	PG	-	-	20	07/28 11:30 AM	11.3	639	023	103.5%	S35	3	11.7	630	007	101.1%				
1	PG	-	-	20	07/28 12:25 PM	11.5	639	021	103.3%	S23	2	11.8	629	007	101.1%				
1	PG	-	-	20	07/28 01:12 PM	11.6	638	010	101.6%	S23	2	11.9	629	006	100.9%				
1	PG	-	-	20	07/28 02:50 PM	11.6	639	050	107.8%	S23	2	11.8	629	010	101.6%				
1	PG	-	-	20	07/28 04:00 PM	11.6	638	092	114.5%	S23	2	11.7	629	015	102.4%				
1	PG	5	80	40	08/01 09:11 AM	11.5	638	021	103.4%	S23	2	11.9	629	011	101.7%				
1	PG	5	80.5	40	08/01 09:48 AM	11.5	638	047	107.4%	S23	2	11.9	629	019	102.9%				
1	PG	6	81	40	08/01 11:15 AM	11.6	638	071	111.2%	S23	2	11.9	629	024	103.9%				
1	PG	7	82	40	08/01 11:55 AM	11.6	637	108	117.1%	S23	2	12.0	629	035	105.7%				
1	PG	6	80	60	08/01 12:35 PM	11.7	638	052	108.2%	S23	2	12.0	628	027	104.3%				
1	PG	6	80.5	60	08/01 01:00 PM	11.7	637	057	109.0%	S23	2	12.0	628	029	104.6%				
1	PG	7	81	60	08/01 01:22 PM	11.7	637	088	113.9%	S23	2	12.0	628	041	106.6%				
1	PG	6	80	60	08/01 01:55 PM	11.8	637	035	105.6%	S23	2	12.1	628	019	103.1%				
1	PG	6	79.5	60	08/01 02:31 PM	11.8	637	008	101.3%	S23	2	12.1	628	009	101.4%				
1	PG	6	79.5	80	08/01 02:55 PM	11.8	637	006	101.0%	S23	2	12.1	628	010	101.5%				
1	PG	6	80	80	08/01 03:18 PM	11.7	637	013	102.0%	S23	2	12.0	628	012	101.9%				
1	PG	6	82	80	08/01 03:35 PM	11.7	637	025	104.0%	S23	2	12.0	628	019	103.1%				
1	PG	8	70	20	08/15 08:38 AM	13.1	640	044	106.9%	S11	1	13.3	632	021	103.2%				
1	PG	8	71	20	08/15 10:48 AM	13.0	640	-018	97.1%	S11	1	13.2	631	-003	99.6%				
1	PG	8	72	20	08/15 11:25 AM	13.0	640	-001	99.8%	S11	1	13.2	632	005	100.7%				

General										HB Reading (CS Meter)					Reading 2 (SA Meter)				
hSTEP	Probe	Tank	Press	Flow	Date & Time	Temp	BP	ΔP	TGP%	Loc	Sta	Temp	BP	ΔP	TGP%	Comments			
1	PG	9	73	20	08/15 12:10 PM	13.0	640	050	107.9%	S11	1	13.3	632	024	103.8%				
1	PG	8	74	20	08/15 12:43 PM	13.0	640	062	109.8%	S11	1	13.2	632	028	104.5%				
1	PG	9	75	20	08/15 01:45 PM	13.0	639	094	114.8%	S11	1	13.2	631	042	106.7%				
1	PG	10	76	20	08/15 02:20 PM	13.0	639	097	115.2%	S11	1	13.1	631	043	106.8%				
1	PG	10	73	40	08/15 02:54 PM	12.9	639	137	121.5%	S11	1	13.1	630	121	119.2%	1.5 minutes			
1	PG	8	65	40	08/16 09:11 AM	12.8	638	-002	99.8%	S11	1	13.1	630	001	100.2%				
1	PG	10	66	40	08/16 11:25 AM	13.1	638	030	104.8%	S11	1	13.3	630	023	103.7%				
1	PG	10	67	40	08/16 03:10 PM	13.1	638	076	112.0%	S11	1	13.3	630	057	108.9%				
1	PG	10	68	40	08/16 03:35 PM	13.0	638	081	112.7%	S11	1	13.3	630	058	109.1%				
1	PG	10	69	40	08/16 03:55 PM	13.1	638	091	114.3%	S11	1	13.3	630	066	110.6%				
1	PG	9	67	60	08/17 01:33 PM	13.1	637	059	109.4%	S11	1	13.3	632	047	107.4%				
1	PG	9	67	60	08/17 01:45 PM	13.0	637	059	109.3%	S11	1	13.2	632	046	107.2%				
1	PG	9	69	60	08/17 02:55 PM	12.8	637	039	106.2%	S11	1	13.0	632	031	104.9%				
1	SW**	11	58	60	08/25 12:47 PM	14.0	635	005	100.8%	S11	1	14.2	631	006	101.0%	1 hole u/s & 1 hole d/s			
1	SW**	11	58	60	08/25 12:56 PM	14.0	635	003	100.5%	S23	2	14.2	631	008	101.3%	1 hole u/s & 1 hole d/s			
1	SW**	11	58	60	08/25 01:08 PM	14.0	635	002	100.3%	S35	3	14.2	631	008	101.3%	1 hole u/s & 1 hole d/s			
1	SW**	11	59	60	08/25 02:01 PM	14.0	635	023	103.5%	S35	3	14.3	632	010	101.5%	1 hole u/s & 1 hole d/s			
1	SW**	11	59	60	08/25 02:11 PM	14.0	635	021	103.2%	S23	2	14.3	631	012	101.9%	1 hole u/s & 1 hole d/s			
1	SW**	11	59	60	08/25 02:22 PM	13.9	635	020	103.0%	S11	1	14.2	631	017	102.7%	1 hole u/s & 1 hole d/s			
1	SW**	11	61	60	08/28 08:28 AM	14.2	631	046	107.3%	S11	1	14.5	627	028	104.5%	1 hole u/s & 1 hole d/s			
1	SW**	11	61	60	08/28 08:37 AM	14.2	631	044	107.1%	S23	2	14.5	628	017	102.6%	1 hole u/s & 1 hole d/s			
1	SW**	11	61	60	08/28 08:47 AM	14.2	631	045	107.2%	S35	3	14.5	628	011	101.7%	1 hole u/s & 1 hole d/s			
1	TB	11	61	60	08/28 08:57 AM	14.2	631	048	107.6%	TB	TB	14.5	628	012	101.9%				
1	SW**	13	64	60	08/28 09:53 AM	14.3	632	074	111.8%	S11	1	14.6	628	046	107.3%	1 hole u/s & 1 hole d/s			
1	SW**	13	64	60	08/28 10:05 AM	14.3	632	075	112.0%	S23	2	14.6	628	024	103.7%	1 hole u/s & 1 hole d/s			
1	SW**	13	64	60	08/28 10:15 AM	14.4	632	077	112.3%	S35	3	14.7	628	013	102.0%	1 hole u/s & 1 hole d/s			
1	TB	13	64	60	08/28 10:25 AM	14.4	632	074	111.8%	TB	TB	14.7	628	014	102.2%				
1	SW**	13	67	60	08/28 10:53 AM	14.4	632	091	114.4%	S11	1	14.9	628	054	108.6%	1 hole u/s & 1 hole d/s			
1	SW**	12	67	60	08/28 11:17 AM	14.3	632	091	114.5%	S23	2	14.8	628	027	104.3%	1 hole u/s & 1 hole d/s			
1	SW**	13	66	60	08/28 11:45 AM	14.3	632	103	116.2%	S35	3	14.8	628	017	102.7%	1 hole u/s & 1 hole d/s			

General										HB Reading (CS Meter)					Reading 2 (SA Meter)				
h _{STEP}	Probe	Tank	Press	Flow	Date & Time	Temp	BP	ΔP	TGP%	Loc	Sta	Temp	BP	ΔP	TGP%	Comments			
1	TB	12	67	60	08/28 11:59 AM	14.4	632	096	115.2%	TB	TB	14.9	628	015	102.4%				
1	SW**	12	67	80	08/28 12:41 PM	14.4	632	115	118.2%	S11	1	14.9	627	080	112.7%	1 hole u/s & 1 hole d/s			
1	SW**	12	67	80	08/28 12:54 PM	14.4	632	118	118.8%	S23	2	15.0	628	049	107.8%	1 hole u/s & 1 hole d/s			
1	SW**	12	67	80	08/28 01:37 PM	14.5	633	092	114.5%	S35	3	15.0	628	022	103.4%	1 hole u/s & 1 hole d/s			
1	SW**	11	62	40	08/29 12:43 PM	14.9	631	044	107.1%	S11	1	15.1	629	020	103.2%	1 hole u/s & 1 hole d/s			
1	SW**	11	62	40	08/29 12:54 PM	14.8	631	048	107.6%	S23	2	15.1	629	013	102.0%	1 hole u/s & 1 hole d/s			
1	SW**	11	62	40	08/29 01:05 PM	14.8	631	052	108.3%	S35	3	15.1	629	008	101.3%	1 hole u/s & 1 hole d/s			
1	PG*	-	-	40	09/01 09:53 AM	15.0	635	028	104.4%	S23	2	15.3	628	017	102.7%	PG moved over to wall			
1	PG*	-	-	40	09/01 10:05 AM	15.0	635	033	105.2%	S23	2	15.3	628	019	103.0%	PG moved over to wall			
1	PG*	-	-	40	09/01 11:13 AM	15.0	635	059	109.2%	S23	2	15.3	628	027	104.2%	PG moved over to wall			
1	SW	-	-	40	09/01 12:10 PM	15.0	635	021	103.3%	S23	2	15.3	628	011	101.8%	Testing phase of SW			
1	SW	-	-	40	09/01 12:55 PM	15.1	634	057	109.0%	S23	2	15.3	627	018	103.0%	Testing phase of SW			
1	SW	15	60	60	09/06 08:48 AM	16.4	634	053	108.4%	S11	1	16.8	628	038	106.0%	Testing phase of SW			
1	SW	15	60	60	09/06 08:58 AM	16.2	634	053	108.4%	S23	2	16.6	628	022	103.6%	Testing phase of SW			
1	SW	15	60	60	09/06 09:13 AM	16.3	634	056	108.9%	S35	3	16.7	628	014	102.2%	Testing phase of SW			
1	SW	16	60	60	09/06 09:41 AM	16.3	634	063	109.9%	S11	1	16.7	628	042	106.7%	Testing phase of SW			
1	SW	16	60	60	09/06 09:55 AM	16.6	634	062	109.8%	S23	2	16.6	629	024	103.8%	Testing phase of SW			
1	SW	16	60	60	09/06 10:12 AM	16.3	634	061	109.7%	S35	3	16.6	629	013	102.0%	Testing phase of SW			
1	SW***	15	61	60	09/06 12:07 PM	16.4	633	057	109.0%	S11	1	16.7	627	041	106.6%	Bottom hole plugged			
1	SW***	15	61	60	09/06 12:29 PM	16.5	634	063	110.0%	S23	2	16.7	627	024	103.9%	Bottom hole plugged			
1	SW***	15	61	60	09/06 12:51 PM	16.5	633	061	109.7%	S35	3	16.8	627	012	101.9%	Bottom hole plugged			
1	TB	15	61	60	09/06 01:26 PM	16.5	633	060	109.5%	TB	TB	16.8	628	014	102.2%				
1	SW***	15	59	60	09/06 02:05 PM	16.6	633	027	104.4%	S11	1	16.8	627	023	103.7%	Bottom hole plugged			
1	SW****	-	60	60	09/08 08:28 AM	16.8	632	061	109.8%	S11	1	17.0	626	038	106.0%	Sealed with silicone			
1	SW****	-	60	60	09/08 08:55 AM	16.8	632	066	110.4%	S23	2	17.1	626	020	103.2%	Sealed with silicone			
1	SW****	-	60	60	09/08 09:12 AM	16.9	632	065	110.3%	S35	3	17.1	627	016	102.5%	Sealed with silicone			
1	SW	17	56	60	09/11 01:22 PM	17.8	634	018	102.9%	S11	1	18.0	628	017	102.6%				
1	SW	17	56	60	09/11 01:33 PM	17.8	634	016	102.6%	S23	2	18.0	628	013	102.1%				
1	SW	17	56	60	09/11 01:43 PM	17.8	634	014	102.2%	S35	3	18.0	628	007	101.1%				
1	TB	17	56	60	09/11 01:51 PM	17.8	634	011	101.8%	TB	TB	18.0	628	010	101.6%				

General										HB Reading (CS Meter)					Reading 2 (SA Meter)				
hSTEP	Probe	Tank	Press	Flow	Date & Time	Temp	BP	ΔP	TGP%	Loc	Sta	Temp	BP	ΔP	TGP%	Comments			
1	SW	17	54.5	80	09/12 09:23 AM	17.9	636	032	105.1%	S11	1	18.1	630	027	104.4%				
1	SW	17	54.5	80	09/12 09:32 AM	17.8	636	031	105.0%	S23	2	18.1	630	019	103.0%				
1	SW	17	54.5	80	09/12 09:43 AM	17.8	636	030	104.8%	S35	3	18.1	631	009	101.4%				
1	TB	17	54.5	80	09/12 09:53 AM	17.9	636	028	104.5%	TB	TB	18.1	631	012	102.0%				
1	SW	18	58	80	09/12 11:00 AM	17.9	636	077	112.2%	S11	1	18.0	630	060	109.5%				
1	SW	18	58	80	09/12 11:11 AM	17.9	636	078	112.4%	S23	2	18.1	631	033	105.3%				
1	SW	18	58	80	09/12 11:24 AM	17.9	636	076	112.0%	S35	3	18.1	631	013	102.0%				
1	TB	18	58	80	09/12 11:32 AM	17.9	630	078	112.3%	TB	TB	18.1	631	014	102.1%				
1	SW	-	60	60	09/12 12:29 PM	17.9	635	093	114.7%	S11	1	18.2	630	062	109.9%				
1	SW	-	60	60	09/12 12:40 PM	17.9	635	092	114.6%	S23	2	18.1	630	030	104.8%				
1	SW	-	60	60	09/12 01:05 PM	17.9	635	089	114.1%	S35	3	18.1	630	012	101.9%				
1	TB	-	60	60	09/12 01:15 PM	17.9	635	101	116.0%	TB	TB	18.1	630	011	101.8%				
1	SW	-	57	40	09/13 10:09 AM	18.1	636	031	105.0%	S23	2	18.3	631	014	102.2%				
1	SW	-	57	40	09/13 10:28 AM	18.1	636	033	105.3%	S35	3	18.3	631	009	101.4%				
1	TB	-	57	40	09/13 10:45 AM	18.1	636	028	104.5%	TB	TB	18.3	631	012	101.9%				
1	SW	-	57	40	09/13 11:01 AM	18.1	637	029	104.7%	S11	1	18.3	631	020	103.2%				
1	SW	-	59	40	09/13 12:23 PM	18.2	636	087	113.8%	S11	1	18.3	630	047	107.5%				
1	SW	-	59	40	09/13 12:38 PM	18.2	636	090	114.2%	S23	2	18.3	630	023	103.7%				
1	SW	-	59	40	09/13 01:03 PM	18.2	636	093	114.7%	S35	3	18.3	630	013	102.1%				
1	TB	-	59	40	09/13 01:13 PM	18.2	636	092	114.5%	TB	TB	18.3	630	012	101.9%				
1	SW	-	61	20	09/13 02:19 PM	18.2	635	116	118.3%	S11	1	18.3	629	041	106.6%				
1	SW	-	61	20	09/13 02:34 PM	18.2	635	107	117.0%	S23	2	18.3	629	015	102.4%				
1	SW	-	61	20	09/13 02:45 PM	18.1	635	104	116.4%	S35	3	18.2	629	008	101.3%				
1	TB	-	61	20	09/13 02:55 PM	18.1	635	103	116.2%	TB	TB	18.2	629	007	101.2%				
1	SW	-	59	20	09/14 09:53 AM	18.0	641	028	104.4%	S11	1	18.1	635	015	102.4%				
1	SW	-	59	20	09/14 10:03 AM	18.0	641	025	103.9%	S23	2	18.1	636	010	101.5%				
1	SW	-	59	20	09/14 10:18 AM	17.9	641	020	103.2%	S35	3	18.1	636	007	101.1%				
1	TB	-	59	20	09/14 10:28 AM	17.9	641	018	102.9%	TB	TB	18.1	636	007	101.1%				
1	SW	-	0	80	09/14 11:09 AM	18.0	641	-035	94.5%	S11	1	18.1	635	-028	95.6%				
1	SW	-	0	80	09/14 11:17 AM	18.0	641	-036	94.4%	S23	2	18.2	635	-005	99.2%				

General										HB Reading (CS Meter)					Reading 2 (SA Meter)				
hSTEP	Probe	Tank	Press	Flow	Date & Time	Temp	BP	ΔP	TGP%	Loc	Sta	Temp	BP	ΔP	TGP%	Comments			
1	SW	-	0	80	09/14 11:25 AM	18.0	641	-036	94.3%	S35	3	18.2	635	003	100.4%				
1	TB	-	0	80	09/14 11:34 AM	18.0	641	-037	94.2%	TB	TB	18.2	635	009	101.4%				
1	SW	-	0	60	09/14 11:45 AM	18.0	641	-037	94.1%	S11	1	18.2	635	-024	96.3%				
1	SW	-	0	60	09/14 11:55 AM	18.0	640	-038	94.1%	S23	2	18.2	635	-002	99.7%				
1	SW	-	0	60	09/14 12:04 PM	18.0	640	-038	94.0%	S35	3	18.2	635	004	100.7%				
1	TB	-	0	60	09/14 12:12 PM	18.0	640	-038	94.0%	TB	TB	18.2	635	009	101.4%				
1	SW	-	0	40	09/14 12:22 PM	18.0	640	-037	94.1%	S11	1	18.2	635	-014	97.8%				
1	SW	-	0	40	09/14 12:31 PM	18.0	640	-037	94.2%	S23	2	18.2	635	001	100.2%				
1	SW	-	0	40	09/14 12:40 PM	18.0	640	-037	94.2%	S35	3	18.2	635	005	100.8%				
1	TB	-	0	40	09/14 12:48 PM	18.0	640	-037	94.2%	TB	TB	18.2	635	007	101.2%				
1	TB	-	0	20	09/14 12:58 PM	18.0	640	-038	94.0%	TB	TB	18.2	635	006	101.0%				
1	SW	-	0	20	09/14 01:05 PM	18.0	640	-038	94.0%	S35	3	18.2	635	005	100.8%				
1	SW	-	0	20	09/14 01:13 PM	18.0	640	-038	94.1%	S23	2	18.2	635	004	100.6%				
1	SW	-	0	20	09/14 01:21 PM	18.0	640	-037	94.3%	S11	1	18.2	635	-007	98.9%				
2	SW	-	0	80	09/18 09:22 AM	17.9	633	-033	94.7%	S6	1	18.0	627	-019	97.1%				
2	SW	-	0	80	09/18 09:32 AM	17.9	633	-034	94.5%	S12	2	17.9	628	002	100.2%				
2	SW	-	0	80	09/18 09:43 AM	17.8	633	-035	94.5%	S18	3	17.9	628	005	100.8%				
2	TB	-	0	80	09/18 09:55 AM	17.8	633	-035	94.5%	TB	TB	17.9	628	010	101.7%				
2	SW	-	0	60	09/18 10:06 AM	17.8	633	-035	94.4%	S6	1	17.8	627	-014	97.9%				
2	SW	-	0	60	09/18 10:18 AM	17.8	633	-035	94.4%	S12	2	17.9	628	003	100.5%				
2	SW	-	0	60	09/18 10:28 AM	17.8	633	-035	94.4%	S18	3	17.9	628	006	100.9%				
2	TB	-	0	60	09/18 10:39 AM	17.8	633	-035	94.4%	TB	TB	17.9	628	008	101.4%				
2	TB	-	0	40	09/18 10:50 AM	17.8	633	-032	94.9%	TB	TB	17.9	628	008	101.2%				
2	SW	-	0	40	09/18 11:01 AM	17.8	633	-032	94.9%	S18	3	17.9	628	006	100.9%				
2	SW	-	0	40	09/18 11:12 AM	17.9	633	-032	95.0%	S12	2	17.9	628	006	100.9%				
2	SW	-	0	40	09/18 11:24 AM	17.9	633	-032	95.0%	S6	1	17.9	627	-007	98.8%				
2	SW	-	0	20	09/18 11:35 AM	17.9	633	-032	94.9%	S6	1	18.0	627	-004	99.5%				
2	SW	-	0	20	09/18 11:48 AM	17.9	633	-032	94.9%	S12	2	17.9	627	006	100.9%				
2	SW	-	0	20	09/18 12:01 PM	17.9	633	-030	95.2%	S18	3	17.9	627	004	100.6%				
2	TB	-	0	20	09/18 12:10 PM	18.0	633	-029	95.4%	TB	TB	17.9	627	006	100.9%				

General										HB Reading (CS Meter)					Reading 2 (SA Meter)				
h _s STEP	Probe	Tank	Press	Flow	Date & Time	Temp	BP	ΔP	TGP%	Loc	Sta	Temp	BP	ΔP	TGP%	Comments			
2	SW	-	58.5	20	09/18 01:28 PM	18.1	632	050	108.0%	S6	1	18.1	626	022	103.5%				
2	SW	-	58.5	20	09/18 02:09 PM	18.1	631	068	110.8%	S12	2	18.0	625	013	102.1%				
2	SW	-	58.5	20	09/18 02:20 PM	18.1	631	068	110.9%	S18	3	18.0	625	005	100.8%				
2	TB	-	58.5	20	09/18 02:34 PM	18.1	631	068	110.7%	TB	TB	18.1	626	006	101.0%				
2	SW	-	59	20	09/19 08:30 AM	17.8	631	063	110.1%	S6	1	17.8	625	023	103.7%				
2	SW	-	60	20	09/19 10:08 AM	17.8	631	083	113.2%	S6	1	17.8	625	028	104.5%				
2	SW	-	60	20	09/19 10:18 AM	17.8	631	082	113.1%	S12	2	17.8	625	014	102.2%				
2	SW	-	60	20	09/19 10:28 AM	17.8	631	083	113.2%	S18	3	17.8	626	005	100.8%				
2	TB	-	60	20	09/19 10:38 AM	17.8	631	085	113.5%	TB	TB	17.8	626	008	101.2%				
2	TB	-	58	40	09/19 12:30 PM	17.9	630	097	115.5%	TB	TB	17.9	625	010	101.5%				
2	SW	-	58	40	09/19 01:15 PM	17.9	630	085	113.5%	S18	3	17.9	625	010	101.6%				
2	SW	-	58	40	09/19 01:25 PM	17.9	631	083	113.2%	S12	2	17.9	624	022	103.5%				
2	SW	-	58	40	09/19 01:35 PM	17.9	631	077	112.3%	S6	1	17.9	625	040	106.4%				
2	SW	-	57	40	09/20 09:55 AM	17.7	635	021	103.3%	S6	1	17.9	631	016	102.6%				
2	SW	-	57	40	09/20 10:15 AM	17.7	635	033	105.2%	S12	2	17.9	631	015	102.3%				
2	SW	-	57	40	09/20 10:25 AM	17.7	635	033	105.3%	S18	3	17.9	631	008	101.3%				
2	TB	-	57	40	09/20 10:35 AM	17.7	635	033	105.2%	TB	TB	17.9	631	008	101.3%				
2	SW	-	57	40	09/20 10:45 AM	17.7	635	033	105.2%	S6	1	17.9	631	023	103.6%				
2	SW	-	55.5	60	09/20 11:52 AM	17.7	636	020	103.2%	S6	1	17.8	630	018	102.8%				
2	SW	-	55.5	60	09/20 12:02 PM	17.7	636	019	103.1%	S12	2	17.8	631	014	102.2%				
2	SW	-	55.5	60	09/20 12:12 PM	17.7	636	019	103.0%	S18	3	17.8	630	009	101.4%				
2	TB	-	55.5	60	09/20 12:22 PM	17.7	636	018	102.9%	TB	TB	17.8	630	011	101.7%				
2	SW	-	58	60	09/20 01:29 PM	17.8	635	062	109.9%	S6	1	17.9	630	041	106.5%				
2	SW	-	58	60	09/20 01:39 PM	17.8	635	062	109.9%	S12	2	17.9	630	023	103.7%				
2	SW	-	58	60	09/20 01:49 PM	17.8	635	061	109.7%	S18	3	17.9	630	011	101.7%				
2	TB	-	58	60	09/20 01:59 PM	17.8	635	061	109.7%	TB	TB	17.9	630	011	101.7%				
2	SW	-	60	60	09/20 02:40 PM	17.7	634	088	114.0%	S6	1	17.9	630	054	108.6%				
2	SW	-	60	60	09/20 03:00 PM	17.7	634	096	115.2%	S12	2	17.9	630	029	104.6%				
2	SW	-	60	60	09/20 03:15 PM	17.7	634	093	114.8%	S18	3	17.9	630	013	102.0%				
2	TB	-	60	60	09/20 03:30 PM	17.7	634	092	114.6%	TB	TB	17.9	630	011	101.7%				

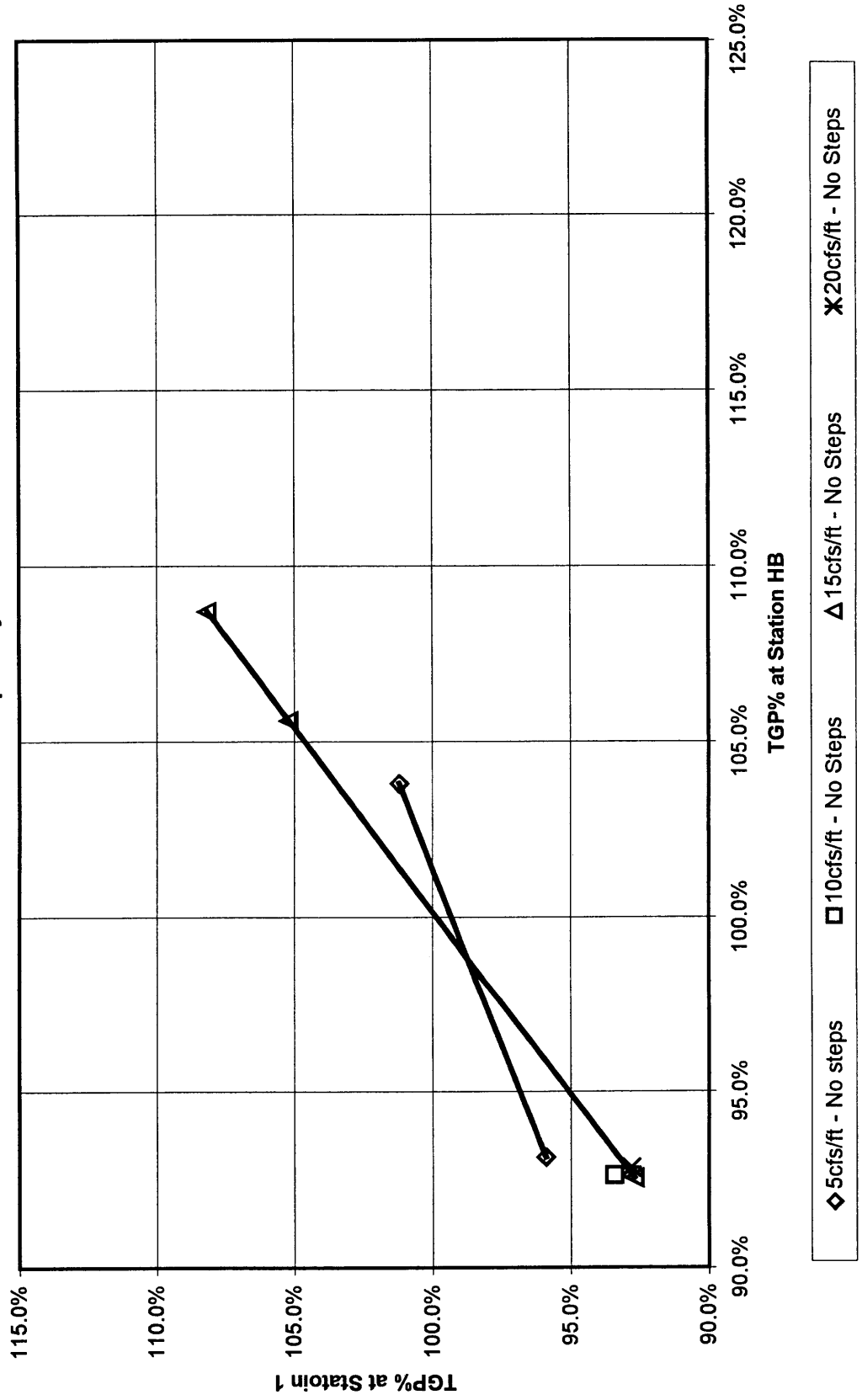
h _{STEP}	General						HB Reading (CS Meter)						Reading 2 (SA Meter)					
	Probe	Tank	Press	Flow	Date & Time		Temp	BP	ΔP	TGP%	Loc	Sta	Temp	BP	ΔP	TGP%	Comments	
2	SW	22	58	80	09/21 09:07 AM		17.7	625	095	115.3%	S6	1	17.8	620	064	110.2%		
2	SW	23	57.5	80	09/21 09:25 AM		17.7	625	098	115.7%	S12	2	17.8	620	035	105.7%		
2	SW	22	57.5	80	09/21 09:45 AM		17.7	625	096	115.4%	S18	3	17.8	620	014	102.3%		
2	TB	23	57.5	80	09/21 10:05 AM		17.7	625	081	113.0%	TB	TB	17.8	620	014	102.3%		
2	TB	-	54	80	09/21 11:05 AM		17.7	624	034	105.5%	TB	TB	17.8	619	011	101.8%		
2	SW	-	54	80	09/21 11:15 AM		17.7	624	033	105.4%	S18	3	17.8	619	010	101.6%		
2	SW	-	54	80	09/21 11:25 AM		17.7	624	033	105.4%	S12	2	17.8	619	019	103.0%		
2	SW	-	54	80	09/21 11:35 AM		17.7	624	036	105.8%	S6	1	17.8	619	030	104.8%		
0	SW	-	57.5	20	09/26 09:39 AM		15.4	636	024	103.8%	1/4	1	15.7	631	008	101.2%		
0	SW	-	57.5	20	09/26 10:02 AM		15.4	636	017	102.7%	1/2	2	15.7	631	009	101.3%		
0	SW	-	58.5	20	09/26 12:00 PM		15.4	636	032	105.0%	3/4	3	15.7	632	009	101.3%	?????	
0	SW	-	57.5	40	09/27 08:55 AM		15.3	638	028	104.5%	1/4	1	15.6	633	000	100.0%	?Not Submerged in flow	
0	HB	-	57.5	40	09/27 09:15 AM		15.3	638	035	105.5%	HB	HB	15.5	633	034	105.4%		
0	SW	-	57.5	40	09/27 09:48 AM		15.4	638	042	106.6%	1/2	2	15.6	633	015	102.3%		
0	SW	-	57.5	40	09/27 10:01 AM		15.4	638	044	106.9%	3/4	3	15.6	633	017	102.7%		
0	TB	-	57.5	40	09/27 10:25 AM		15.4	638	037	105.8%	TB	TB	15.6	633	007	101.1%		
0	TB	-	59	40	09/27 11:30 AM		15.4	638	045	107.2%	TB	TB	15.6	633	009	101.4%		
0	SW	-	59	40	09/27 11:45 AM		15.4	638	045	107.1%	1/4	1	15.6	633	000	100.0%	?Not Submerged in flow	
0	SW	-	60	40	09/27 12:48 PM		15.6	638	090	114.2%	1/4	1	15.7	632	005	100.7%	?Not Submerged in flow	
0	SW	-	60	40	09/27 02:20 PM		15.6	638	103	116.2%	1/2	2	15.7	631	033	105.2%		
0	SW	-	60	40	09/27 02:31 PM		15.6	638	102	116.0%	3/4	3	15.7	632	032	105.1%		
0	TB	-	60	40	09/27 02:45 PM		15.6	638	097	115.2%	TB	TB	15.7	632	014	102.2%		
0	TB	-	59	20	09/27 03:00 PM		15.5	638	090	114.2%	TB	TB	15.7	632	008	101.2%		
0	SW	-	0	80	09/28 08:40 AM		15.3	637	-045	92.8%	1/2	2	15.5	632	-029	95.4%		
0	SW	-	0	80	09/28 08:52 AM		15.3	637	-046	92.7%	3/4	3	15.5	632	-019	97.0%		
0	SW	-	0	60	09/28 09:55 AM		15.3	637	-047	92.6%	3/4	3	15.5	633	-011	98.4%		
0	SW	-	0	60	09/28 10:08 AM		15.3	637	-047	92.5%	1/2	2	15.5	633	-026	95.9%		
0	SW	-	0	60	09/28 10:20 AM		15.3	637	-047	92.5%	1/4	1	15.5	633	-046	92.7%		
0	SW	-	0	40	09/28 10:25 AM		15.3	637	-047	92.6%	1/4	1	15.5	633	-042	93.4%		
0	SW	-	0	40	09/28 10:35 AM		15.3	637	-045	92.8%	1/2	2	15.5	633	-012	98.1%		

General										HB Reading (CS Meter)					Reading 2 (SA Meter)				
h _{STEP}	Probe	Tank	Press	Flow	Date & Time	Temp	BP	ΔP	TGP%	Loc	Sta	Temp	BP	ΔP	TGP%	Comments			
0	SW	-	0	40	09/28 10:45 AM	15.3	637	-045	92.8%	3/4	3	15.5	633	000	100.0%				
0	TB	-	0	40	09/28 10:55 AM	15.3	637	-045	92.8%	TB	TB	15.5	633	001	100.2%				
0	TB	-	0	20	09/28 11:05 AM	15.3	637	-045	92.8%	TB	TB	15.5	633	002	100.4%				
0	SW	-	0	20	09/28 11:15 AM	15.3	637	-046	92.7%	3/4	3	15.5	633	004	100.6%				
0	SW	-	0	20	09/28 11:25 AM	15.4	637	-045	92.9%	1/2	2	15.6	633	000	100.0%				
0	SW	-	0	20	09/28 11:35 AM	15.4	637	-044	93.1%	1/4	1	15.7	633	-026	95.9%				
0	SW	-	0	80	09/28 11:59 AM	15.4	637	-045	92.8%	1/4	1	15.6	633	-045	92.8%				
0	SW	-	56.5	60	09/29 09:15 AM	15.3	634	035	105.6%	1/4	1	15.7	628	032	105.2%				
0	SW	-	56.5	60	09/29 09:25 AM	15.3	634	033	105.3%	1/2	2	15.7	628	023	103.7%				
0	SW	-	56.5	60	09/29 09:35 AM	15.3	634	030	104.8%	3/4	3	15.7	628	022	103.5%				
0	TB	-	56.5	60	09/29 09:45 AM	15.3	634	034	105.5%	TB	TB	15.7	628	011	101.7%				
0	SW	-	58	60	09/29 10:30 AM	15.4	634	055	108.7%	1/4	1	15.6	628	052	108.2%				
0	SW	-	58	60	09/29 10:40 AM	15.4	634	055	108.8%	1/2	2	15.6	628	035	105.7%				
0	SW	-	58	60	09/29 10:55 AM	15.4	634	050	108.0%	3/4	3	15.5	628	030	104.9%				
0	TB	-	58	60	09/29 11:05 AM	15.4	634	050	108.0%	TB	TB	15.5	628	013	102.0%				
0	SW*	-	58	60	09/29 01:50 PM	15.4	633	058	109.3%	1/2	2	15.6	627	038	106.1%	Top SW removed			
0	SW*	-	58	60	09/29 02:40 PM	15.5	632	056	108.9%	3/4	3	15.7	627	033	105.2%	Top SW removed			

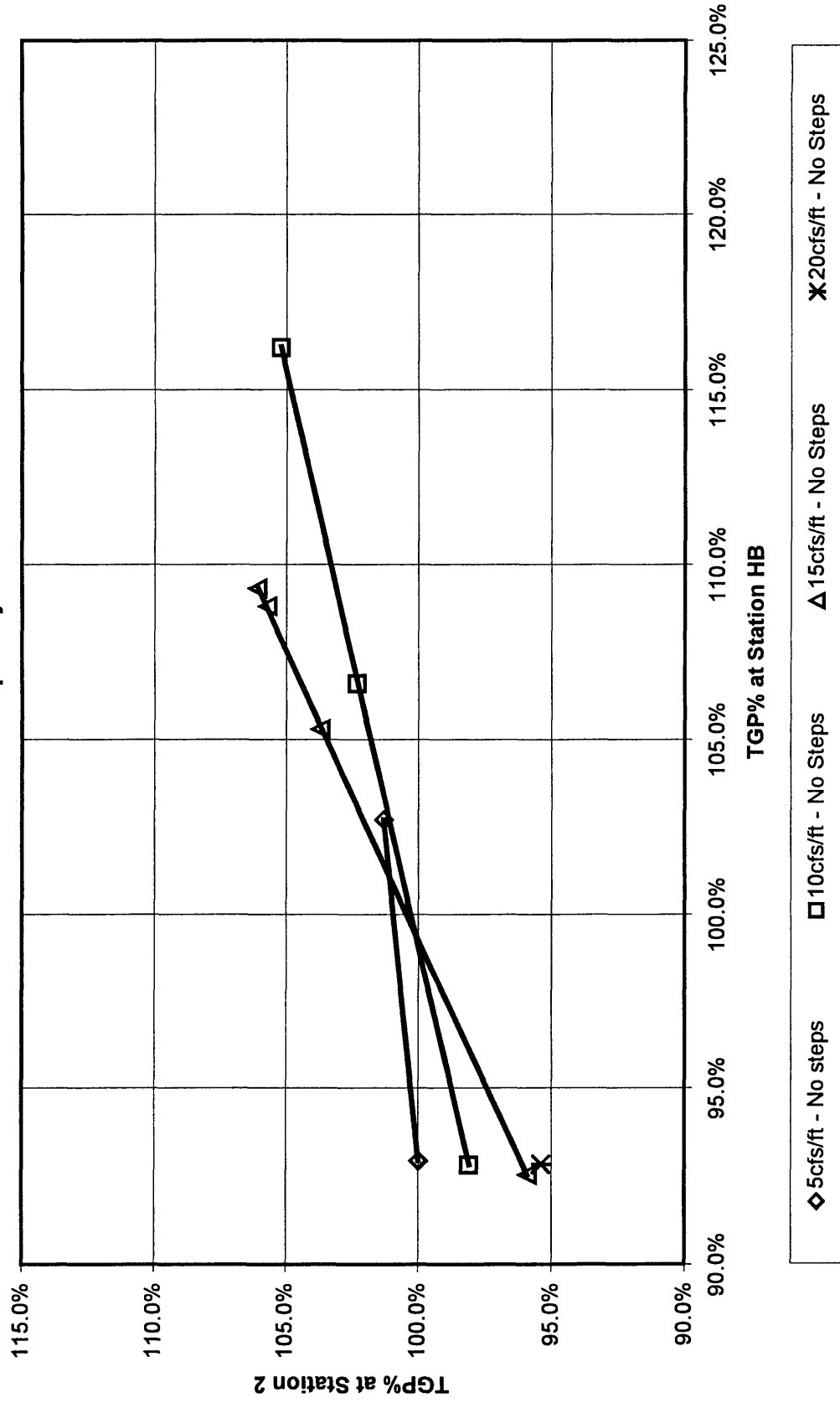
APPENDIX B

PLOTS OF TGP% IN HEAD BOX VS TGP% ON SLOPE

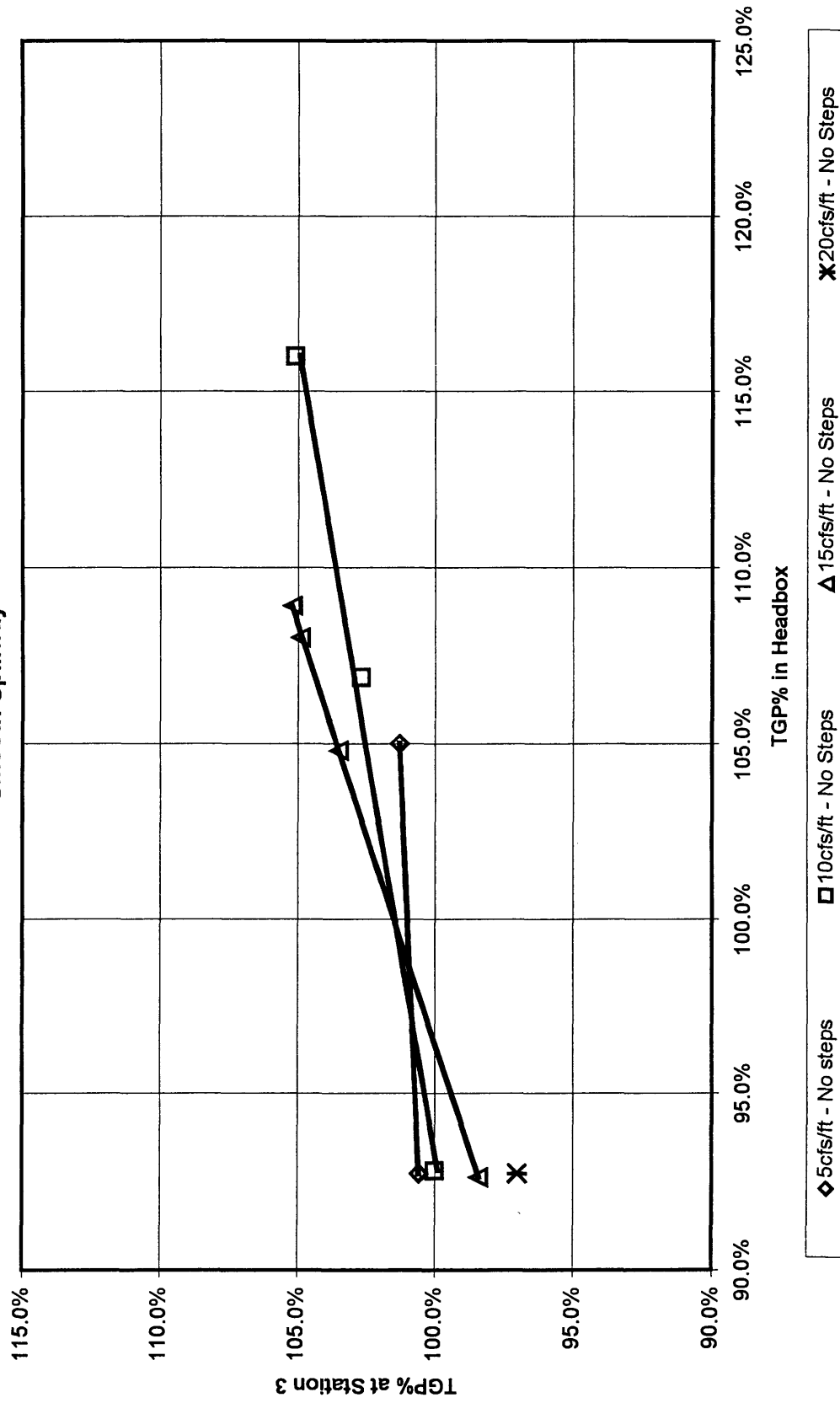
TGP% at Station HB vs Station 1
Smooth Spillway



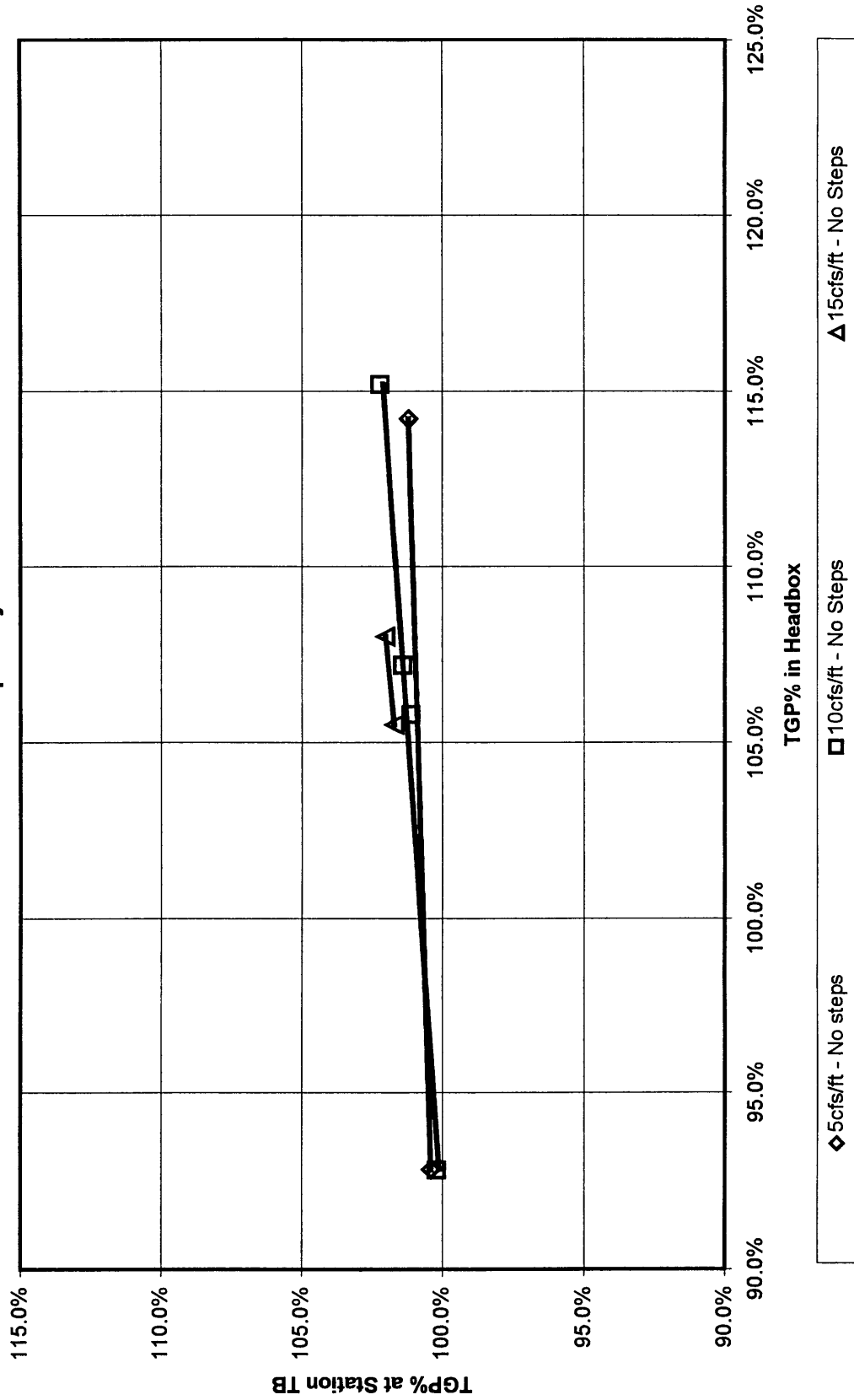
TGP% at Station HB vs. Station 2
Smooth Spillway



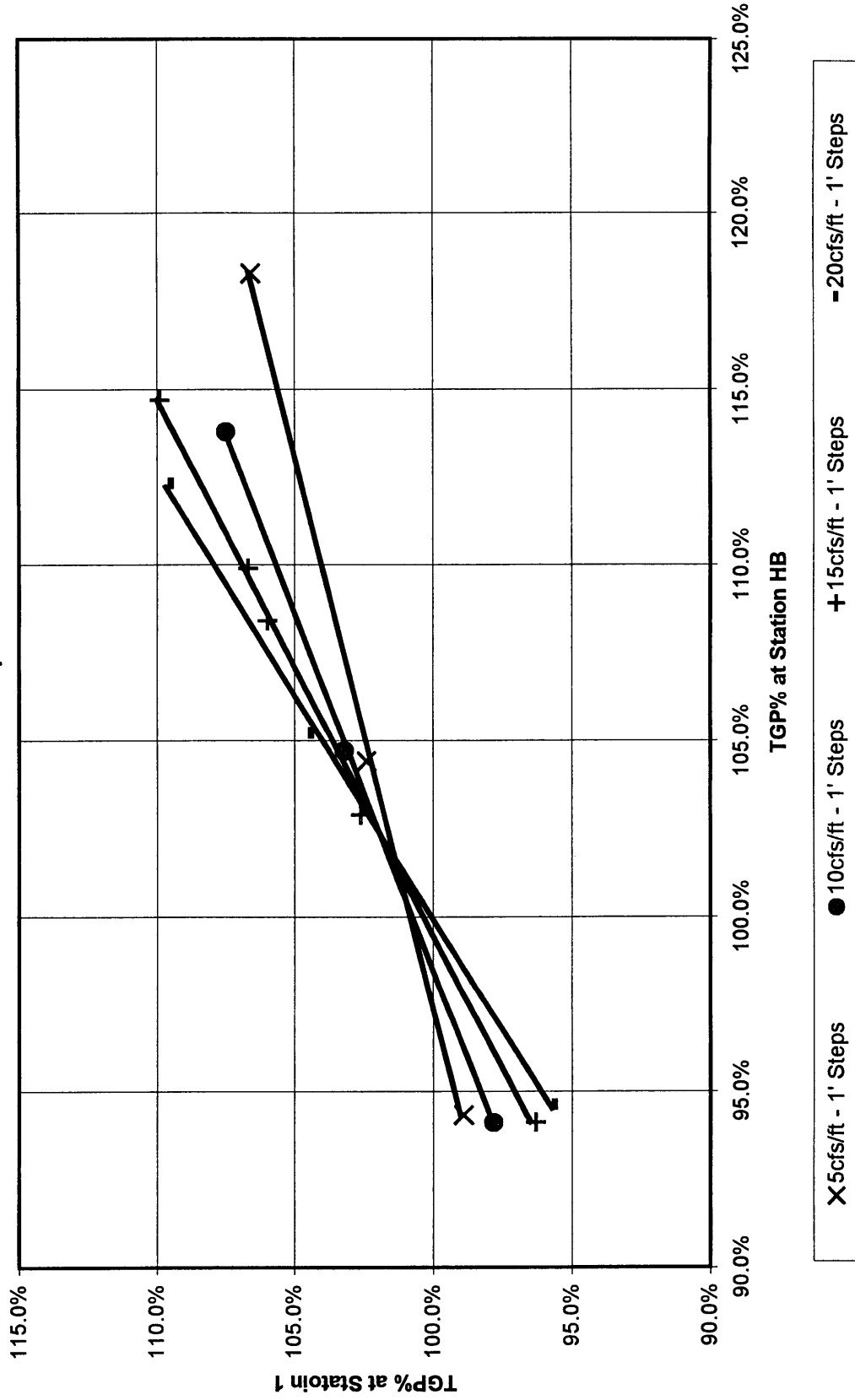
TGP% at Station HB vs. Station 3
Smooth Spillway



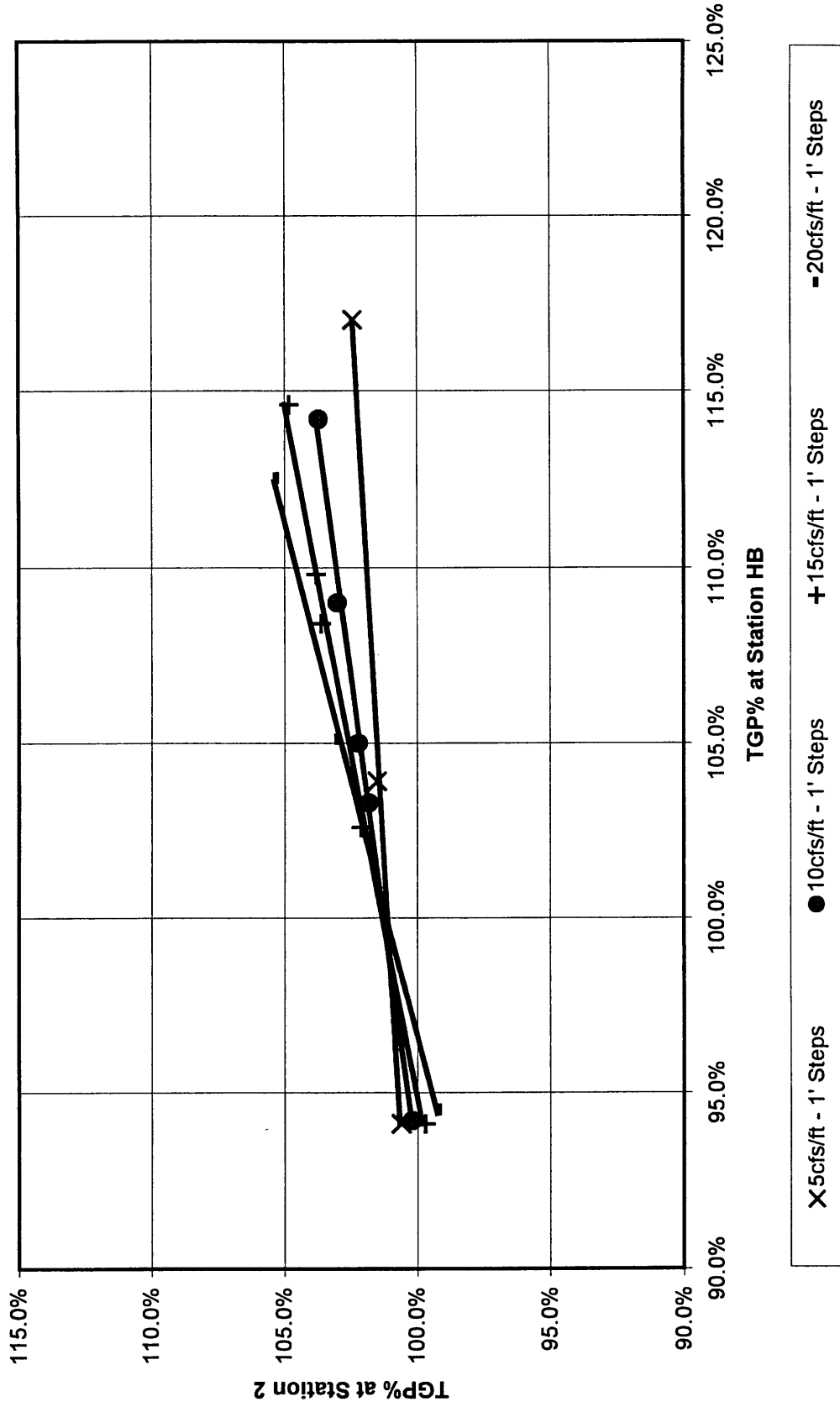
**TGP% at Station HB vs. Station TB
Smooth Spillway**



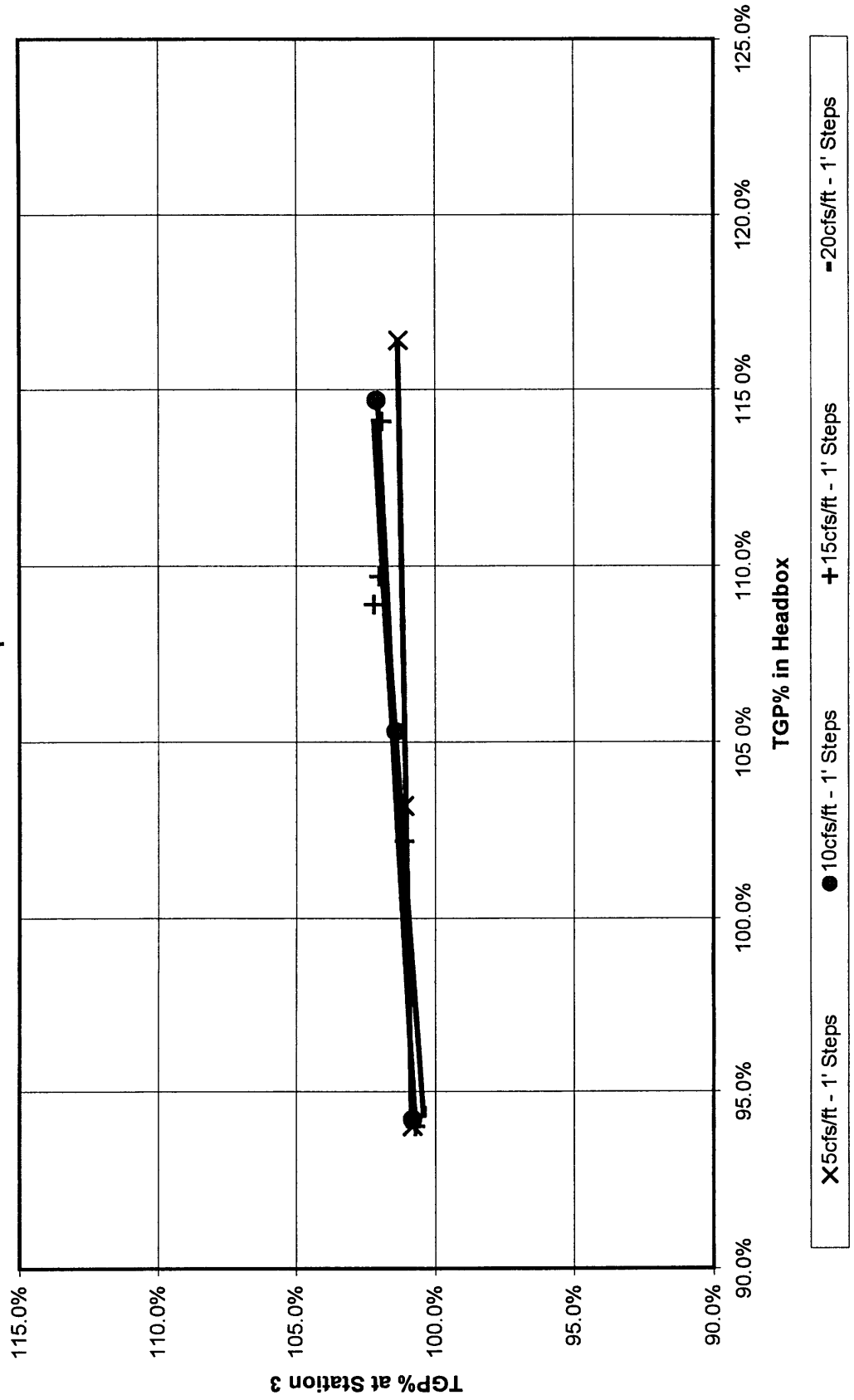
TGP% at Statoin HB vs Station 1
1-Foot Steps



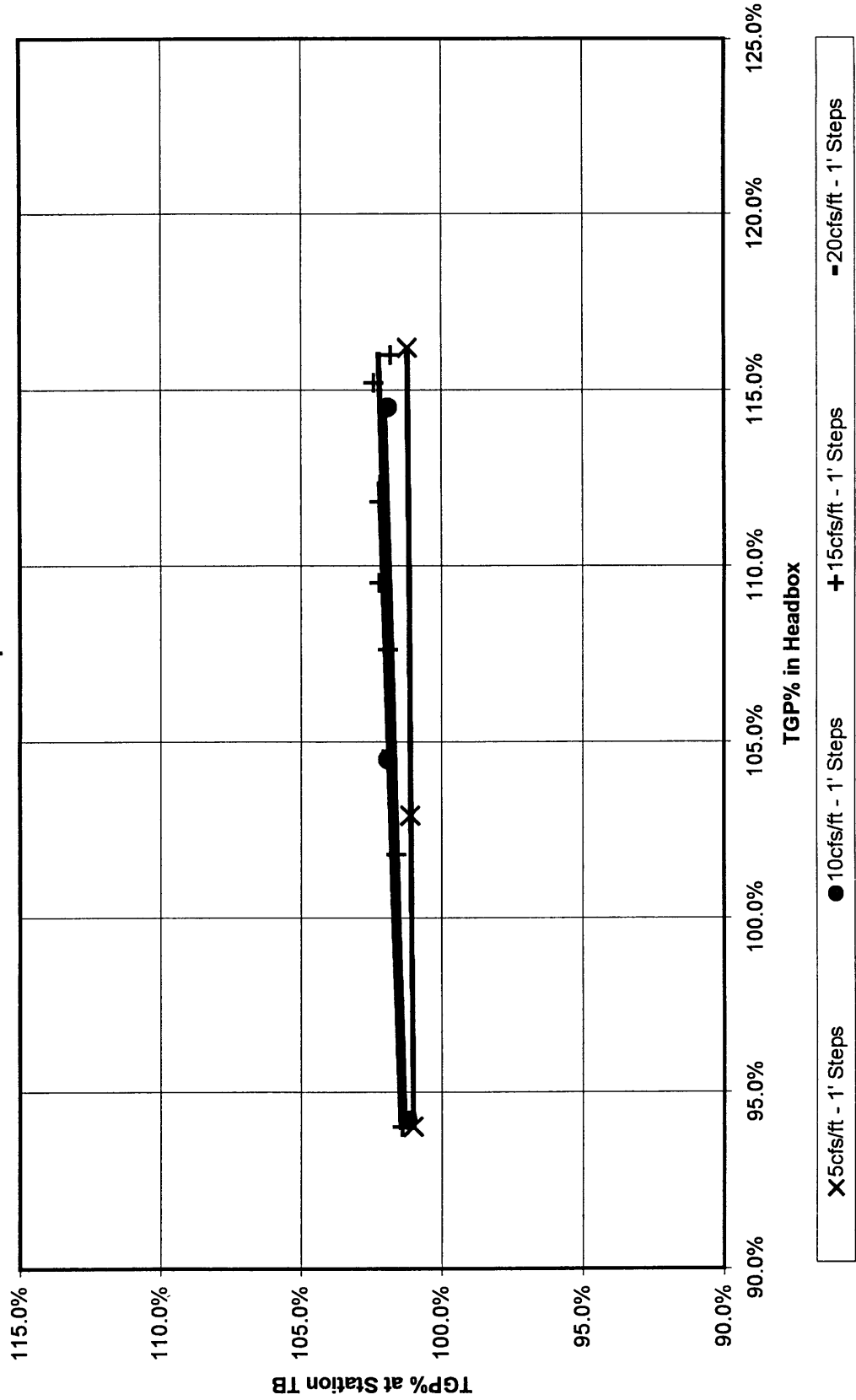
**TGP% at Station HB vs. Station 2
1-Foot Steps**



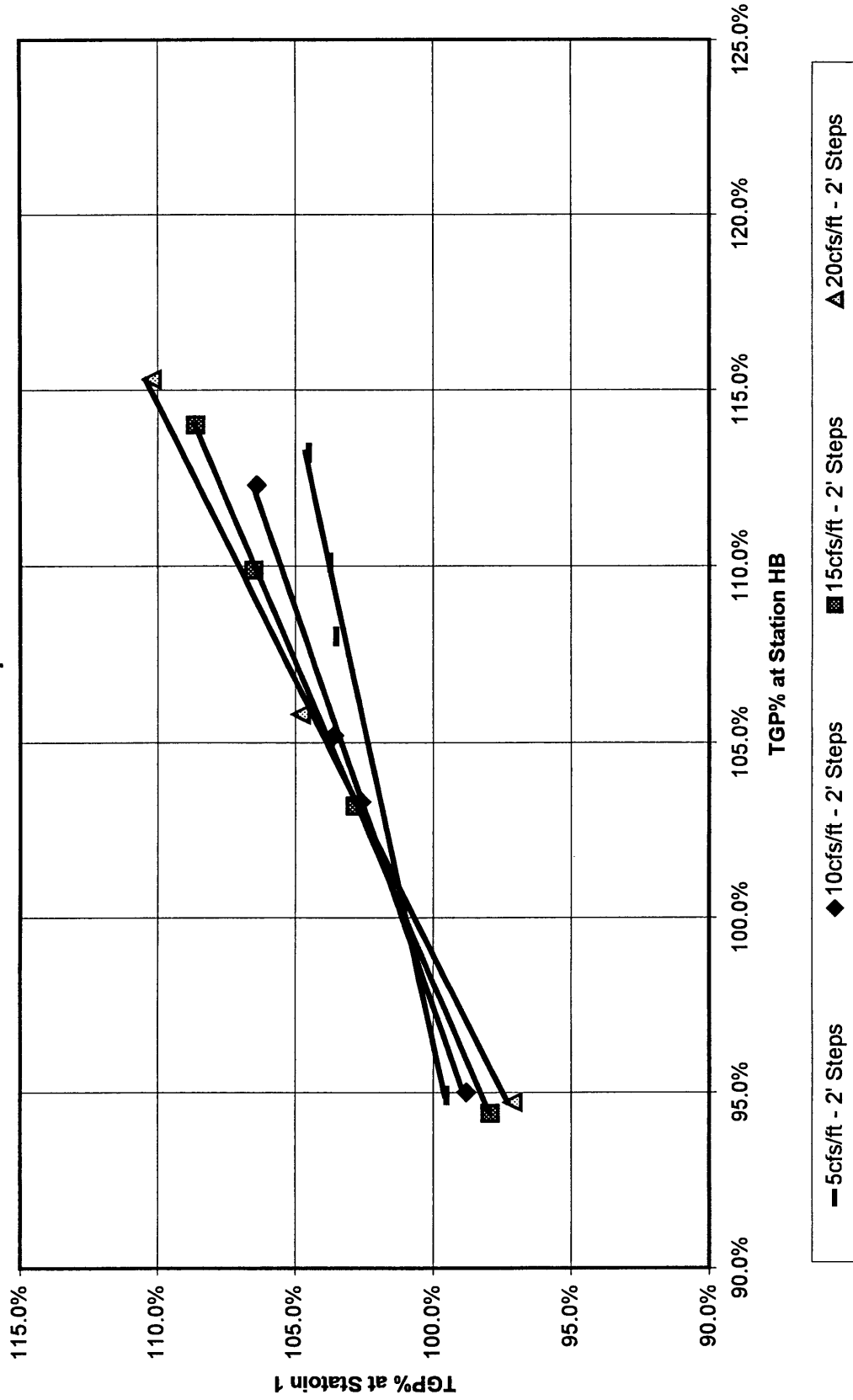
**TGP% at Station HB vs. Station 3
1-Foot Steps**



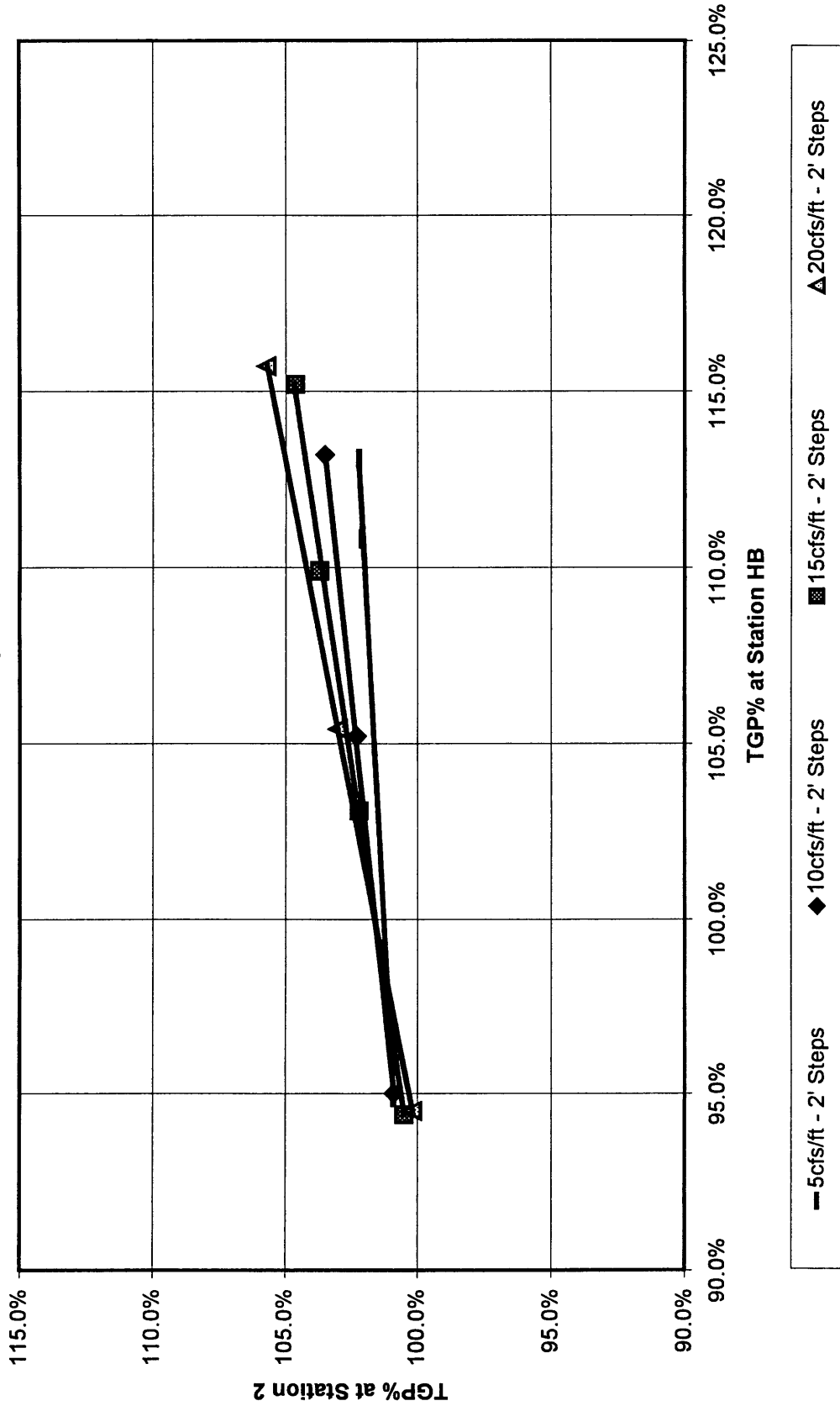
**TGP% at Station HB vs. Station TB
1-Foot Steps**



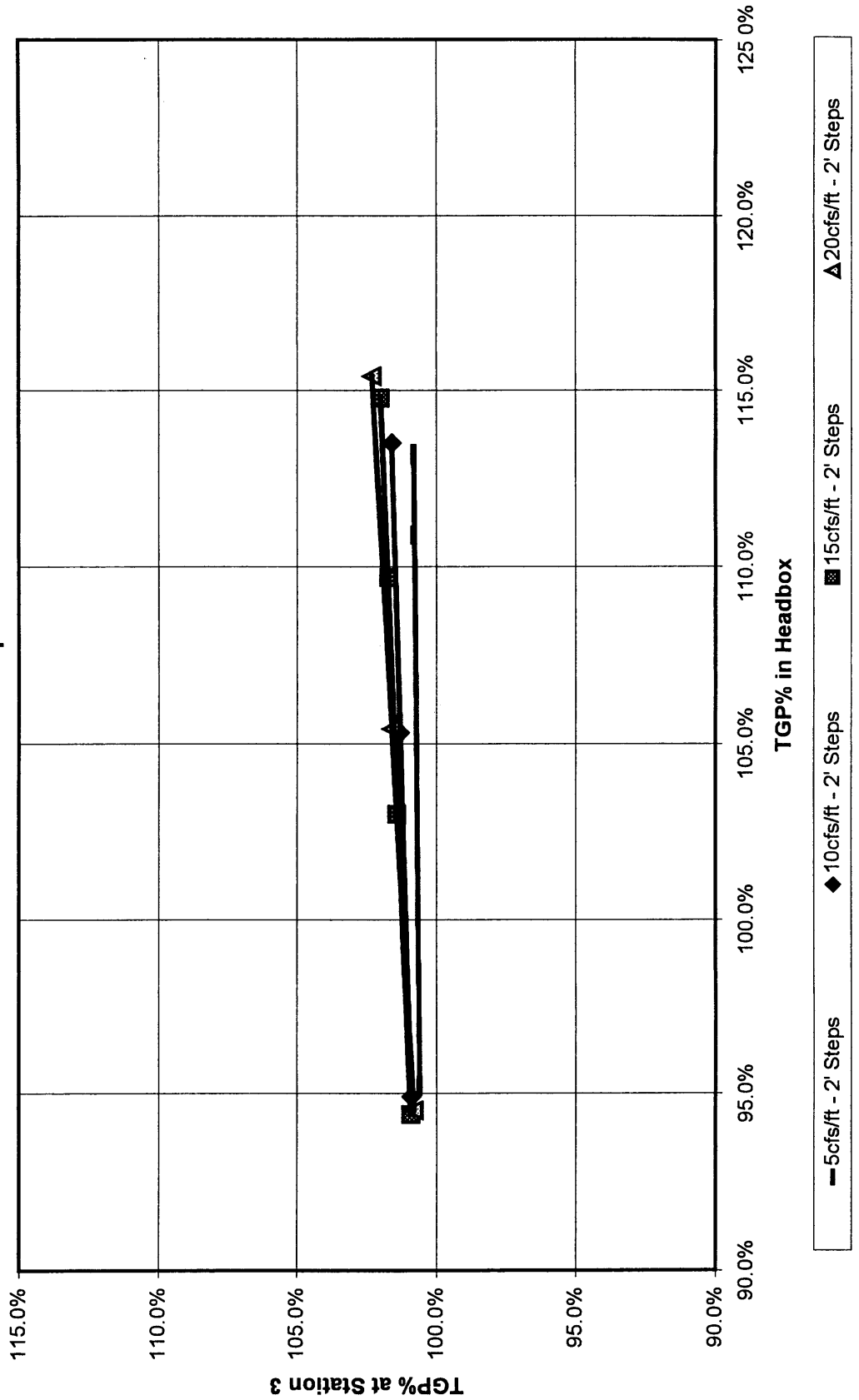
**TGP% at Station HB vs Station 1
2-Foot Steps**



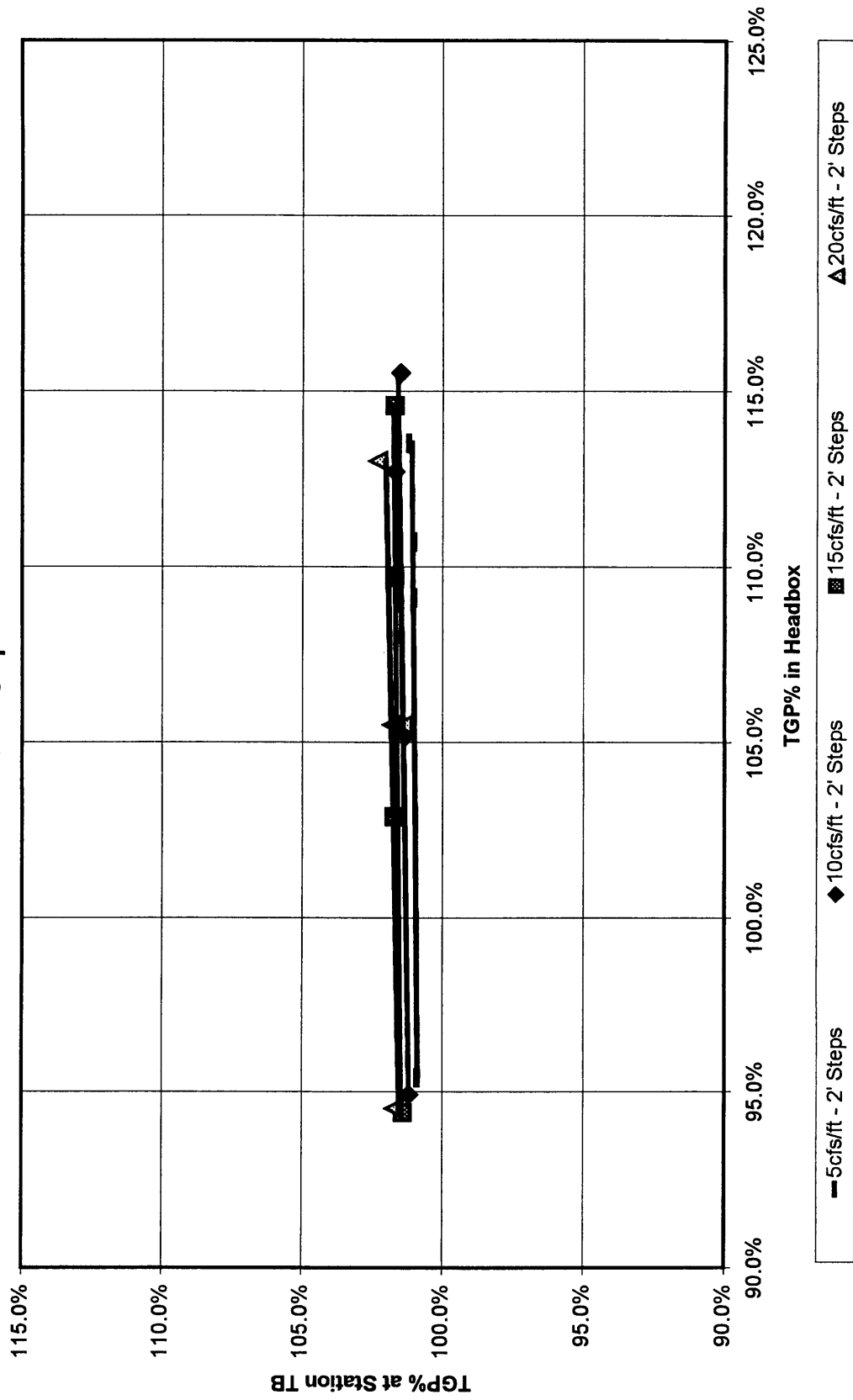
TGP% at Station HB vs. Station 2
2-Foot Steps



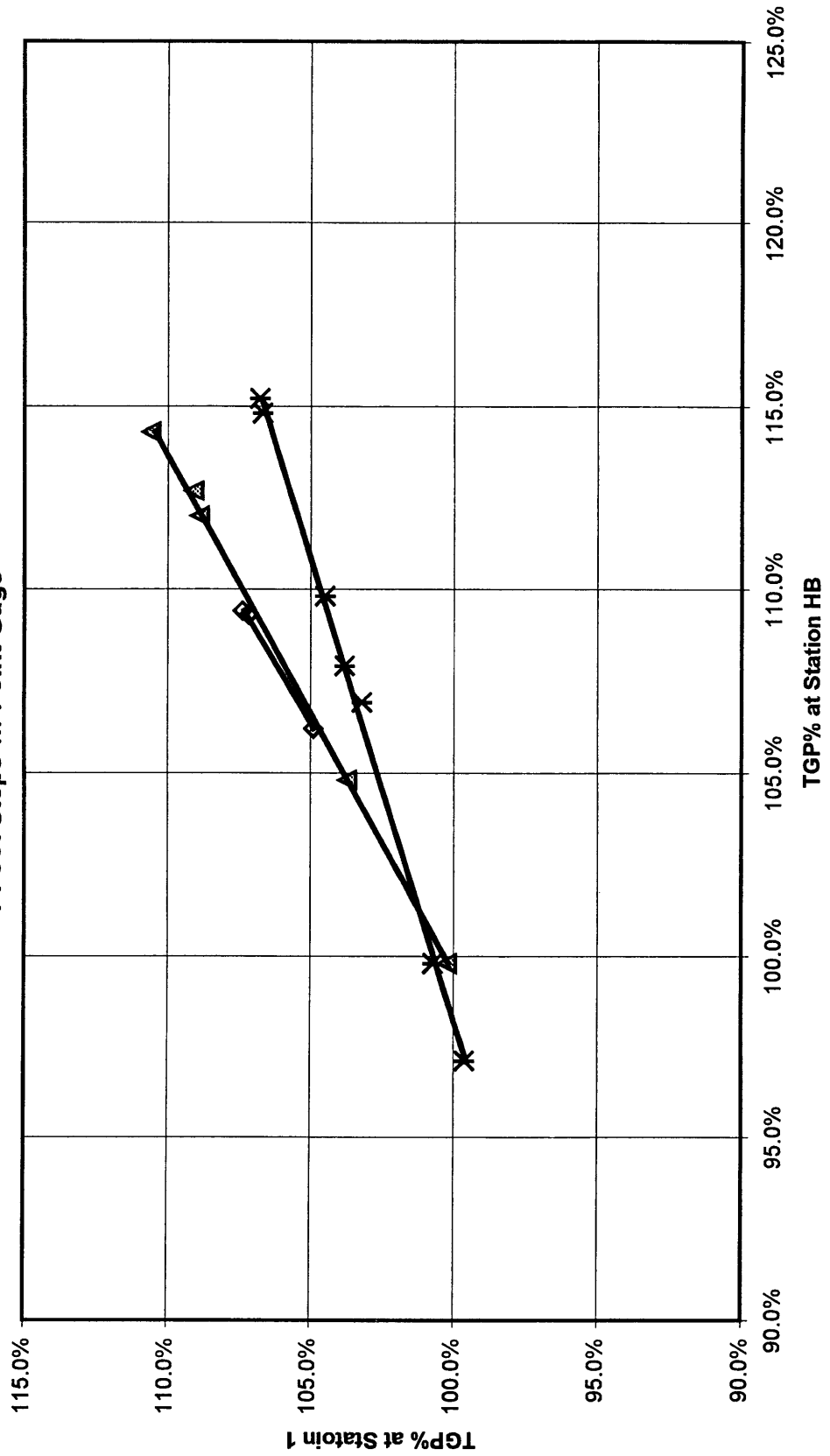
**TGP% at Station HB vs. Station 3
2-Foot Steps**



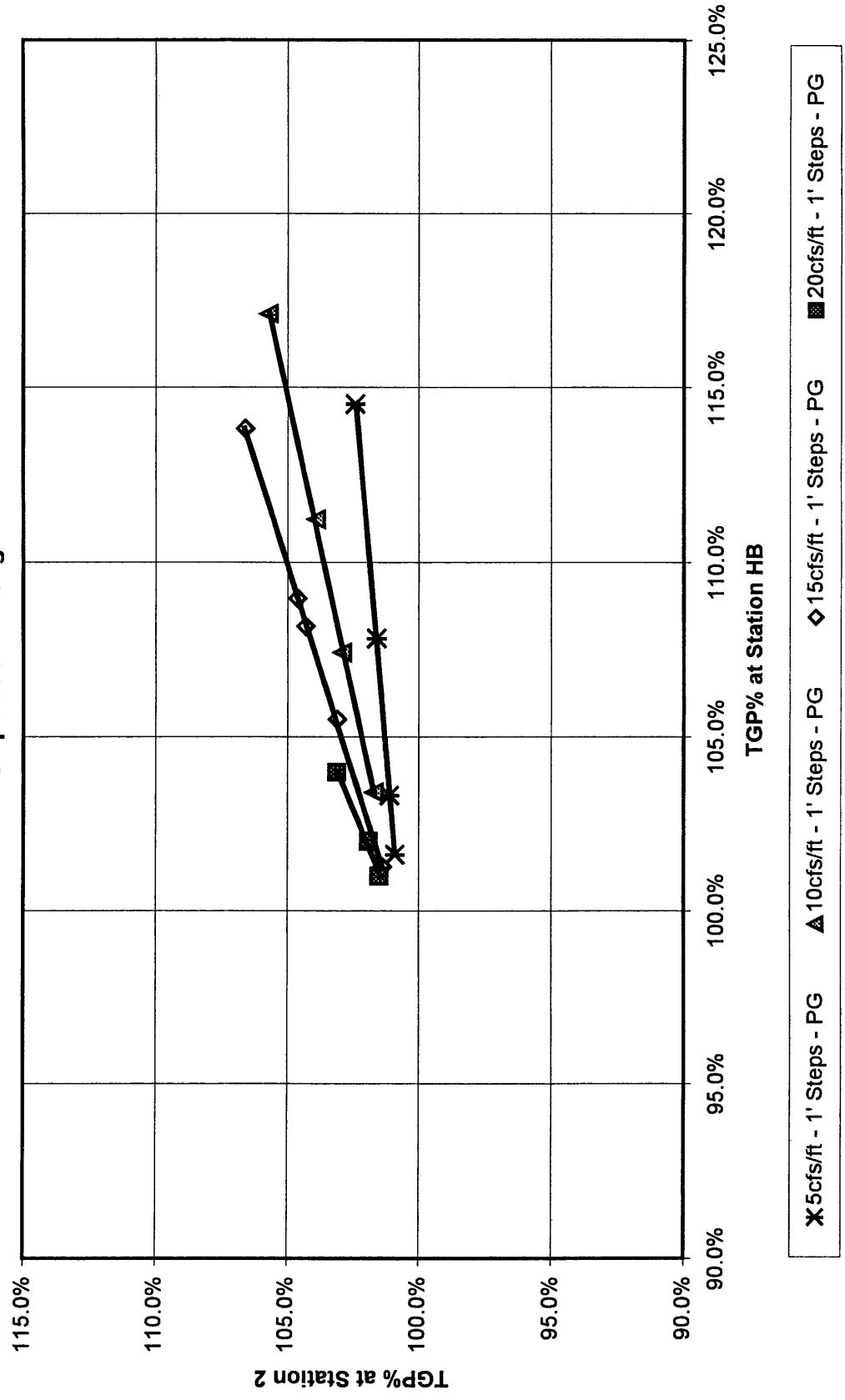
**TGP% at Station HB vs. Station TB
2-Foot Steps**



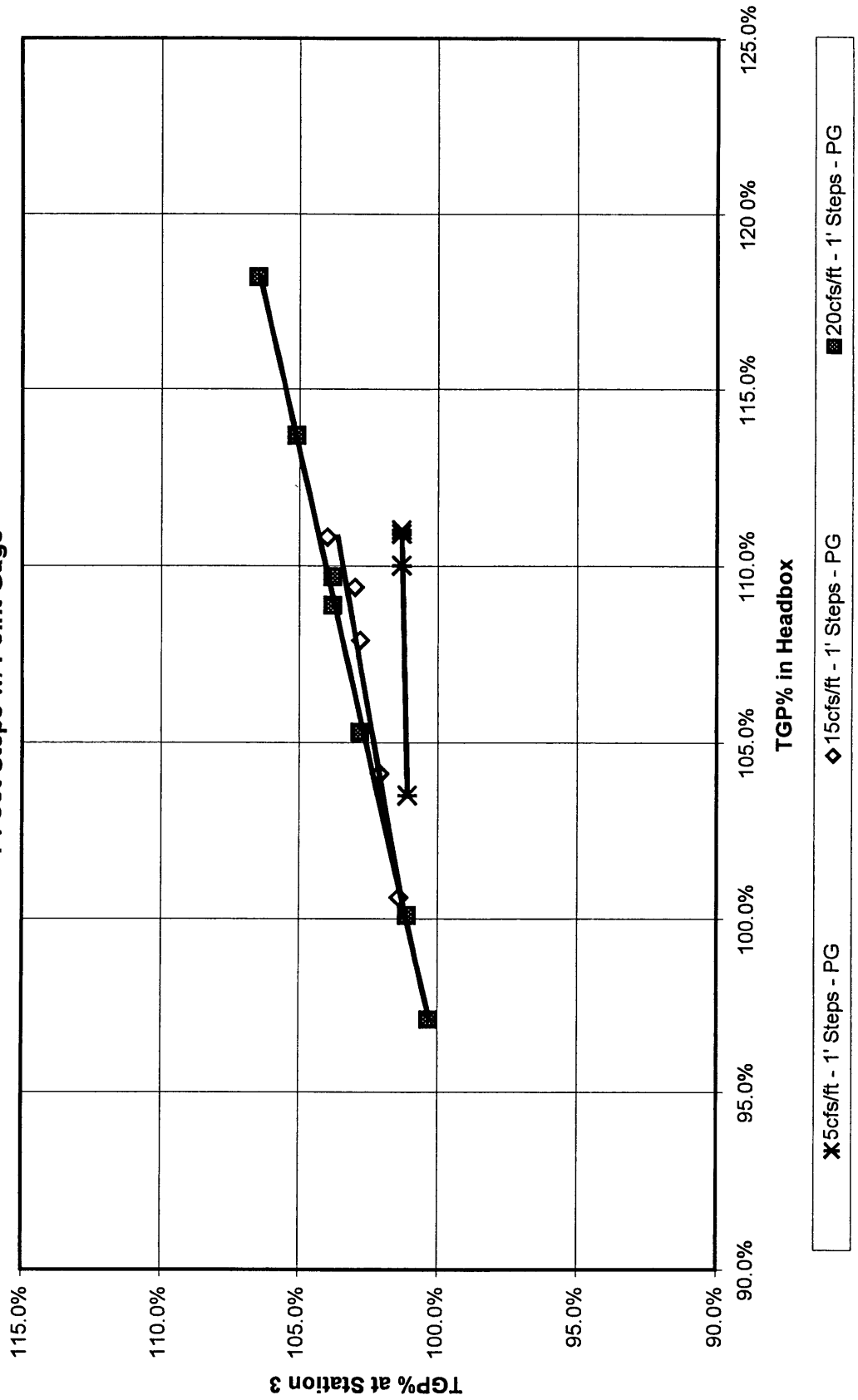
**TGP% at Station HB vs Station 1
1-Foot Steps w/ Point Gage**



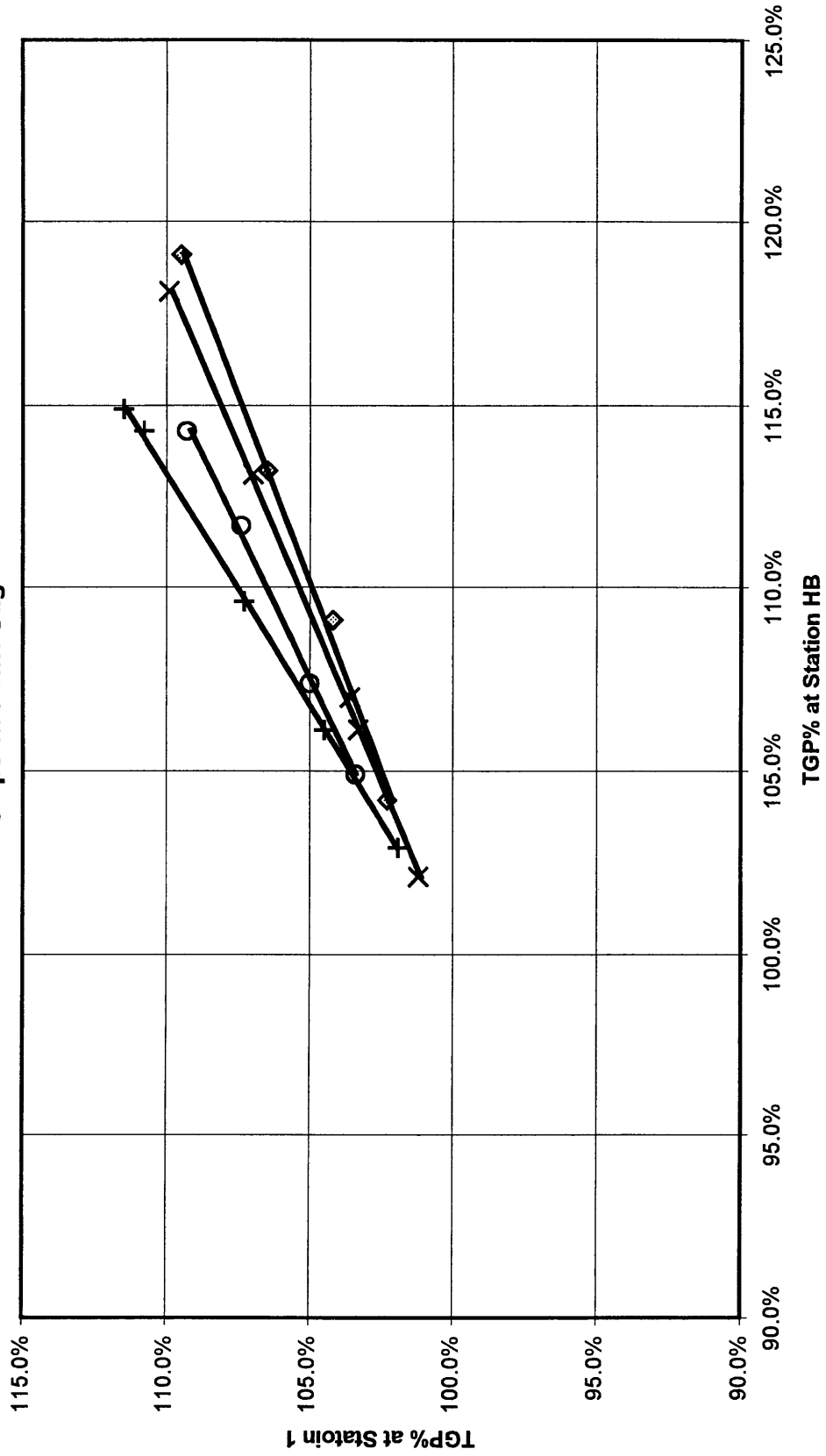
**TGP% at Station HB vs. Station 2
1-Foot Steps w/ Point Gage**



**TGP% at Station HB vs. Station 3
1-Foot Steps w/ Point Gage**

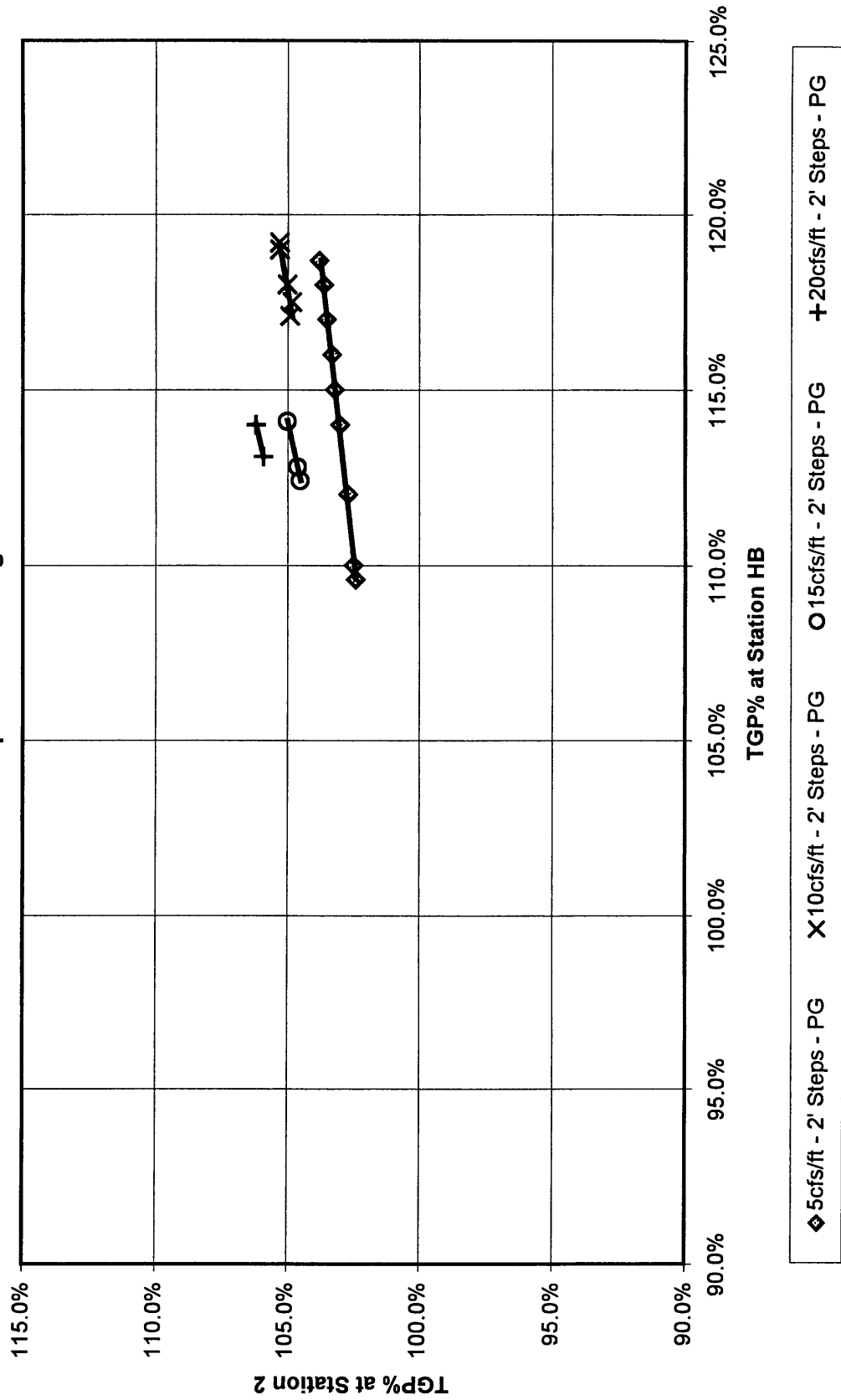


**TGP% at Station HB vs Station 1
2-Foot Steps w/ Point Gage**



◆ 5cfs/ft - 2' Steps - PG X 10cfs/ft - 2' Steps - PG O 15cfs/ft - 2' Steps - PG + 20cfs/ft - 2' Steps - PG

TGP% at Station HB vs. Station 2
2-Foot Steps w/ Point Gage

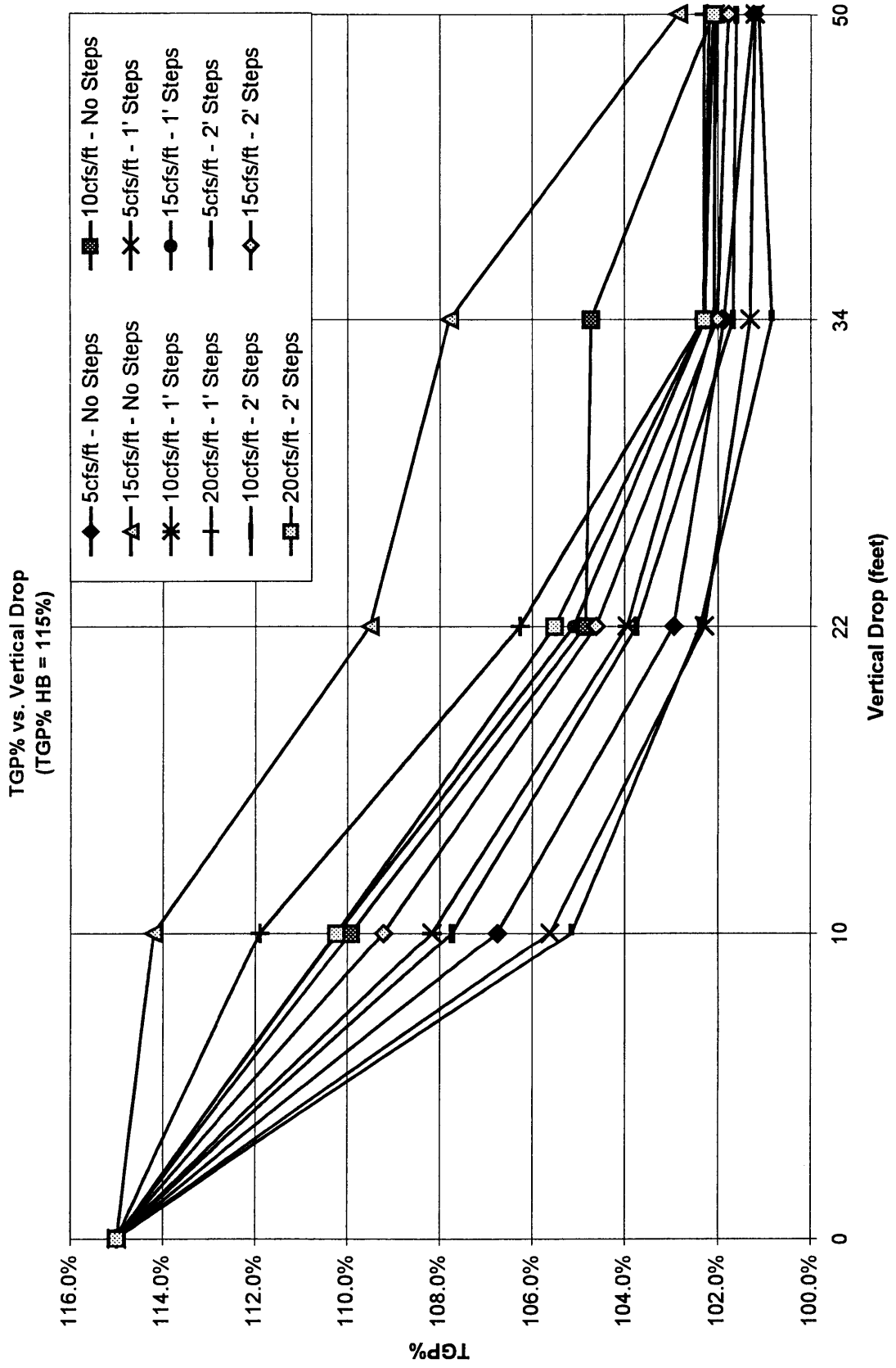


APPENDIX C
LINEAR REGRESSION EQUATIONS

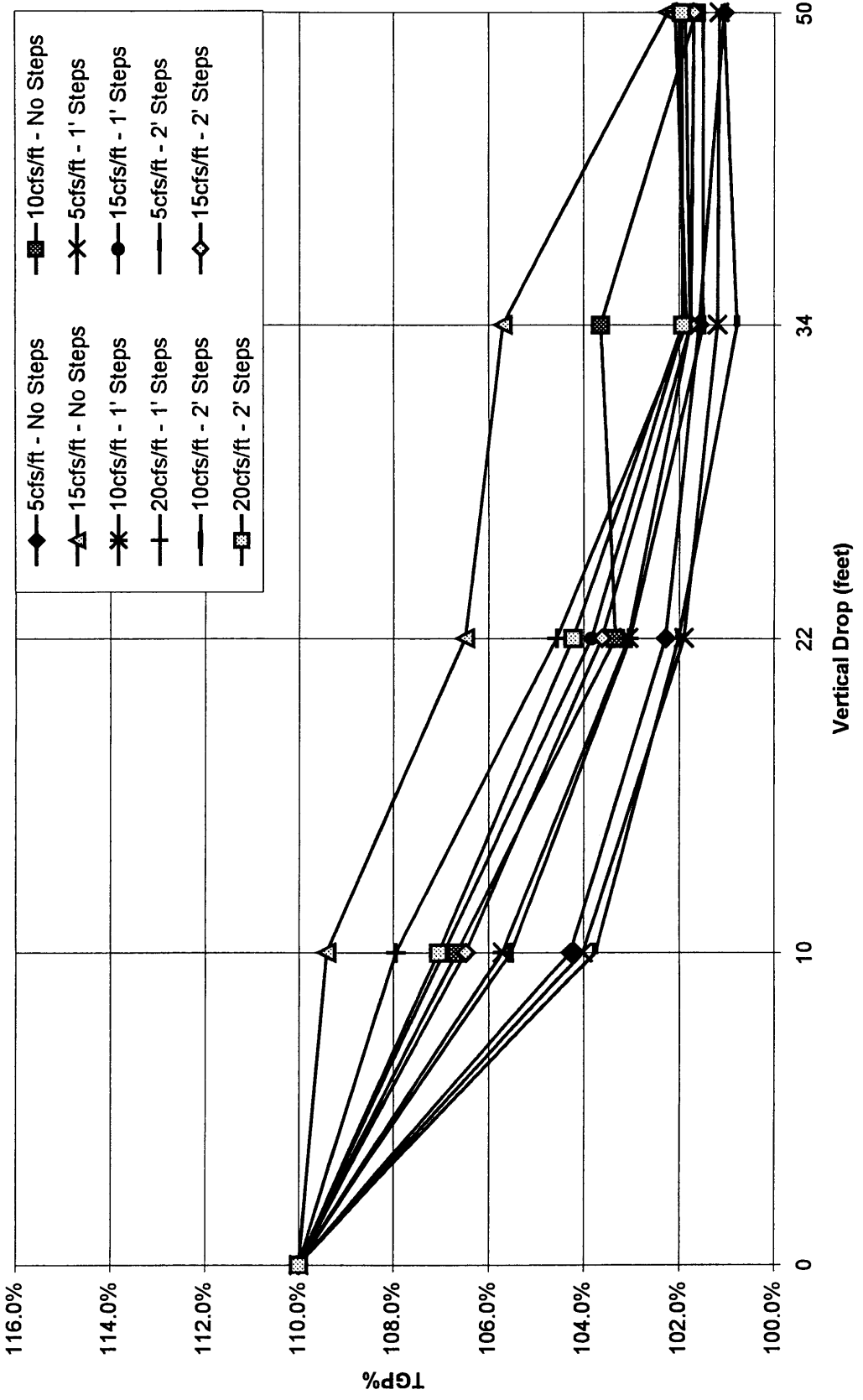
h _{STEP}	Probe	Flow	Vert Drop	Station	Slope	y-inter	E	R ²	Points
0	SW	5	10	1	0.4953	0.498	0.505	1	2
0	SW	5	22	2	0.1327	0.877	0.867	1	2
0	SW	5	34	3	0.0569	0.953	0.943	1	2
0	SW	5	50	TB	0.0374	0.969	0.963	1	2
0	SW	10	10	1	-	-	-	-	1
0	SW	10	22	2	0.3035	0.699	0.697	1	3
0	SW	10	34	3	0.2174	0.797	0.783	0.9919	3
0	SW	10	50	TB	0.0881	0.920	0.912	0.9781	4
0	SW	15	10	1	0.956	0.043	0.044	1	3
0	SW	15	22	2	0.6048	0.400	0.395	0.9999	4
0	SW	15	34	3	0.4192	0.596	0.581	0.9999	4
0	SW	15	50	TB	0.12	0.890	0.880	1	2
0	SW	20	10	1	-	-	-	-	1
0	SW	20	22	2	-	-	-	-	1
0	SW	20	34	3	-	-	-	-	1
0	SW	20	50	TB	-	-	-	-	0
1	SW	5	10	1	0.3197	0.689	0.680	0.9985	3
1	SW	5	22	2	0.0781	0.933	0.922	0.9931	3
1	SW	5	34	3	0.0218	0.988	0.978	0.9534	3
1	SW	5	50	TB	0.0089	1.002	0.991	0.9871	3
1	SW	10	10	1	0.4929	0.515	0.507	0.9995	3
1	SW	10	22	2	0.1786	0.834	0.821	0.9955	5
1	SW	10	34	3	0.0631	0.948	0.937	0.9915	3
1	SW	10	50	TB	0.0347	0.981	0.965	0.7574	3
1	SW	15	10	1	0.6561	0.348	0.344	0.9981	5
1	SW	15	22	2	0.2515	0.762	0.749	0.9937	5
1	SW	15	34	3	0.0745	0.937	0.926	0.819	5
1	SW	15	50	TB	0.0361	0.980	0.964	0.6179	7
1	SW	20	10	1	0.7888	0.212	0.211	0.9985	3
1	SW	20	22	2	0.3402	0.671	0.660	0.9985	3
1	SW	20	34	3	0.0907	0.919	0.909	0.9987	3
1	SW	20	50	TB	0.0397	0.977	0.960	0.906	3
2	SW	5	10	1	0.2772	0.733	0.723	0.9919	4
2	SW	5	22	2	0.0729	0.940	0.927	0.9978	3
2	SW	5	34	3	0.0117	0.995	0.988	0.9862	3
2	SW	5	50	TB	0.0125	0.997	0.988	0.6448	4
2	SW	10	10	1	0.4413	0.570	0.559	0.9977	4
2	SW	10	22	2	0.1426	0.873	0.857	0.9994	3
2	SW	10	34	3	0.0377	0.973	0.962	0.9998	3
2	SW	10	50	TB	0.0203	0.993	0.980	0.7076	4
2	SW	15	10	1	0.5478	0.462	0.452	0.9998	4
2	SW	15	22	2	0.1998	0.816	0.800	0.9984	4
2	SW	15	34	3	0.0531	0.959	0.947	0.9974	4
2	SW	15	50	TB	0.0143	1.001	0.986	0.7003	4
2	SW	20	10	1	0.6375	0.369	0.363	0.9968	3
2	SW	20	22	2	0.2594	0.757	0.741	1	3
2	SW	20	34	3	0.0718	0.940	0.928	0.9998	3
2	SW	20	50	TB	0.0278	0.989	0.972	0.3215	4

APPENDIX D

PLOTS OF TGP% AS A FUNCTION OF VERTICAL DROP



TGP% vs. Vertical Drop
(TGP% HB = 110%)



TGP% vs. Vertical Drop
(TGP% HB = 105%)

